

SPACE STATION
AUXILIARY THRUST CHAMBER TECHNOLOGY

Final Report

Prepared For:

National Aeronautics and Space Administration
Lewis Research Center
Cleveland, Ohio 44135

July 1990

Contract NAS 3-24398

Approved By:



B. L. Reimer,
Program Manager
Space Propulsion

Prepared By:



P. J. Robinson
Project Engineer
Space Station Propulsion

GenCorp Aerojet
Propulsion Division
Sacramento, California 95813

TABLE OF CONTENTS

	<u>Page</u>
I. Summary	1
II. Introduction	2
III. Space Station Thruster No. 1	6
A. Design Approach	6
1. Design Background	6
2. Design Concept	6
3. Design Point	9
B. Design Analysis	9
1. Ignition Analysis	9
2. Thermal Analysis	9
3. Performance Analysis	22
4. Chamber Life Analysis	22
C. Design Description and Fabrication	25
D. Test	30
1. Test Setup	30
2. Instrumentation	30
3. Test Summary	30
4. Experimental Results	39
E. Evaluation of Results	44
F. Conclusions	55
IV. Space Station Thruster No. 2	56
A. Design Approach	56
1. Design Background	56
2. Design Concept	56
3. Design Point	59
B. Design Analysis	59
1. Ignition Analysis	59
2. Thermal Analysis	65
3. Performance Analysis	65
4. Chamber Life Analysis	65
C. Design Description and Fabrication	65

TABLE OF CONTENTS (cont.)

	<u>Page</u>
D. Test	72
1. Test Setup	72
2. Instrumentation	72
3. Test Summary	76
4. Experimental Results	86
E. Evaluation of Results	86
F. Conclusions	114
V. References	115
Appendix A: Detail Drawings, Thruster No. 1	A-1
Appendix B: Test Data, Thruster No. 1	B-1
Appendix C: Performance Prediction Methodology	C-1
Appendix D: Detail Drawings, Thruster No. 2	D-1

LIST OF TABLES

<u>Table No.</u>		<u>Page</u>
I	Design Requirements for Thruster No. 1	4
II	Design Requirements for Thruster No. 2	5
III	Thruster No. 1 Design Point	10
IV	Space Station Thruster No. 1 Spark Igniter Operating Characteristics	15
V	Test Instrumentation Space Station Thruster No. 1	35
VI	Thruster No. 1 Test Summary for Mixture Ratio Range	37
VII	Thruster No. 1 Test Summary for Percent Fuel Film Cooling Range	38
VIII	Design Points, NASA LeRC Space Station Thrusters	63
IX	Space Station Thruster No. 2 Spark Igniter Operating Characteristics	64
X	Design Point Performance Prediction for Thruster No. 2	67
XI	Test Instrumentation Space Station Thruster No. 2	77
XII	Thruster No. 2 Test Summary	84
XIII	Thruster No. 2 Test Summary for Percent Film Cooling Range	85
XIV	Test Data Summary for Test No. 166	92
XV	Test Data Summary for Test No. 193	93
XVI	Test Data Summary for Test No. 199	94
XVII	Test Data Summary for Test No. 207	95
XVIII	Test Data Summary for Test No. 227	96

LIST OF FIGURES

<u>Figure No.</u>		<u>Page</u>
1	Vacuum Specific Impulse vs Mixture Ratio	3
2	Proven Spark Torch Igniter Concept	7
3	Cutaway of Thruster No. 1 Assembly	8
4	Paschen's Low Curve for Air	11
5	Flame Quenching Limit for O ₂ /H ₂	12
6	Minimum Spark Energy Requirements for O ₂ /H ₂ Propellants	13
7	Spark Ignition Limits: High Pressure, Low Pressure, Minimum Energy Limits	14
8	Experimentally Determined Effect of Fuel Film Coolant on Delivered Specific Impulse and Mixing Efficiency	16
9	Typical Fit of Reference 5 Thermocouple Data with Conduction Code Prediction	18
10	Space Station Thruster Convergent Section Cg Profile	19
11	Comparison of Throat Heat Transfer with Turbulent and Laminar Correlations	20
12	Comparison of Reference 5 Thruster Adiabatic Wall Temperature Profile with HOCOOL Prediction	21
13	Predicted Mixing Efficiency, E _m , for Overall Mixture Ratio	23
14	Predicted Performance for Overall Mixture Ratio	24
15	Manson-Halford Method of Universal Slopes for Low Cycle Fatigue	26
16	Machined ZrCu Chamber Liner - Thruster No. 1	27
17	Completed Chamber Assembly - Thruster No. 1	28
18	Sleeve Insert	29
19	Aerojet Altitude Test Facility for Small Thrusters	31
20	Thruster Mounted to the Thrust Measuring Test Stand	32
21	Test Cell with Mounted Test Stand	33
22	Chamber Thermocouple Location	34
23	Backside Temperature Profile with 60 Percent FFC	40
24	Backside Temperature Profile with 75 Percent FFC	41
25	Maximum Backside Temperature Variation with FFC	42
26	Maximum Backside Temperature Variation with Mixture Ratio	43
27	Performance Variation with Percent FFC	45
28	Performance Variation with Mixture Ratio	46
29	Two Mixing Zones of Thruster Design	47

LIST OF FIGURES (cont.)

<u>Figure No.</u>		<u>Page</u>
30	Energy Release Efficiency and Specific Impulse Trends with Increasing O/F	50
31	Energy Release for Constant % FFC and Velocity Ratio	51
32	Current Space Station Thruster Has Inadequate H ₂ /O ₂ Momentum Flux Ratio and Mixing Length for Core Flow at High Mixing Ratio	52
33	Momentum Flux Ratio for Different % FFC and O/F	53
34	ERE for Increasing % FFC and Momentum Flux Ratio	54
35	Mixing Efficiency, E _T , for Thruster No. 1	57
36	Thruster No. 2 Assembly	58
37	Redesign of Injector/Sleeve Interface	60
38	Momentum Flux Ratio Compared for Thruster Nos. 1 and 2	61
39	Mixing Efficiency, E _T , Compared for Thruster Nos. 1 and 2	62
40	Predicted Gas-Side Wall Temperature Profile for Nominal Chamber Pressure	66
41	Predicted Gas-Side Wall Temperature Profile for 40 Percent of Nominal Chamber Pressure	68
42	Predicted Gas-Side Wall Temperature Profile for 135 Percent of Nominal Chamber Pressure	69
43	Performance Predictions for Operating Range of Thruster No. 2	70
44	Effects of Nozzle Extensions on Delivered Performance	71
45	Machined ZrCu Chamber Liner for Thruster No. 2	73
46	Thruster Chamber Assembly - Aft End	74
47	Thruster Chamber Assembly - Head End	75
48	Instrumentation Schematic for Space Station Thruster No. 2	79
49	Axial Positions of Thermocouples	80
50	Internal Thermocouple (TCI) Row Designations	81
51	Row A and Row C Thermocouples	82
52	Row B and Row D Thermocouples	83
53	Predicted vs Measured Performance for an Assumed Injector ERE of 97.0%	87
54	Predicted vs Measured Performance for an Assumed Injector ERE of 96.1%	88
55	Measured vs Predicted Wall Temperatures at the Design Point	89
56	Thermocouple Grid Positions	91
57	Measured Back-Side Wall Temperatures for Test No. 166	97
58	Measured Back-Side Wall Temperatures for Test No. 193	98

LIST OF FIGURES (cont.)

<u>Figure No.</u>		<u>Page</u>
59	Measured Back-Side Wall Temperatures for Test No. 199	99
60	Measured Back-Side Wall Temperatures for Test No. 207	100
61	Measured Back-Side Wall Temperatures for Test No. 227	101
62	Predicted vs Measured Back-Side Wall Temperatures for the Thruster Design Point	102
63	Cgn Profile for Calibrated Model	103
64	Predicted Stream Tube Mixture Ratios	104
65	Predicted Adiabatic Wall Temperatures	105
66	Predicted vs Measured Back-Side Wall Temperatures for Test No. 193	106
67	Predicted vs Measured Back-Side Wall Temperatures for Test No. 207	107
68	Predicted vs Measured Back-Side Wall Temperatures for Test No. 227	108
69	Predicted vs Measured Back-Side Wall Temperatures for Test No. 166	109
70	Predicted Maximum Wall Temperatures for Design Point	111
71	Revised Space Station Thruster Performance Predictions for Calibrated Thermal Model	112
72	Performance Improvement for Space Station Thruster No. 2	113

I. SUMMARY

The objective of the program documented herein was to establish a technical data base to support future development of GO_2/GH_2 flight thrusters for a Space Station Auxiliary Propulsion System. Specific issues of concern were thruster performance and cycle life. To address these issues, NASA funded Aerojet to design, fabricate and altitude test two 25-lbf GO_2/GH_2 thrusters. The first thruster was designed to operate at a nominal mixture ratio (O/F) of 4.0, and expansion area ratio (ϵ) of 100:1. It was tested over a range of O/F from 2.0 to 8.0, achieving a range of specific impulse (I_{sp}) from 440 to 310 lbf-sec/lbm. The second thruster was optimized for a nominal O/F of 8.0 at a lower nozzle expansion area ratio ϵ of 30:1. This second thruster was tested over an O/F range of 3.0 to 9.5, achieving an I_{sp} range of 416 to 332 lbf-sec/lbm, respectively. At O/F = 8.0, the I_{sp} was 360 lbf-sec/lbm, as predicted.

II. INTRODUCTION

The development of the Space Shuttle has made it possible to develop a Space Station. Such a Space Station requires an onboard auxiliary propulsion system (APS) to provide for vehicle reboost, attitude control, and docking and avoidance maneuvers. A key component of this onboard APS is the thruster design. To develop the required thruster technology base to support the Space Station Project, the National Aeronautics and Space Administration (NASA) Lewis Research Center (LeRC) has sponsored a development program under Contract No. NAS 3-24398. During this NASA LeRC sponsored program, two similar, yet distinct, 25-lbf gaseous oxygen/hydrogen (GO_2/GH_2) thrusters have been designed, fabricated and altitude tested to provide the necessary technology base for the future design of the Space Station APS thrusters.

The initial thruster was designed for operation at a nominal mixture ratio (O/F) of 4.0. This mixture ratio provided the maximum theoretical specific impulse, as indicated in Figure 1. Design requirements for this initial thruster, designated Thruster No. 1, are provided in Table I. During the course of the analysis, design and fabrication of Thruster No. 1, the Space Station propulsion requirements evolved. Specifically, the operating mixture ratio changed from 4.0 to 8.0, which was consistent with water electrolysis, the proposed method of generating the onboard GO_2/GH_2 propellants. Thruster No. 1 was completed as originally designed to meet the requirements of Table I; however, during the testing phase, the hot-fire mixture ratio range was extended from 3-5 to 2-8, to be responsive to the evolved requirements. The performance at the higher O/F values was not optimum, because those values lay in an off-design regime.

To evaluate a thruster optimized at an O/F of 8.0, NASA LeRC funded a redesign of the 25 lbf thruster, specifically the injector. The results of the test data evaluation from Thruster No. 1 were used to calibrate the thermal and hydraulic models utilized in the redesign effort. The new requirements, as given in Table II, were established by NASA LeRC. This redesigned thruster, designated Thruster No. 2, was fabricated and altitude tested, yielding excellent results and confirming the design and analysis methodology employed.

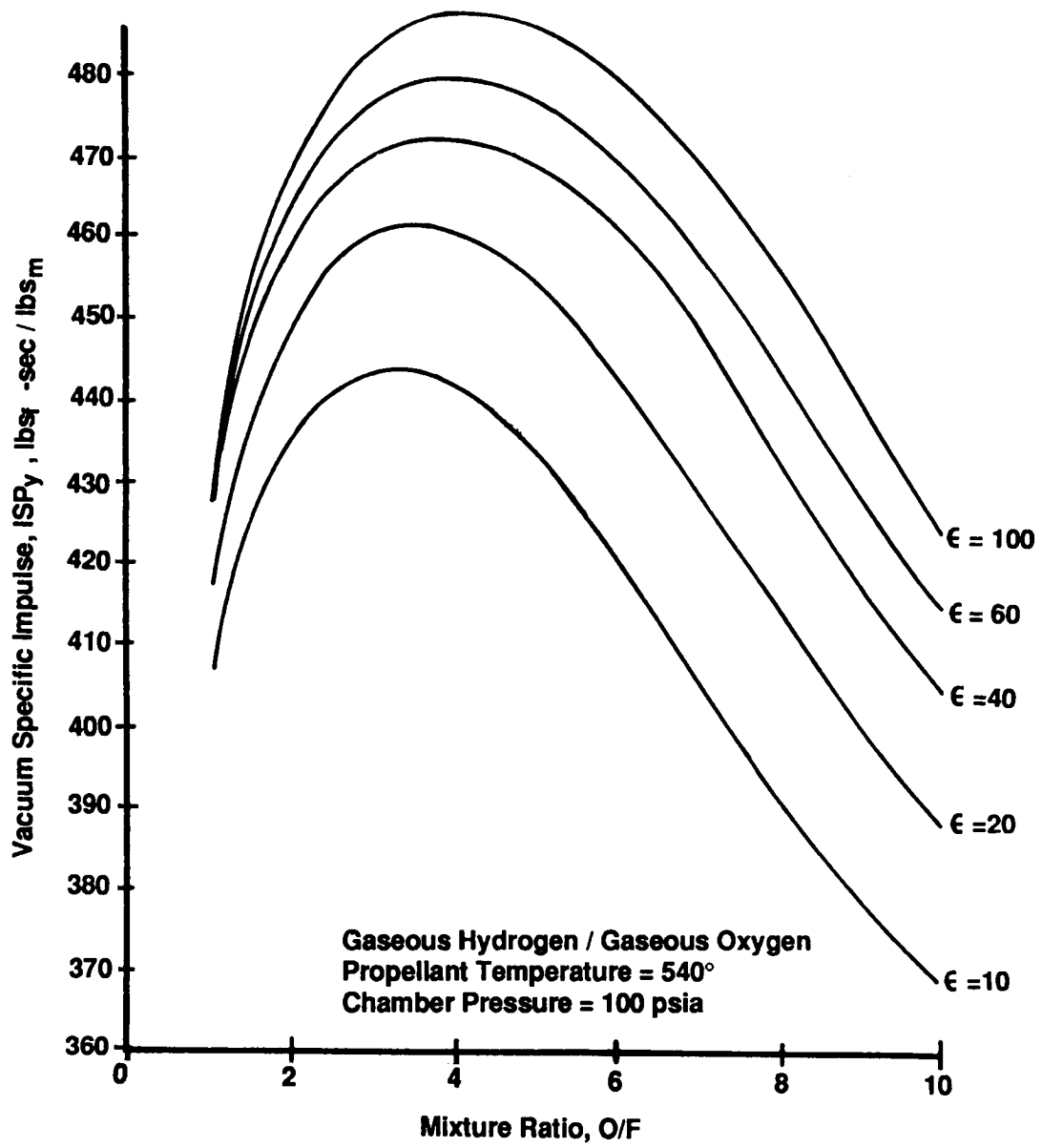


Figure 1. Vacuum Specific Impulse vs. Mixture Ratio ($P_c = 100$ psia)

TABLE I

DESIGN REQUIREMENTS FOR THRUSTER NO. 1

Propellants	GO₂/GH₂
Mixture Ratio, O/F	4.0 ± 1.0
Specific Impulse, ISP	≥ 400 lbf-sec/lbm
Fuel Inlet Temperature, TFI	200° - 530°R
Oxidizer Inlet Temperature, TOI	300° - 530°R
Total Impulse, I_{tot}	2.0 x 10⁶ lbf-sec
Minimum Impulse Bit, I_{bit}	2.0 lbf-sec

TABLE II

DESIGN REQUIREMENTS FOR THRUSTER NO. 2

Propellants	GO ₂ /GH ₂
Mixture Ratio, O/F	8.0
Thrust, F	25.0 lbf
Specific Impulse, ISP	346 lbf-sec/lbm*
Fuel Inlet Temperature, TFI	200° - 530°R
Oxidizer Inlet Temperature, TOI	300° - 530°R
Total Impulse, I _{tot}	6.0 x 10 ⁶ lbf-sec
Minimum Impulse Bit, I _{bit}	2.0 lbf-sec
Throttling, % of Nominal P _c	50% - 125%

*Minimum specific impulse (Isp) required for an expansion area ratio (ϵ) of 30:1. An Isp of 346 lbf-sec/lbm at $\epsilon = 30$ would ensure an Isp of 380 lbf-sec/lbm at $\epsilon = 100$.

III. SPACE STATION THRUSTER NO. 1

A. DESIGN APPROACH

1. Design Background

Several programs^{1,2,3} conducted by Aerojet for NASA in the early 1970's provided the basis for the current thruster design, namely a proven spark torch igniter. This igniter concept utilized two-stage ignition, as shown in Figure 2. The first stage injected a small portion (10%) of the fuel into all of the oxidizer that flowed around the spark plug tip and ignited at Point ① of Figure 2. This oxidizer-rich (O/F = 50) mixture flowed down the center (Point ②) of a sleeve insert which was regeneratively cooled with the remaining (90%) of the fuel. At Point ③, the balance of the fuel was injected into the oxidizer-rich core, resulting in a fuel-rich (O/F = 2.0) torch at Point ④ which, in turn, ignited the main injector. This igniter design was demonstrated with GO₂/GH₂ in more than 100,000 firings over a mixture ratio range of 2 to about 250 and inlet temperatures from normal boiling point to ambient.

Aerojet suspected that the igniter, used in these programs involving larger thrusters, could be operated continuously with a small regeneratively cooled chamber to meet the requirements of a small (25-lbf) O₂/H₂ thruster. This concept was designated the integral igniter injector with regeneratively cooled thrust chamber, i.e., I³-Regen, and was demonstrated in a program in the early 1980's. A residual igniter from the 1970's programs was used as the injector for both radiation and regeneratively cooled thrusters developed by Aerojet in a program⁴ sponsored by the Jet Propulsion Laboratory (JPL). The JPL test results served as the starting point for the NASA LeRC Space Station thruster design.

2. Design Concept

The assembly for Thruster No. 1, as shown in the cutaway of Figure 3, consists of a combination (integral) igniter injector, a regeneratively cooled thrust chamber, fuel balancing orifices and a sleeve insert at the chamber forward end. Integral, directly-actuated poppet-type valves control the flow of propellants to the thruster. Fuel is first used to regeneratively cool the thrust chamber, flowing counter to the combustion gases. As the fuel exits the chamber coolant channels at the forward end, it is collected in an annular manifold formed at the interface between the integral igniter injector and the thrust chamber. This annular manifold feeds two sets of radial flow passages. One set of passages supplies hydrogen to the injector where it impinges radially on the axial flow of spark-energized oxygen, causing ignition in the

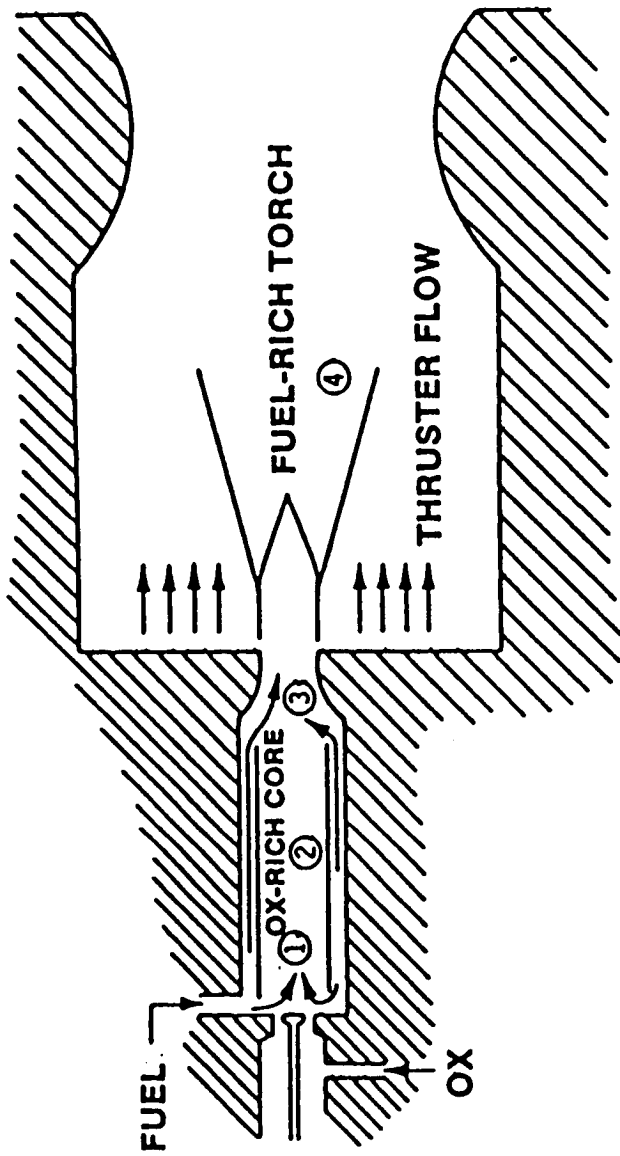


Figure 2. Proven Spark Torch Igniter Concept

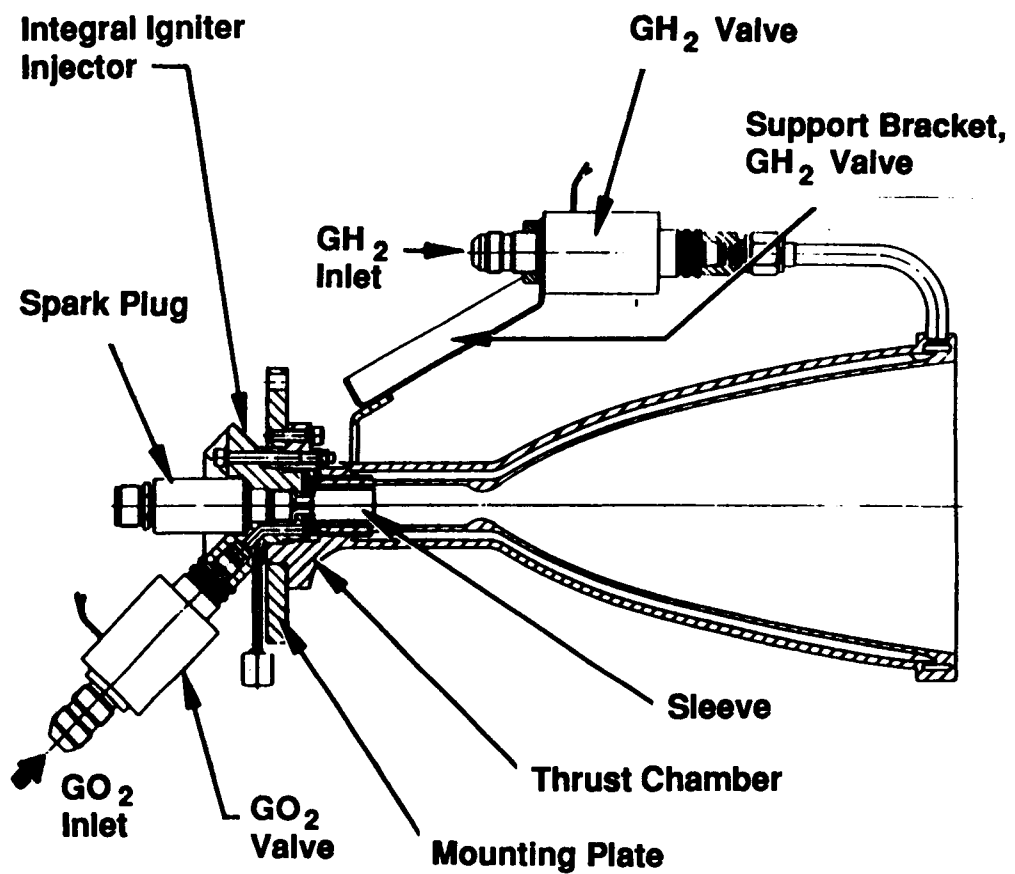


Figure 3. Cutaway of Thruster No.1 Assembly

III, A, Design Approach (cont.)

oxidizer-rich core. For an overall mixture ratio of four (4.0), the core O/F is 16.0. The second set of radial flow passages meters the remainder of the hydrogen into axially-slotted passages on the outer surface of the sleeve insert. This hydrogen is injected axially as film or barrier cooling along the inner wall of the thrust chamber. The film coolant and injector core streams progressively mix as the core flow is entrained into the film coolant stream, achieving the nominal overall O/F of 4.0.

3. Design Point

The design point for Thruster No. 1, based on the original contract requirements, is presented in Table III. Evolution of the Space Station APS requirements to be synergistic with water electrolysis occurred subsequent to the establishment and implementation of this design point.

B. DESIGN ANALYSIS

1. Ignition Analysis

An extensive data base and analytical/design capability have been established for spark-initiated igniters highlighted by the curves in Figures 4, 5, and 6^{1,2}. These curves define the ignition/no ignition boundaries for high pressure, low pressure, and minimum energy limits, as illustrated in Figure 7. Based on this extensive data base, the spark igniter operating characteristics for Thruster No. 1 are as indicated in Table IV.

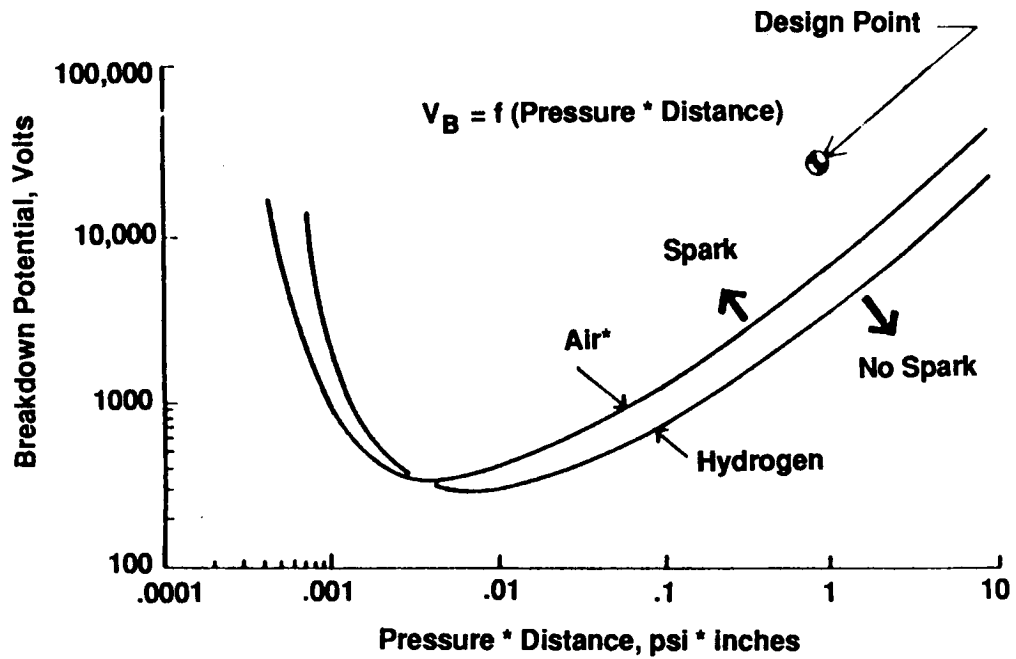
2. Thermal Analysis

Optimum thruster performance occurred with 60 percent fuel film cooling (FFC), as indicated by the JPL performance data of Figure 8; however, since the thruster sleeve cooling was predicted to be marginal at 60 percent fuel film cooling, 75 percent fuel film cooling was selected for the thruster baseline design.

A thermal model of the thruster was developed with the computer code HOCOOL^{6,7} which was used for determining coolant requirements and for predicting thermal response of rocket thrust chambers, specifically those with hydrogen film and regenerative cooling. HOCOOL required the input of two empirical constants: the heat transfer correlation

TABLE III**THRUSTER NO. 1 DESIGN POINT**

Thrust, F-lbf	25
Chamber Pressure, P_c -psia	75
% FFC	75
Overall Mixture Ratio, MR	4.0 ± 1.0
Core Mixture Ratio, MR_{core}	16.0 ± 4.0
Fuel Inlet Temperature, TFI-°R	200 - 530
Oxidizer Inlet Temperature, TOI-°R	300 - 530
Throat Diameter, D_T -in.	.500
Chamber Diameter, D_C -in.	.750
Contraction Area Ratio, ϵ_c	2.25
Expansion Area Ratio, ϵ	100
Chamber Length, L' , in.	1.925



*Air is assumed to Behave Like Oxygen

Figure 4. Paschen's Law Curve for Air*

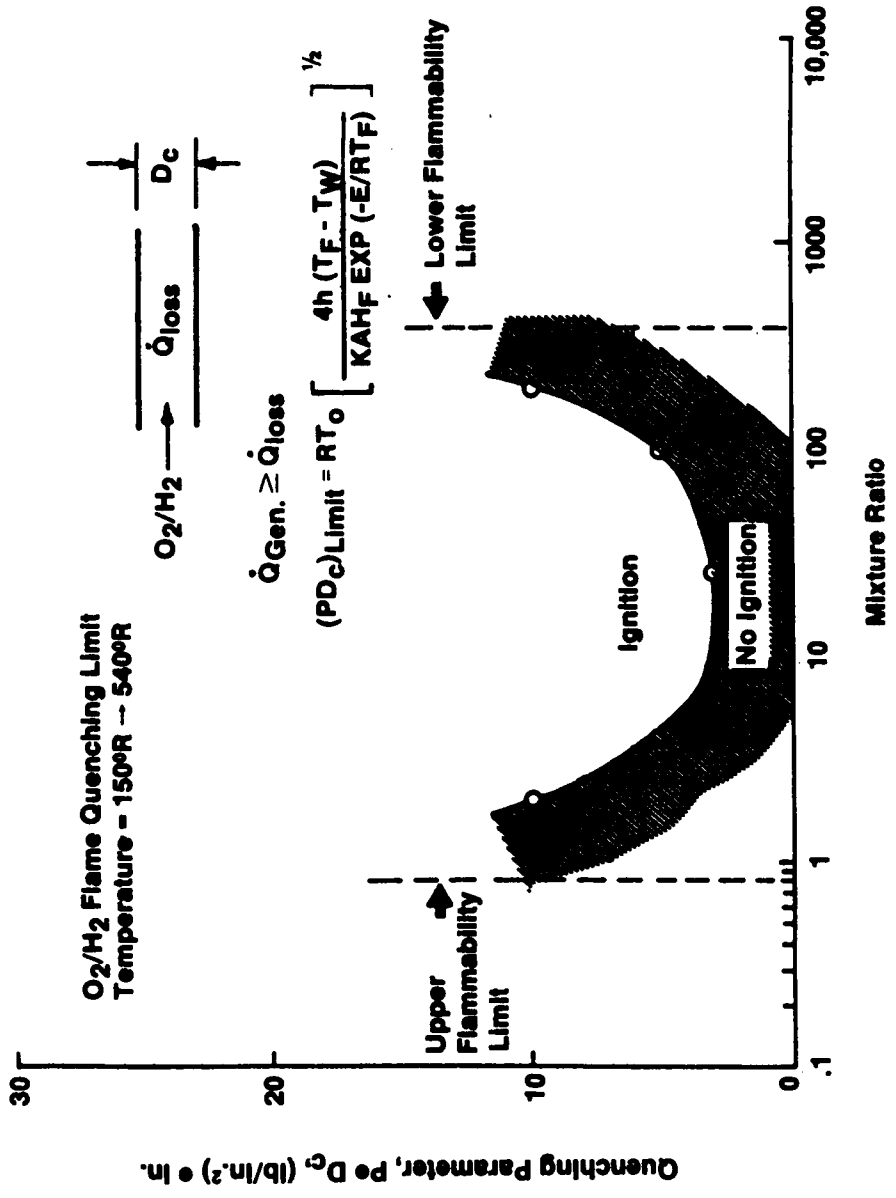


Figure 5. Flame Quenching Limit for O₂ /H₂

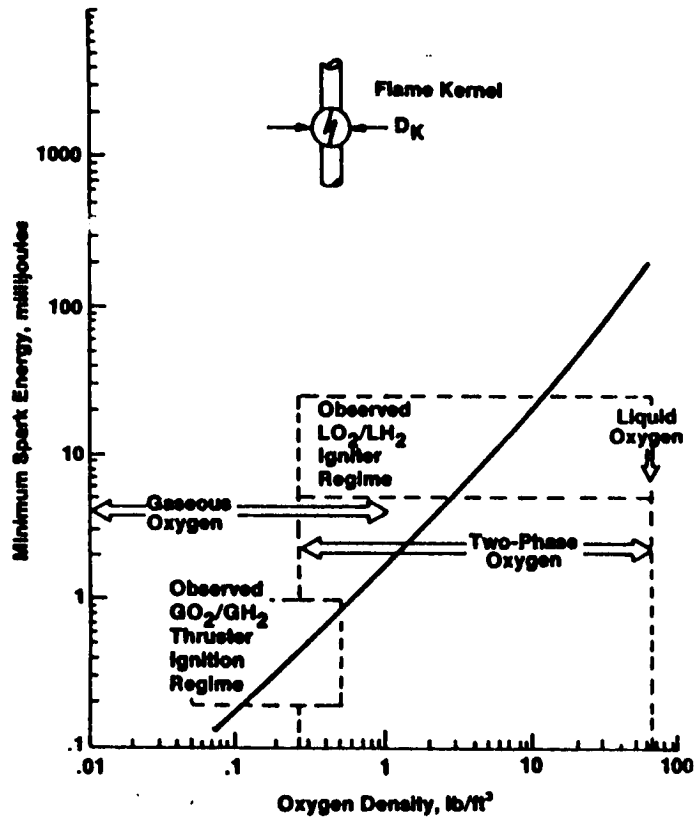


Figure 6. Minimum Spark Energy Requirements for O₂ /H₂ Propellants

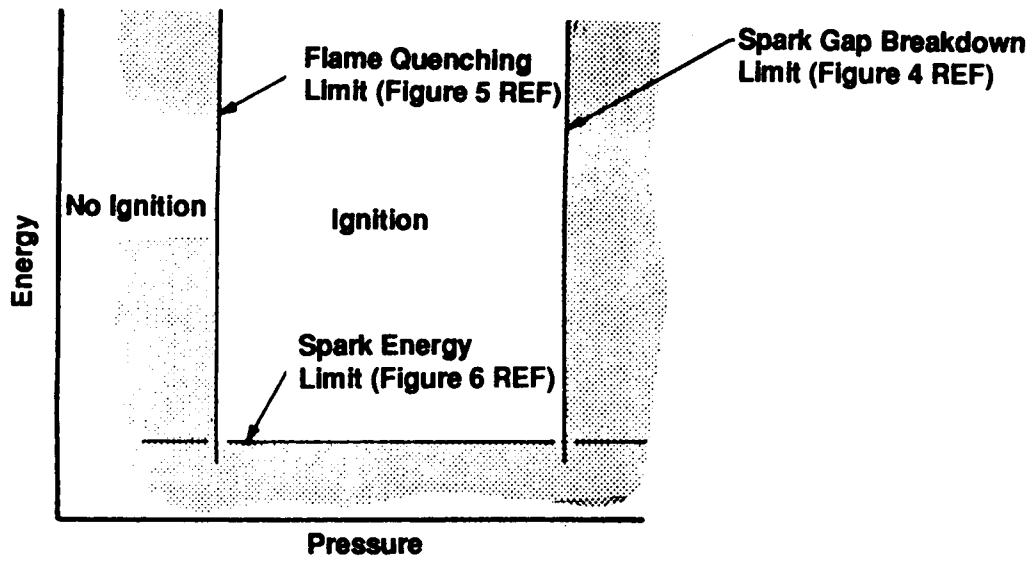


Figure 7. Spark Ignition limits: High Pressure, Low Pressure, Minimum Energy Limits

TABLE IV

SPACE STATION THRUSTER NO. 1
SPARK IGNITER OPERATING CHARACTERISTICS

Spark Igniter Energy, mJ	10 min
Spark Rate, SPS (Hz)	300
Spark Gap, in.	0.050
Igniter Sleeve I.D., in.	0.575
Breakdown Potential, Volts	30,000 min.
Minimum Ignition Pressure, psia	9
Maximum Ignition Pressure, psia	110
Predicted Nominal Cold Flow Pressure, psia	22

REF. 5 Data

O/F = 2.8 to 3.0

Pc = 30 psia

Tox T_F = 75°F

ℓ = 100 : 1

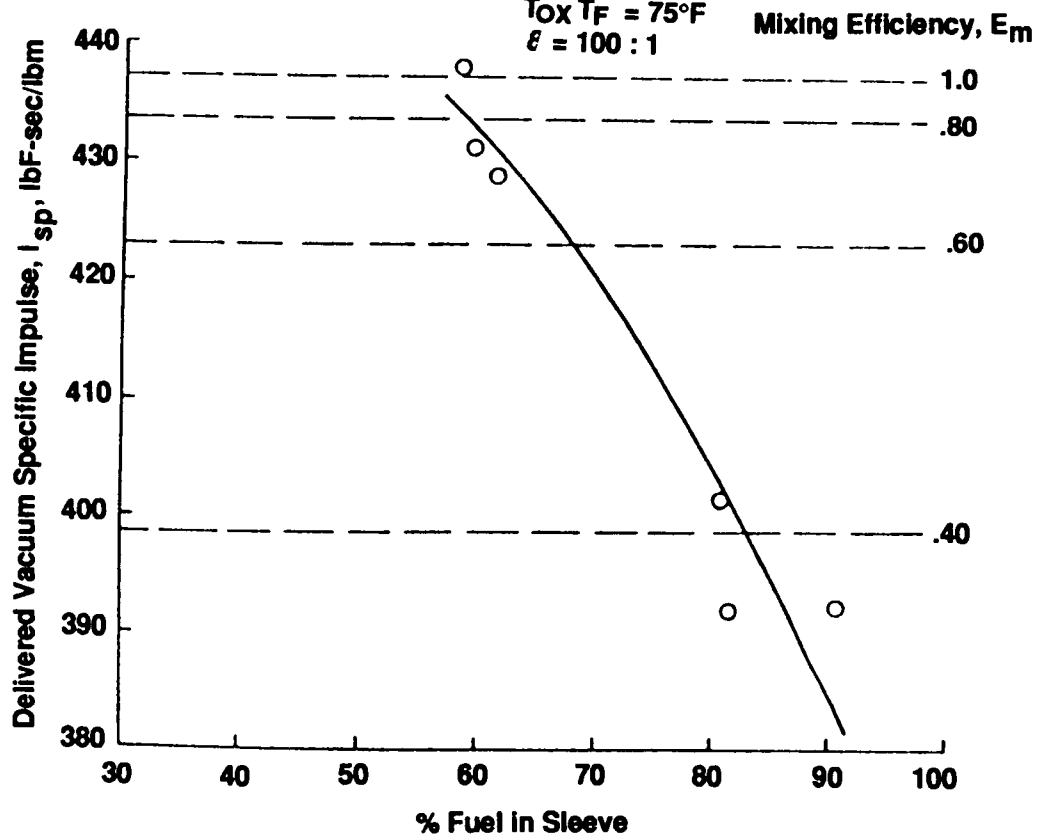


Figure 8. Experimentally Determined Effect of Fuel Film Coolant on Specific Impulse and Mixing Efficiency

III, B, Design Analysis (cont.)

coefficient, C_{g_n} , and the entrainment fraction, KSO. The first constant, C_{g_n} , modified the classical Bartz heat transfer coefficient to account for flow acceleration effects and injector characteristics on chamber heat transfer.

The entrainment model of HOCOOL utilized a two stream tube mixing model. In this model, the core gases from the main injector were considered to be entrained by and to mix with the film coolant. This mixing layer comprised one of the stream tubes. The other stream tube was the mixed oxidizer-rich core of combustion gases. The rate of entrainment of the core gases into the mixing layer was defined by the entrainment fraction, KSO.

The C_{g_n} profile and the entrainment fraction were based on the JPL thruster test program. During this program, a thin-walled 100:1 area ratio rhenium thruster was fired over a range of chamber pressure from 30 to 190 psia and mixture ratios from 2.0 to 3.4. Analysis of thermocouple data defined the C_{g_n} and the adiabatic wall temperature profiles, the latter of which determines the entrainment fraction.

a. C_{g_n} and Adiabatic Wall Temperature Profiles

By performing transient wall analyses with a one-dimensional heat conduction code, thermocouple transients from the test data were matched to determine heat transfer coefficients and adiabatic wall temperatures. Figure 9 presents a typical match between the transient data and computer code calculations. Very good agreement was obtained. The heat transfer coefficients determined with the conduction code have been correlated to the Bartz coefficient for non-reactive turbulent flow. The convergent section C_{g_n} profile resulting from this correlation is shown in Figure 10.

Possible flow relaminarization in the convergent section may reduce the heat transfer coefficient due to the different functional dependence on Reynolds number as shown in Figure 11. The turbulent correlation was used for design purposes, thus providing a potential 30% design margin.

b. Entrainment Fraction

The entrainment fraction was inferred from the adiabatic wall temperature profiles. A typical comparison of the empirical adiabatic wall temperatures with HOCOOL calculations is shown in Figure 12. HOCOOL very accurately predicted the throat adiabatic wall

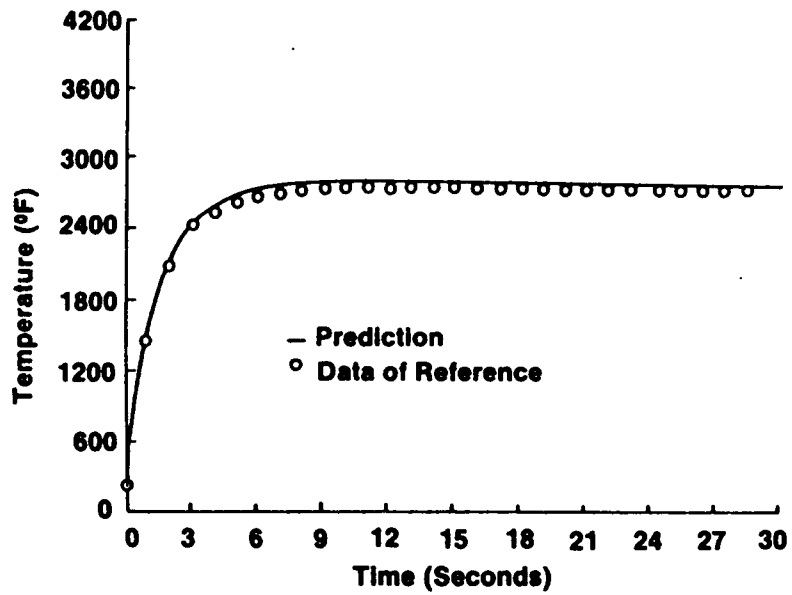


Figure 9. Typical Fit of Reference 5 Thermocouple Data with Conduction Code Prediction

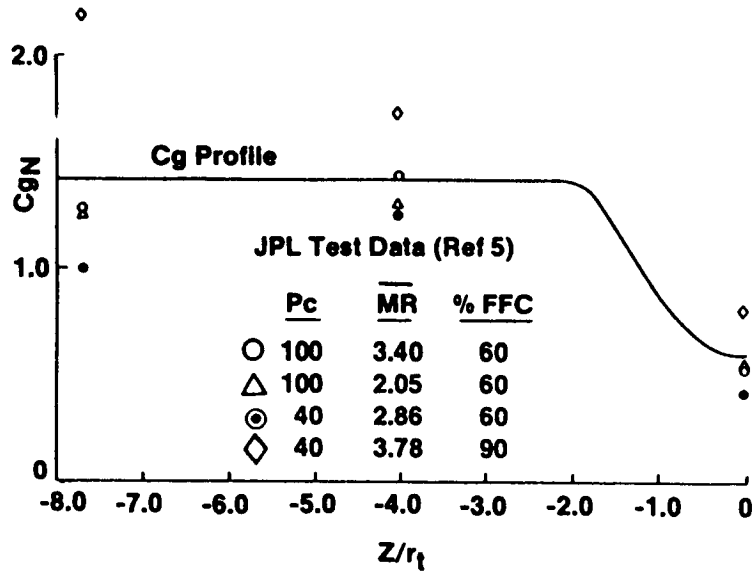


Figure 10. Space Station Thruster Convergent Section Cg Profile

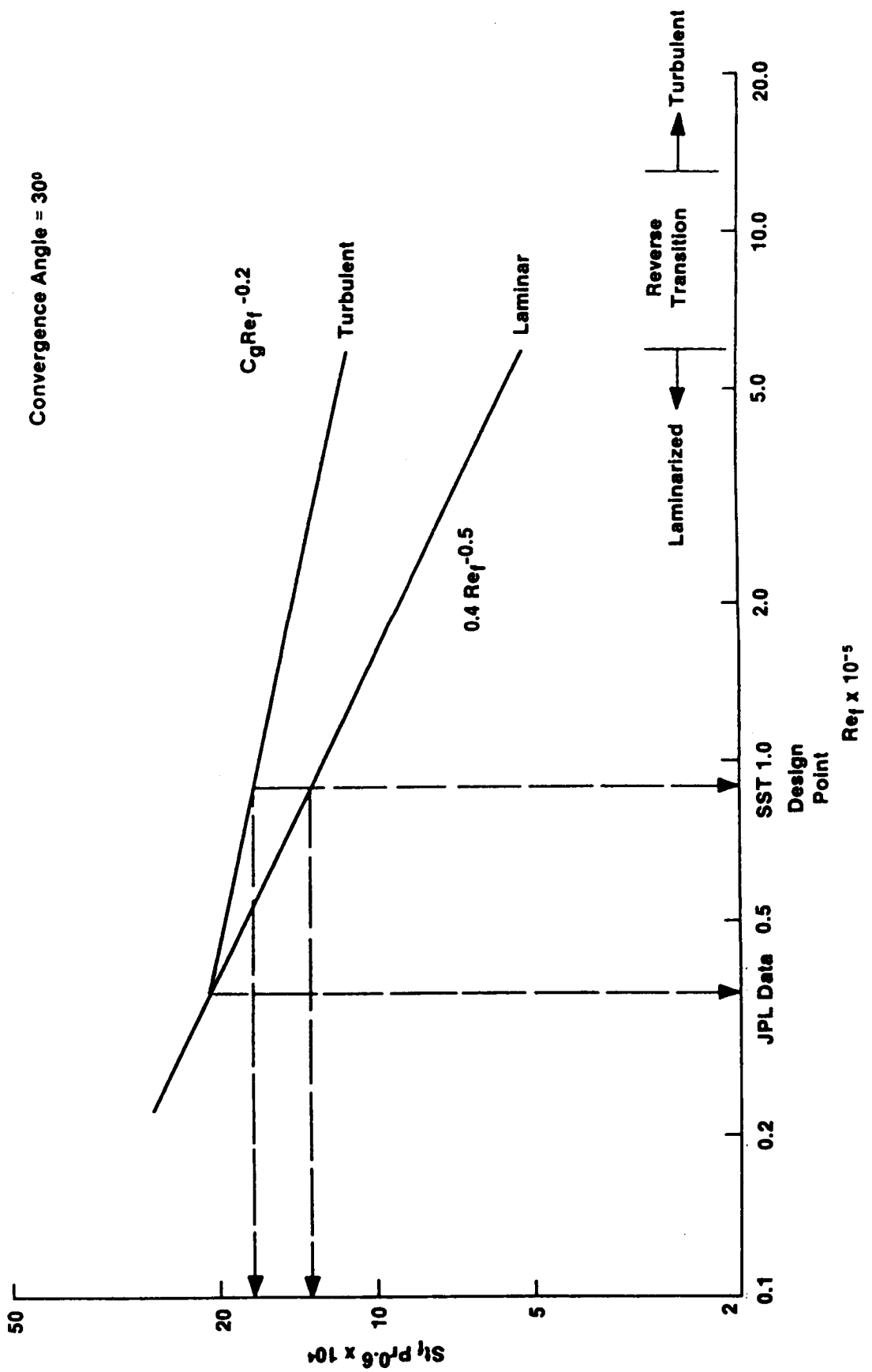


Figure 11. Comparison of Throat Heat Transfer with Turbulent and Laminar Correlations

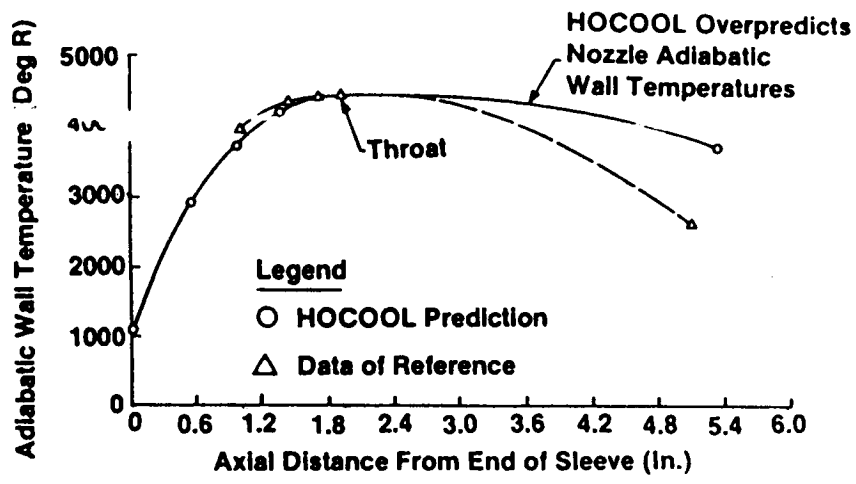


Figure 12. Comparison of Reference 5 Thruster Adiabatic Wall Temperature Profile with HOCOOL Prediction

III, B, Design Analysis (cont.)

temperature but somewhat over-predicted divergent nozzle temperatures. Appropriate modifications were made to the latter for design purposes.

3. Performance Analysis

Combustion performance of GO_2/GH_2 was evaluated parametrically over broad ranges of design points and operating conditions using the TDK and TBL computer programs^{8,9}. The results of these parametric studies were incorporated into a performance prediction model called ROCKET. To account for the impact of incomplete mixing, ROCKET utilized a mixing efficiency parameter, E_m ,¹⁰ which is defined for the simplified two stream tube flow characterization as follows:

$$E_m = \left\{ 1 - X_o \left[\frac{(O/F)_o - (O/F)}{1 + (O/F)_o} \right] - X_f \left[\frac{(O/F) - (O/F)_f}{(O/F)[1 + (O/F)_f]} \right] \right\}$$

where:

- $(O/F)_o$ = mixture ratio of oxidizer-rich stream tube
- $(O/F)_f$ = mixture ratio of fuel-rich stream tube
- X_o = mass fraction of oxidizer-rich stream tube
- X_f = mass fraction of fuel-rich stream tube

Performance predictions were based on thermal analysis of the JPL test data which characterizes the mixing between the core and the film coolant streams in terms of E_m values. Subsequent analysis using ROCKET and these E_m values determined the predicted specific impulse (I_{sp}) for the various operating points being evaluated. Figures 13 and 14 show the predicted E_m and I_{sp} values, respectively, as a function of overall mixture ratio. The predicted values in these two figures were for an injector energy release efficiency (ERE) of 100 percent, i.e., a perfect injector.

4. Chamber Life Analysis

The 2.0×10^6 lbf-sec impulse requirement equates to a total firing duration of 22.2 hours at a thrust of 25 lbf. During the 10-year design life, the actual duty cycle is expected to comprise about 500 deep thermal cycles and perhaps 100,000 impulse bits. The thruster will easily meet these requirements. The cycle life estimate is based on the Manson-Halford method of universal slopes.¹¹ The thermal strain in the chamber wall is determined at the point of

E_m vs MR

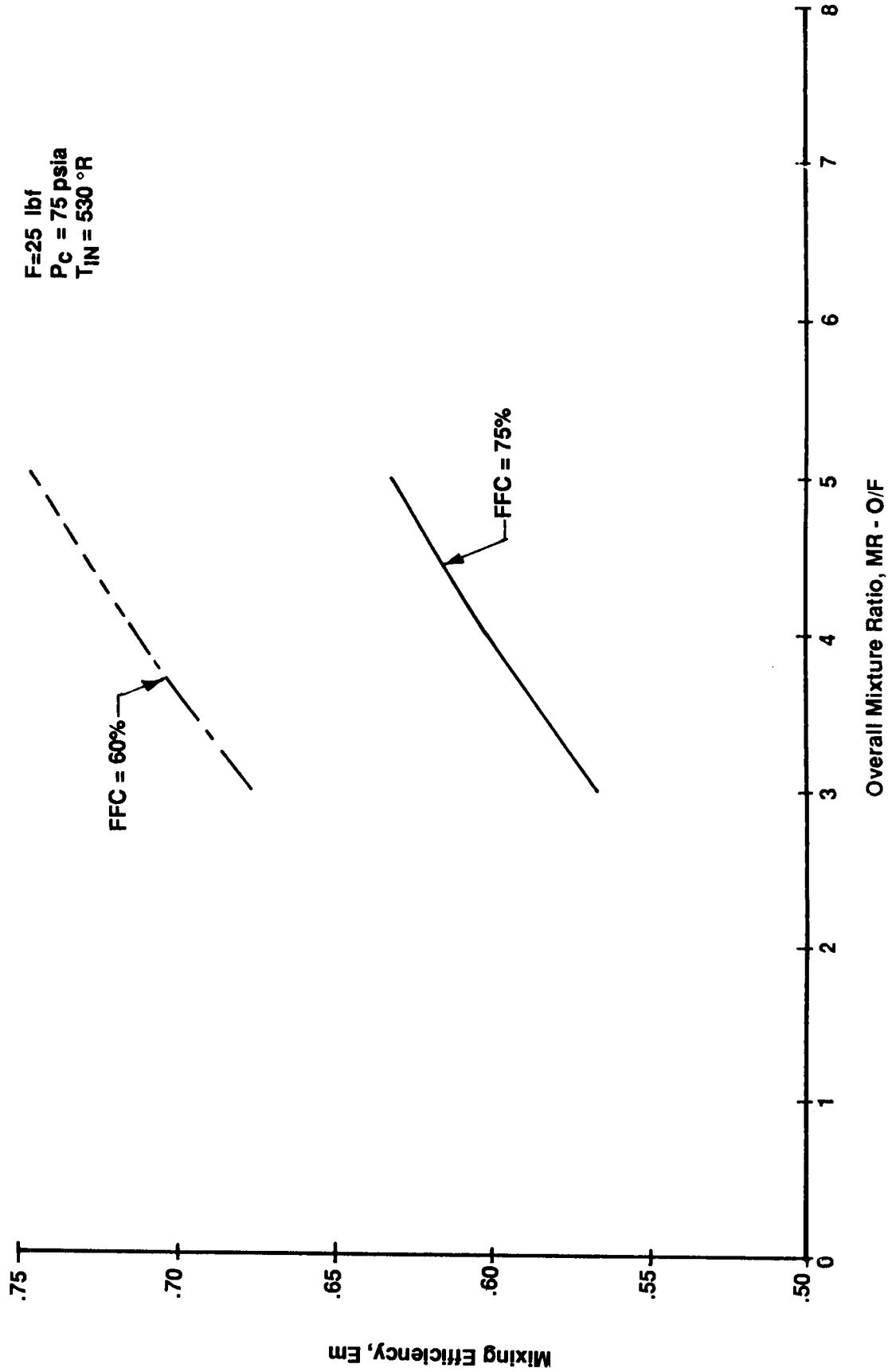


Figure 13. Predicted Mixing Efficiency, E_m , for Overall Mixture Ratio

Isp vs MR

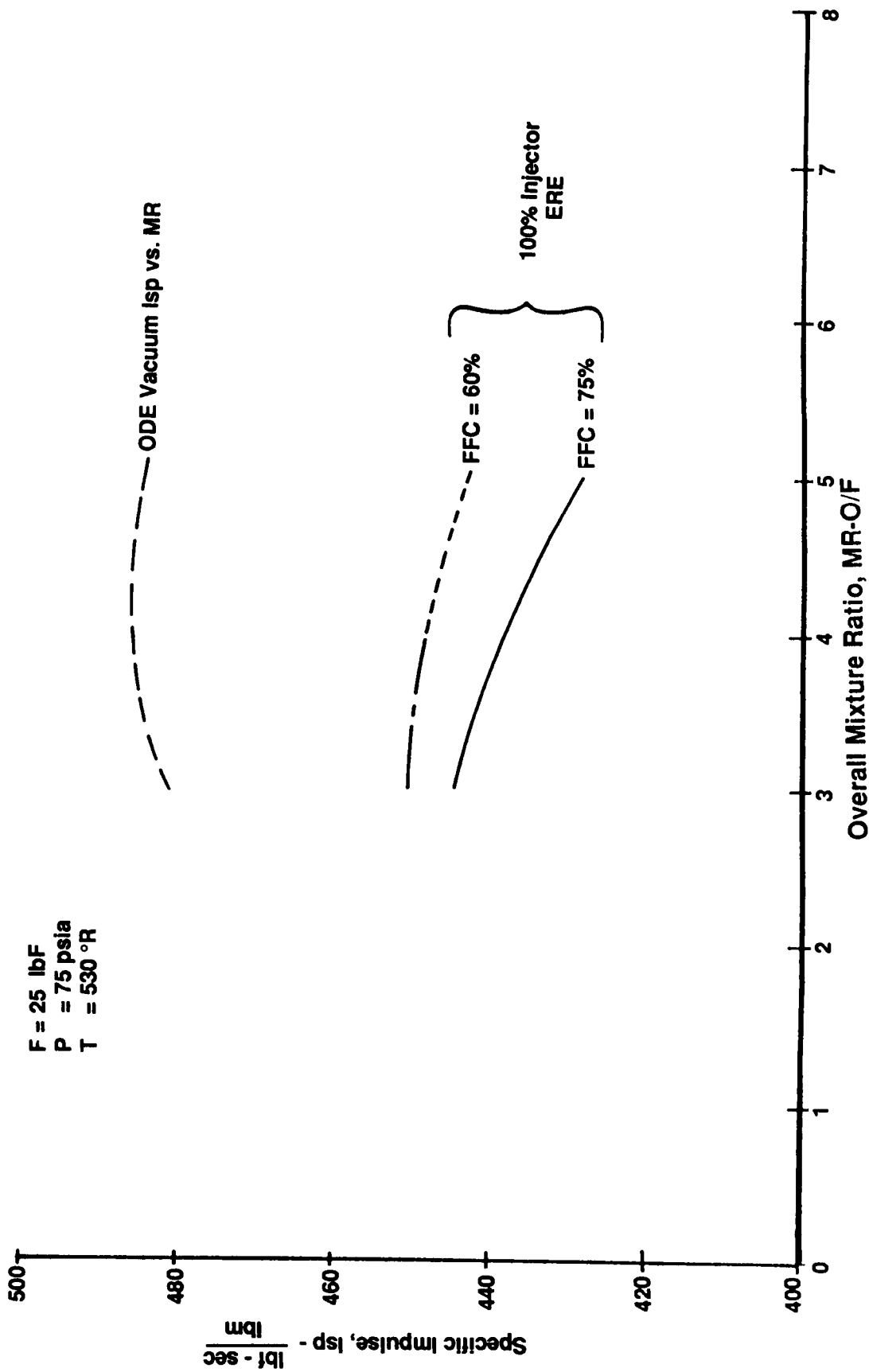


Figure 14. Predicted Performance for Overall Mixture Ratio

III, B, Design Analysis (cont.)

maximum gas side temperature, using finite element thermal and structural models. The calculated strain range is used, as shown in Figure 15, to obtain the predicted cycle life for a given temperature and time at temperature.

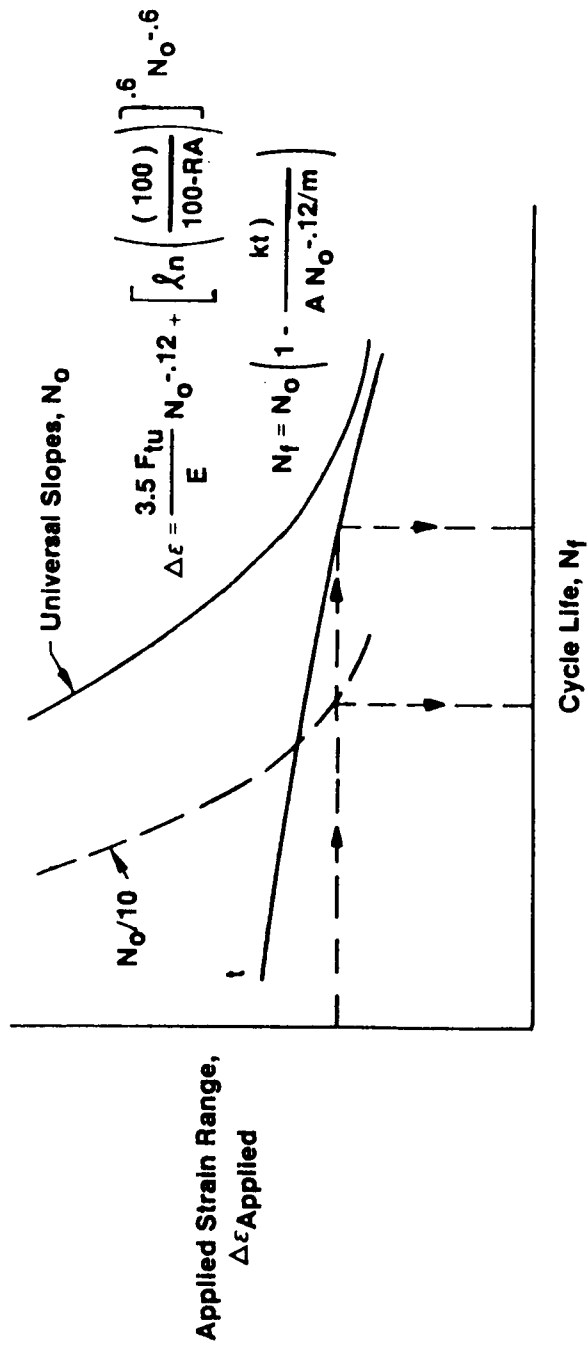
Chamber life for the thruster has been estimated to exceed 500 deep thermal cycles. About seventy deep thermal cycles have been demonstrated in test. Based on wall temperatures being lower than predicted, the updated life prediction is about 2000 deep thermal cycles. Impulse bit capability is effectively infinite because very little thermal strain is developed during short firings.

C. DESIGN DESCRIPTION AND FABRICATION

The thruster design consists of three major components: the thrust chamber, the sleeve insert, and the integral igniter injector. The thrust chamber is made of an axially slotted zirconium-copper liner that has an electroformed nickel (EFNi) outer jacket. The EFNi jacket closes out the 24 chamber coolant channels and provides structural support for the copper liner. The diverging section of the chamber is an optimized Rao contour with a potential flow expansion area ratio of 100:1. Figure 16 shows the machined chamber liner and Figure 17 shows the completed thrust chamber.

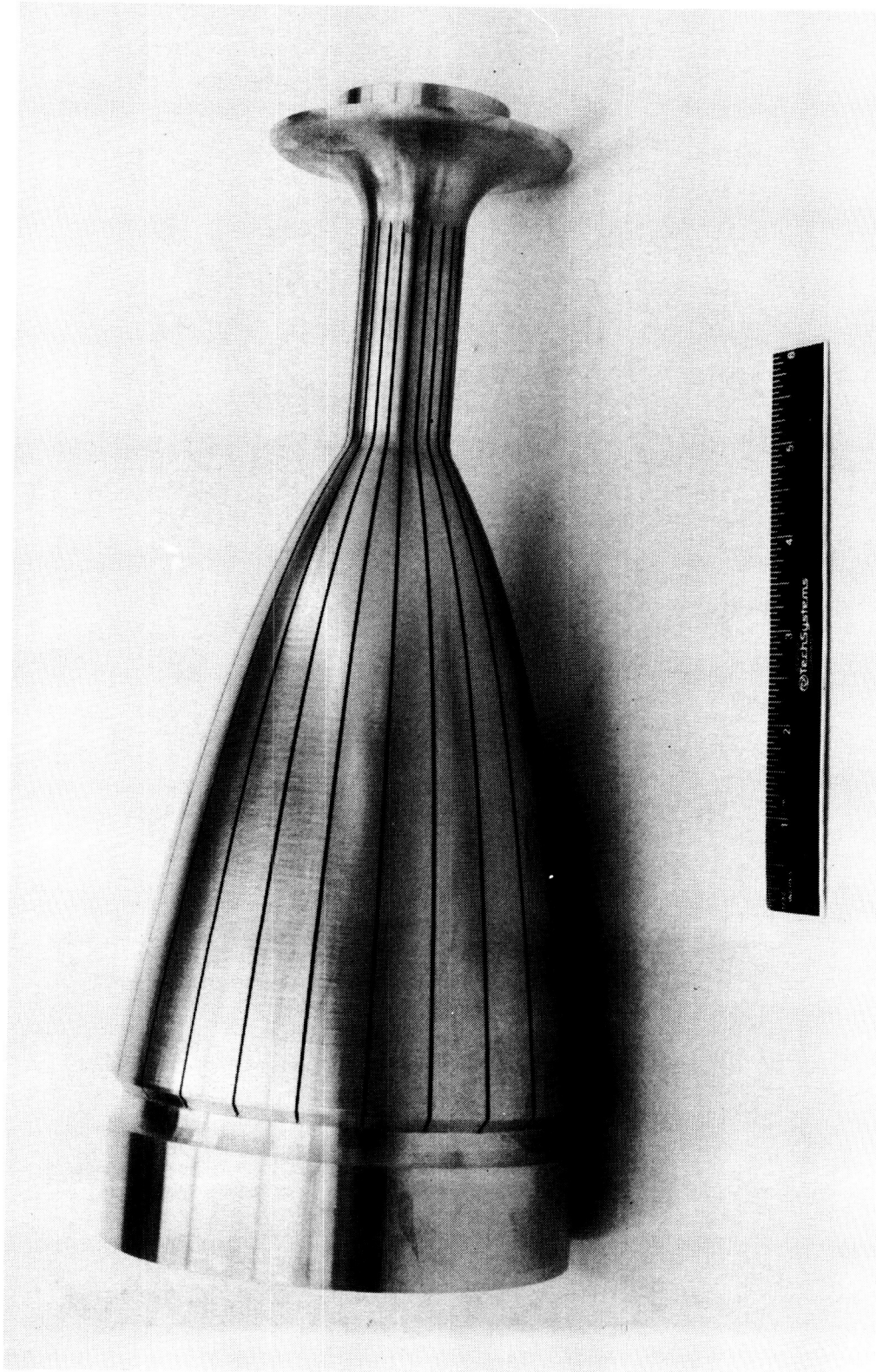
The sleeve insert, shown in Figure 18, is designed to fit into the forward end of the thrust chamber. Flow-balancing orifices divide the hydrogen flow, which exits the chamber coolant channels between the injector and the sleeve. The sleeve is made of nickel (Ni-200) and has 18 axial slots cut into the outer diameter for regenerative cooling and axial injection.

The integral igniter injector consists of a machined stainless steel igniter body and a nickel (Ni-200) platelet injector. Propellant distribution and metering occur within the photoetched flow passages of the individual injector platelets. These individual platelets are diffusion-bonded to form a homogeneous structure which becomes the injector. The injector is brazed to the igniter body to complete the assembly. Provisions are made within the igniter body to mount the spark plug, the chamber pressure transducer and the oxidizer valve. Both propellant valves mount directly onto the thruster. Figure 3 shows a cutaway of the thruster assembly with all of the thruster components identified.



Enter Curve at $\Delta\epsilon$ Applied and Define N_f as Minimum N_f from Cumulative Time Curve, t , or $N_0/10$, whichever is Less.

Figure 15. Manson-Halford Method of Universal Slopes for Low Cycle Fatigue



C1185 2790

Figure 16. Machined ZrCu Chamber Liner - Thruster No. 1

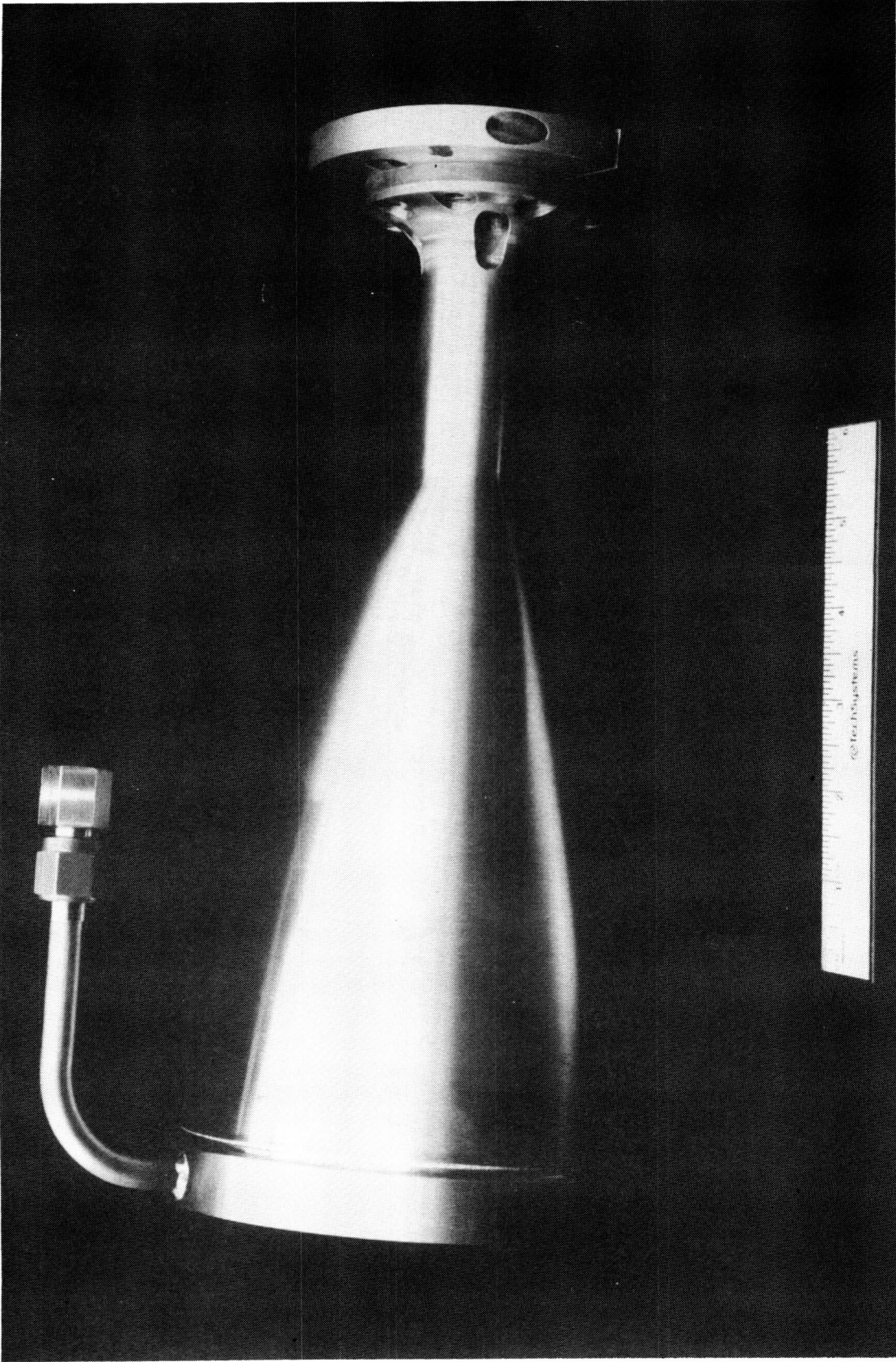
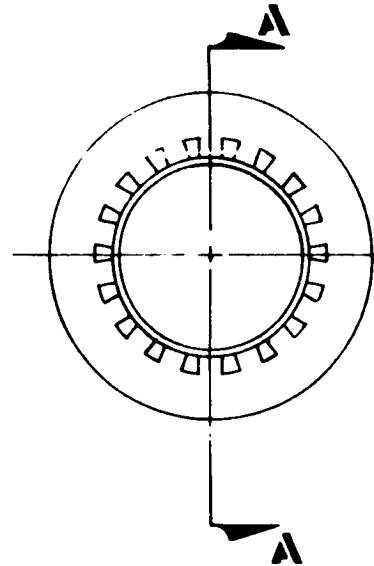
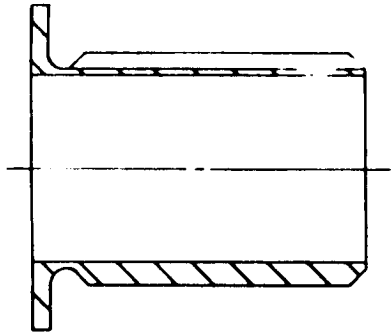


Figure 17. Completed Chamber Assembly - Thruster No. 1



SECTION A-A

Figure 18. Sleeve Insert

III, Space Station Thruster No. 1 (cont.)

D. TEST

1. Test Setup

The space station thruster was tested in the altitude test facility shown in Figure 19, which was equipped with a hardware test cell, an 11,000 cubic foot altitude chamber, and the necessary auxiliary instrumentation, controls, and data recording equipment. The thruster hardware mounted to a test stand designed to measure thrust, as shown in Figure 20. The thruster and stand were installed as a subassembly into the test cell, as shown in Figure 21, where the thruster nozzle was positioned to exhaust into a water-cooled diffuser linking the test cell with the altitude chamber. The diffuser maintained required cell pressure, and ensured that the thruster nozzle flowed full. Propellant supply lines were plumbed to the test cell from a standard GH_2 trailer and a 50 cubic foot, 6000 psi facility gaseous oxygen supply.

The altitude chamber was equipped with two two-stage pump units, each unit being composed of a first-stage reciprocating pump and a second-stage blower. These two units could pump at a combined rate of 4800 CFM to maintain a simulated altitude of 100,000 to 130,000 feet at a maximum continuous thrust of 25 lbf.

2. Instrumentation

The thruster test assembly was instrumented to measure thrust, propellant flowrates, inlet pressures and temperatures, coolant bulk temperature rise, thrust chamber pressure and chamber backside wall temperatures. There were 16 backside thermocouples, located in two rows located 180 degrees apart, the rows being designated "A" and "B." Each row had a thermocouple positioned at eight axial stations along the chamber, thus providing a temperature measurement (A or B) at each axial station, i.e., Station 1, Station 2, ... etc. These axial stations were located according to Figure 22, while the test instrumentation is summarized in Table V.

3. Test Summary

Thruster No. 1 was tested extensively, covering a broad range of mixture ratio (O/F) and percentage fuel film cooling (FFC). Tables VI and VII provide a summary of tests run with regard to O/F and percent FFC, respectively. The thruster was tested from an O/F of 2.2 to 8.1, far exceeding the design range of 3.0 to 5.0. Furthermore, testing covered percent FFC from

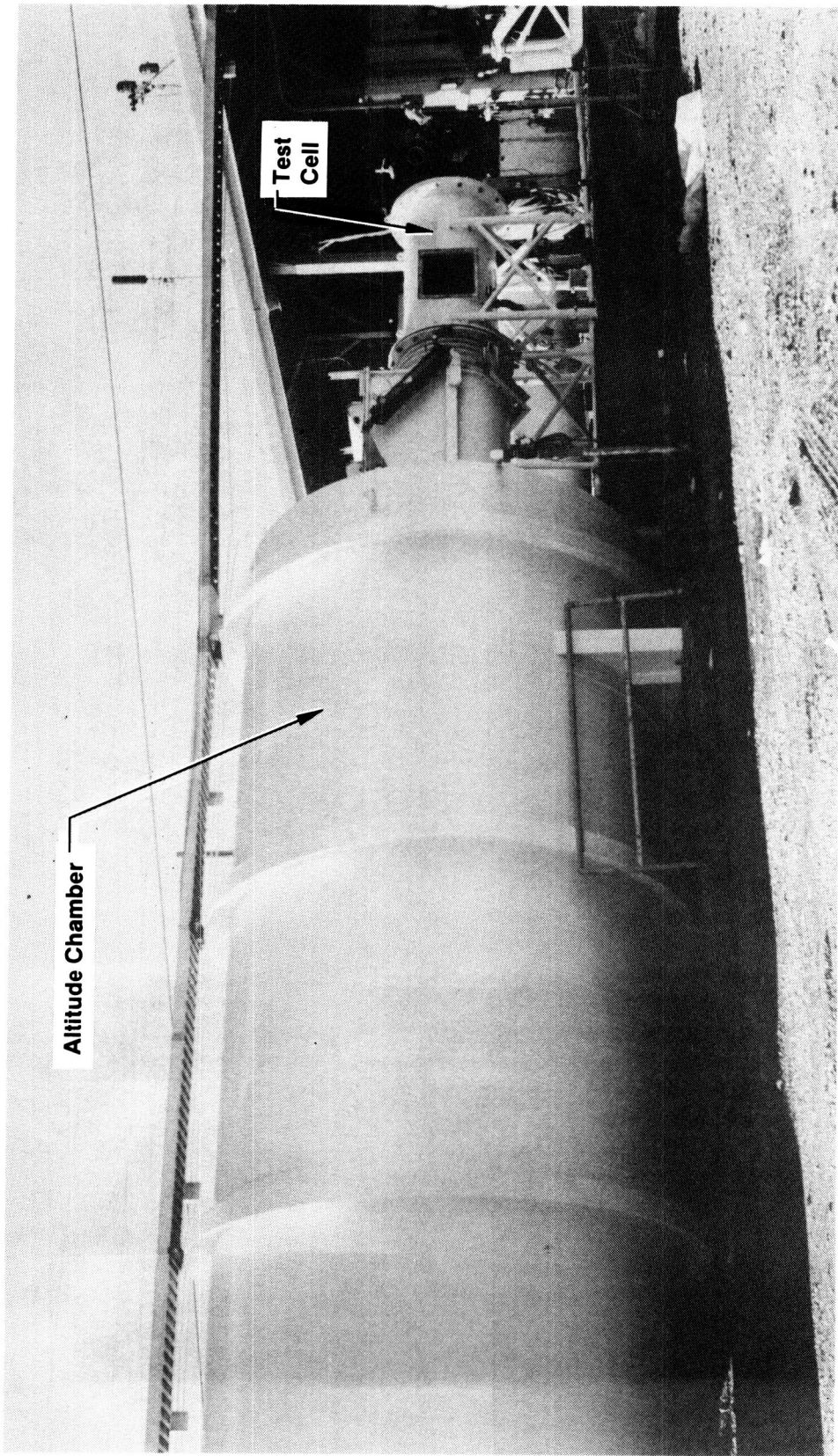


Figure 19. Aerojet Altitude Test Facility for Small Thrusters

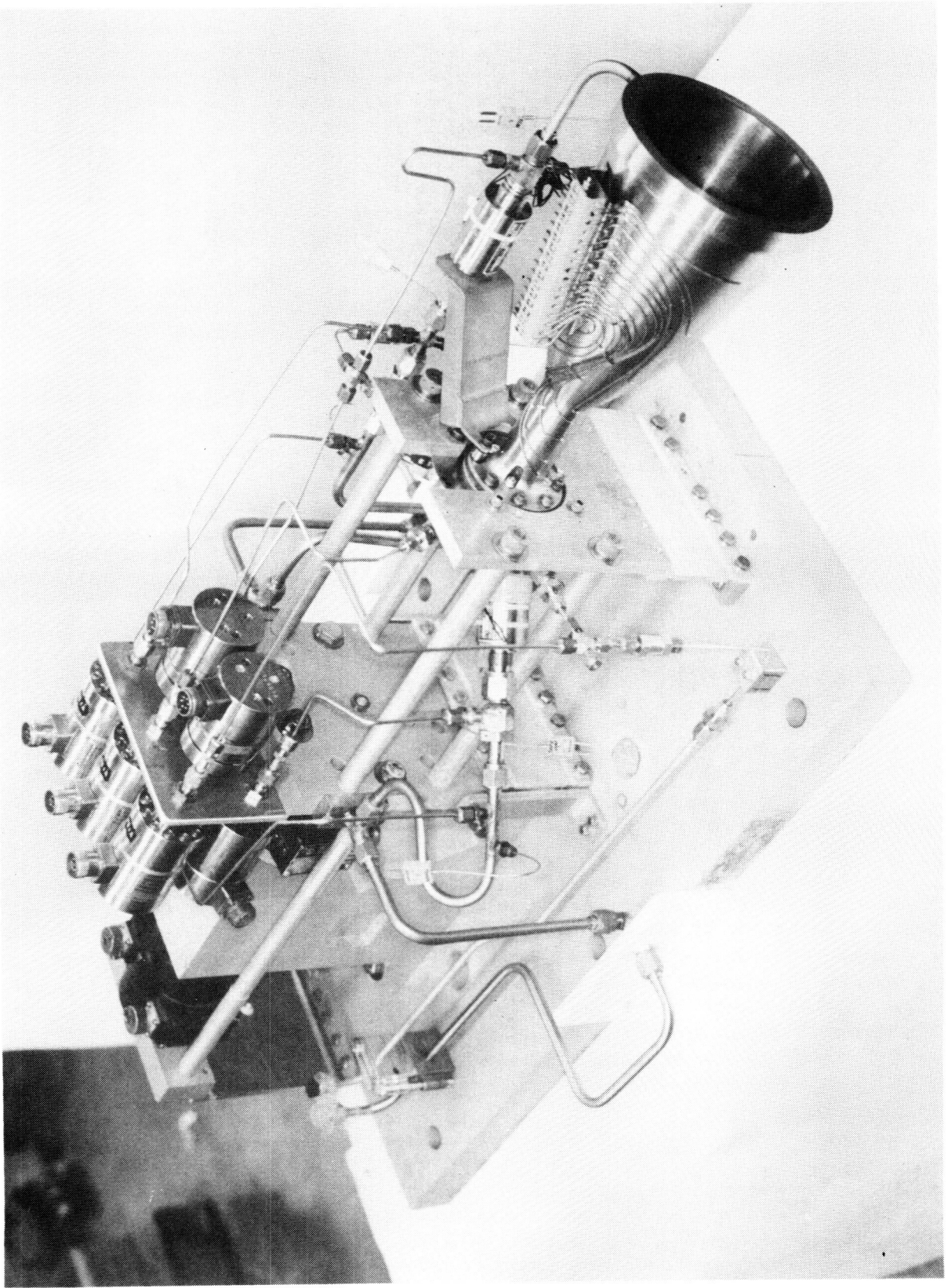


Figure 20. Thruster Mounted to the Thrust Measuring Test Stand

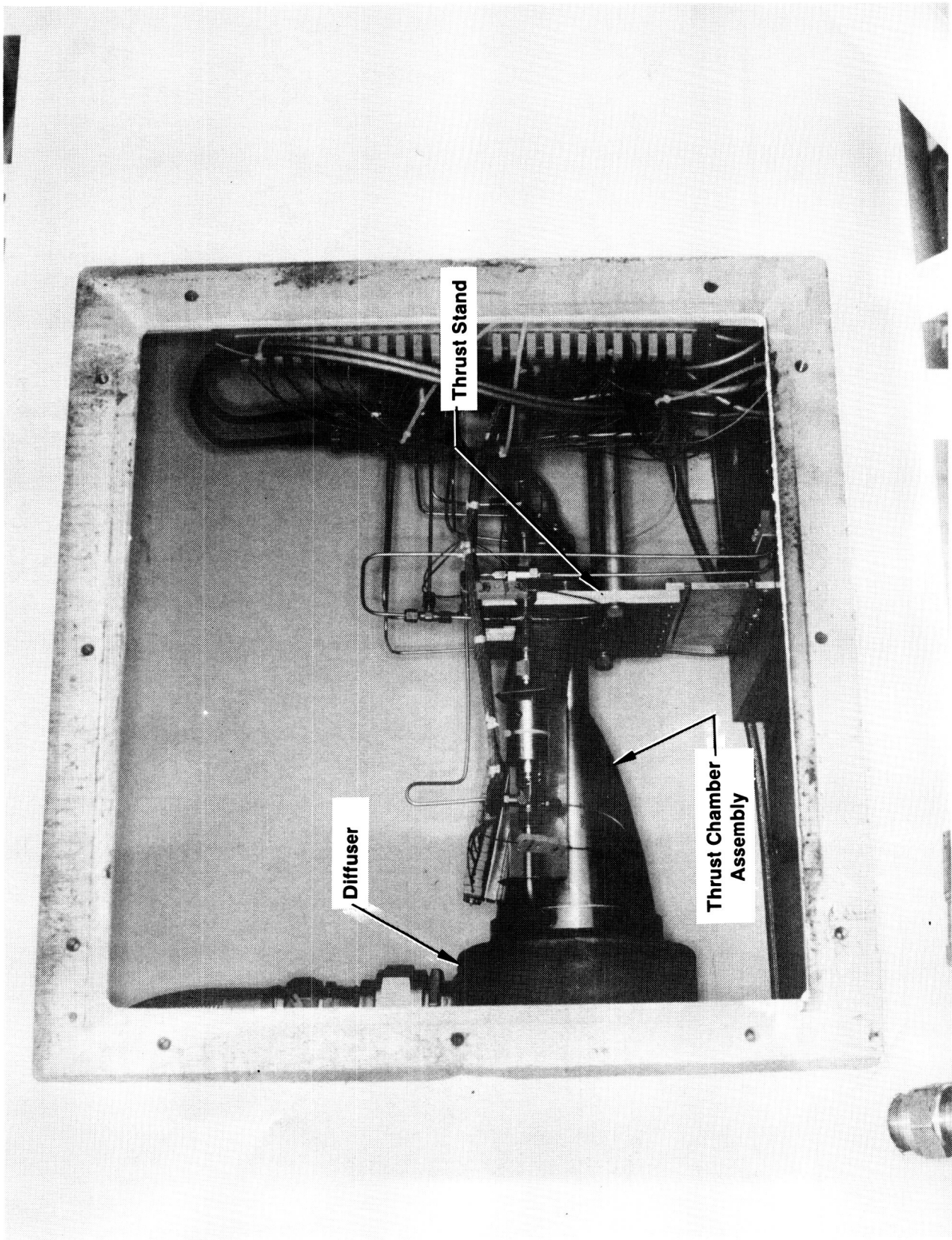


Figure 21. Test Cell with Mounted Test Stand

TC	x (in.)	z (in.)
TCA 1, TCB 1	1.10	-2.50
TCA 2, TCB 2	1.68	-1.92
TCA 3, TCB 3	2.50	-1.10
TCA 4, TCB 4	3.25	-0.35
TCA 5, TCB 5	3.60	0
TCA 6, TCB 6	5.90	2.30
TCA 7, TCB 7	8.30	4.70
TCA 8, TCB 8	10.65	7.05

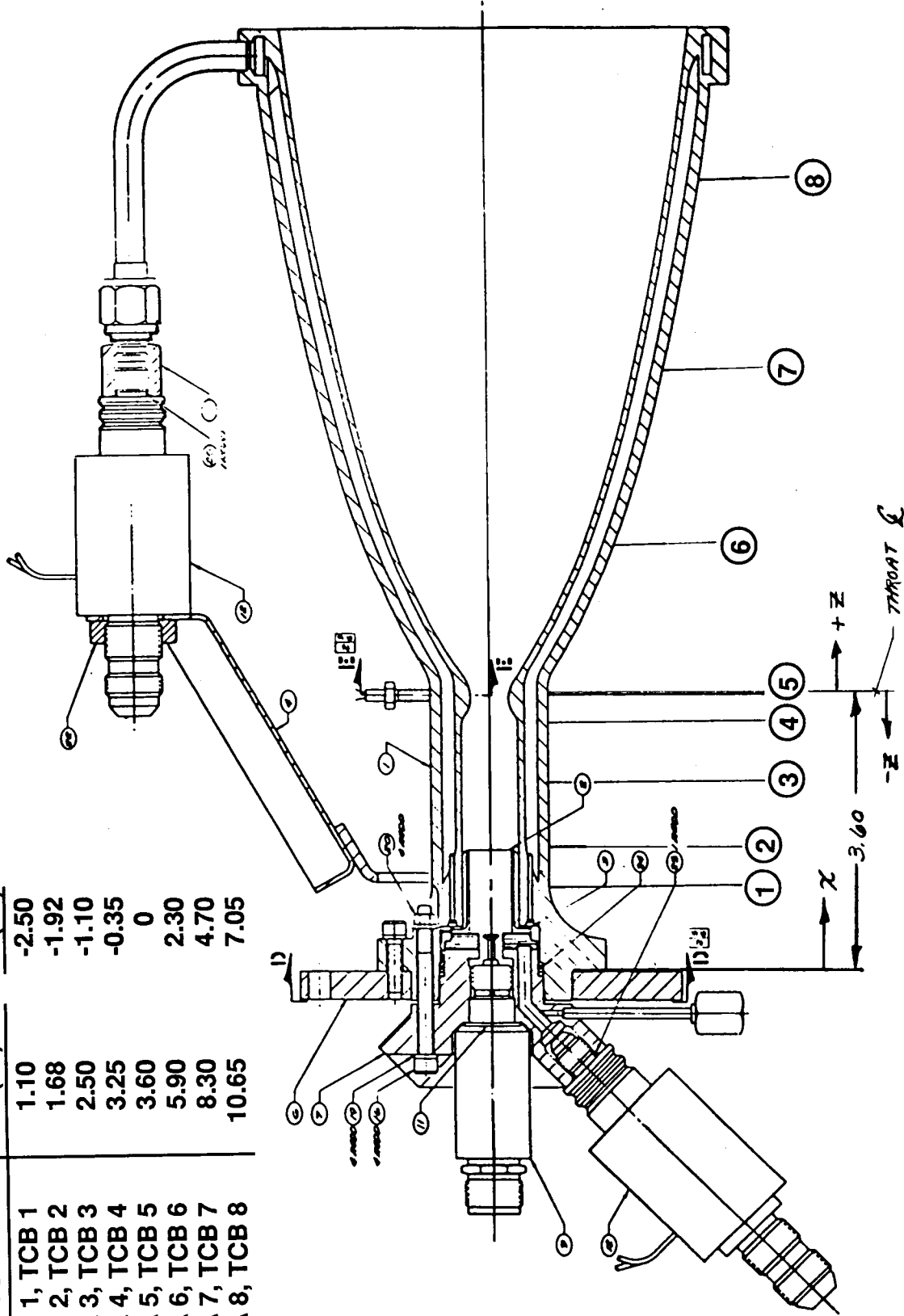


Figure 22. Chamber Thermocouple Location

TABLE V
 TEST INSTRUMENTATION
 SPACE STATION THRUSTER NO. 1

Parameter	Symbol	Range
<u>Pressure</u>		
Fuel Tank Pressure	PFT	As Required
Fuel Venturi Inlet Pressure	PFVI	As Required
Fuel Thrust Chamber Valve JN	PFTCVI	100 - 300 psia
Fuel Chamber Inlet Pressure	PFCI	80 - 200 psia
Oxidizer Tank Pressure	POT	As Required
Oxidizer Venturi Inlet Pressure	POVI	As Required
Oxidizer Thruster Chamber Valve Injector	POTCVI	100 - 300 psia
Oxidizer Injector Manifold	POJ	75 - 300 + psia
Chamber Pressure	PC	50 - 150 psia
Spark Plug Cavity Pressure	PSPC	50 - 150 psia
<u>Thrust</u>		
Measured Thrust, Bridge A	F _A	15 - 50 lbf
Measured Thrust, Bridge B	F _B	15 - 50 lbf
<u>Propellant Temperatures</u>		
Fuel Venturi Inlet Temperature	TFVI	32° - 2300°F
Fuel Chamber Inlet Temperature	TFCI	32° - 2300°F
Fuel Injector Manifold Temperature	TFJ	32° - 2300°F
Oxidizer Venturi Inlet Temperature	TOVI	32° - 2300°F
Igniter Body Temperature	TBIG	32° - 2300°F

TABLE V
TEST INSTRUMENTATION
SPACE STATION THRUSTER NO. 1
(Continued)

Parameter	Symbol	Range	Location, x (in.)
<u>Chamber Temperature</u>			
Forward Sleeve	TCA1;TCB1	32° - 2300°F	1.10
Sleeve Exit	TCA2;TCB2	32° - 2300°F	1.68
Mid-Barrel Section	TCA3;TCB3	32° - 2300°F	2.50
Convergent Section	TCA4;TCB4	32° - 2300°F	3.25
Throat	TCA5;TCB5	32° - 2300°F	3.60
Forward Divergent Section	TCA6;TCB6	32° - 2300°F	5.90
Middle Divergent Section	TCA7;TCB7	32° - 2300°F	8.30
Aft Divergent Section	TCA8;TC81	32° - 2300°F	10.65

TABLE VI

THRUSTER NO. 1 TEST SUMMARY FOR MIXTURE RATIO RANGE

<u>Mixture Ratio O/F</u>	<u>Total Duration (sec)</u>	<u>Total Impulse (lbf-sec)</u>
2	60	1,302
3	240	5,107
4	3,735	89,526
5	224	5,576
6	221	4,728
7	17,563	428,997
8	<u>155</u>	<u>3,221</u>
Total	22,198	538,457

TABLE VII

THRUSTER NO. 1 TEST SUMMARY FOR PERCENT FUEL FILM COOLING RANGE

Fuel Film Cooling (%)	Mixture Ratio (O/F)	Total Duration (sec)	Total Impulse (lbf-sec)
59	3	60	1,662
	4	980	26,221
	5	55	1,386
	6	19	456
64	3	60	1,602
	4	687	16,458
	5	72	1,749
74	4	1,547	35,949
	5	97	2,441
85	4	271	6,314
	7	17,219	420,063
	8	51	1,056
87	2	60	1,302
	4	120	2,184
	6	120	2,376
	8	66	1,332
88	6	60	1,314
	8	38	833
92	3	120	1,843
	4	130	2,400
	6	22	582
95	7	344	8,934
	Total	<u>22,198</u>	<u>538,457</u>

III, D, Test (cont.)

59 to 95. Appendix B contains a test log and reduced data of all the tests that were run for Thruster No. 1.

4. Experimental Results

The wide range of mixture ratio was incorporated into the test plan after completion of hardware fabrication to demonstrate the feasibility of successfully operating a thruster on the products of water electrolysis (O/F = 8.0). At the time, mission studies showed that additional hydrogen may be available from other sources, such that O/F capability from 4.0 to 8.0 was likely, with the average O/F falling between 4.5 and 5.2. Potentially, only 20 percent of the total impulse may be generated at an O/F of 8.0; nevertheless, most of the impulse (432,000 lbf-sec) for thruster No. 1 was obtained at mixture ratios from 7.0 to 8.0, with the longest firing duration being 2200 seconds at an O/F of 7.5. The thrust chamber showed absolutely no sign of any degradation from the testing.

Thermal data agree reasonably well with predicted values for the thruster design point, indicating that the thermal model was satisfactory. Measured and predicted backside wall temperature profiles were compared at a mixture ratio of 4.0 in Figures 23 and 24 for 60 and 75 percent fuel film cooling, respectively. An excellent correlation existed between predicted and measured values for the diverging section of the chamber. For the converging and cylindrical sections, it appeared that axial conduction averted the highs and lows predicted by the one-dimensional HOCOOL model. In Figures 23 and 24, the maximum measured backside temperature was within a few percent of the average predicted chamber values. Likewise, measured coolant bulk temperature rises were within 10 percent of predicted values.

Additional thermal data are given in Figures 25 and 26. Figure 25 shows maximum backside temperature variations with percent fuel film cooling. Maximum backside temperatures decreased linearly with increasing film cooling and appeared to be much more sensitive to mixture ratio. Figure 21 supported this conclusion of a stronger dependence on mixture ratio than on film cooling. The high mixture ratio (7 to 8) tests were also indicated in Figures 25 and 26, where it was apparent that the wall temperatures were high at these off-design operating points.

The igniter body, oxidizer valve body and thruster mounting plate temperatures were also monitored during testing, never exceeding values of 200°F, 75°F, and 250°F, respectively. These values were maintained regardless of operating point or test duration, even for the

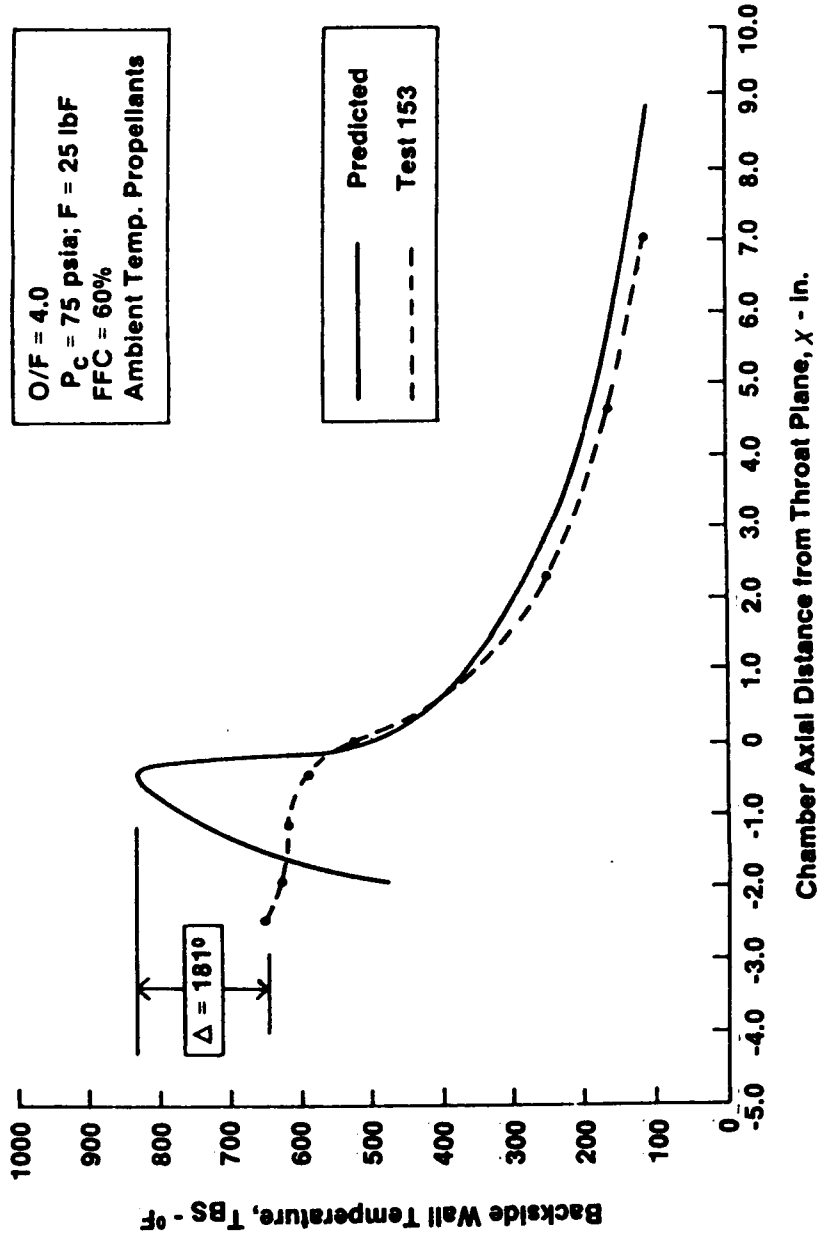


Figure 23. Backside Temperature Profile with 60 Percent FFC

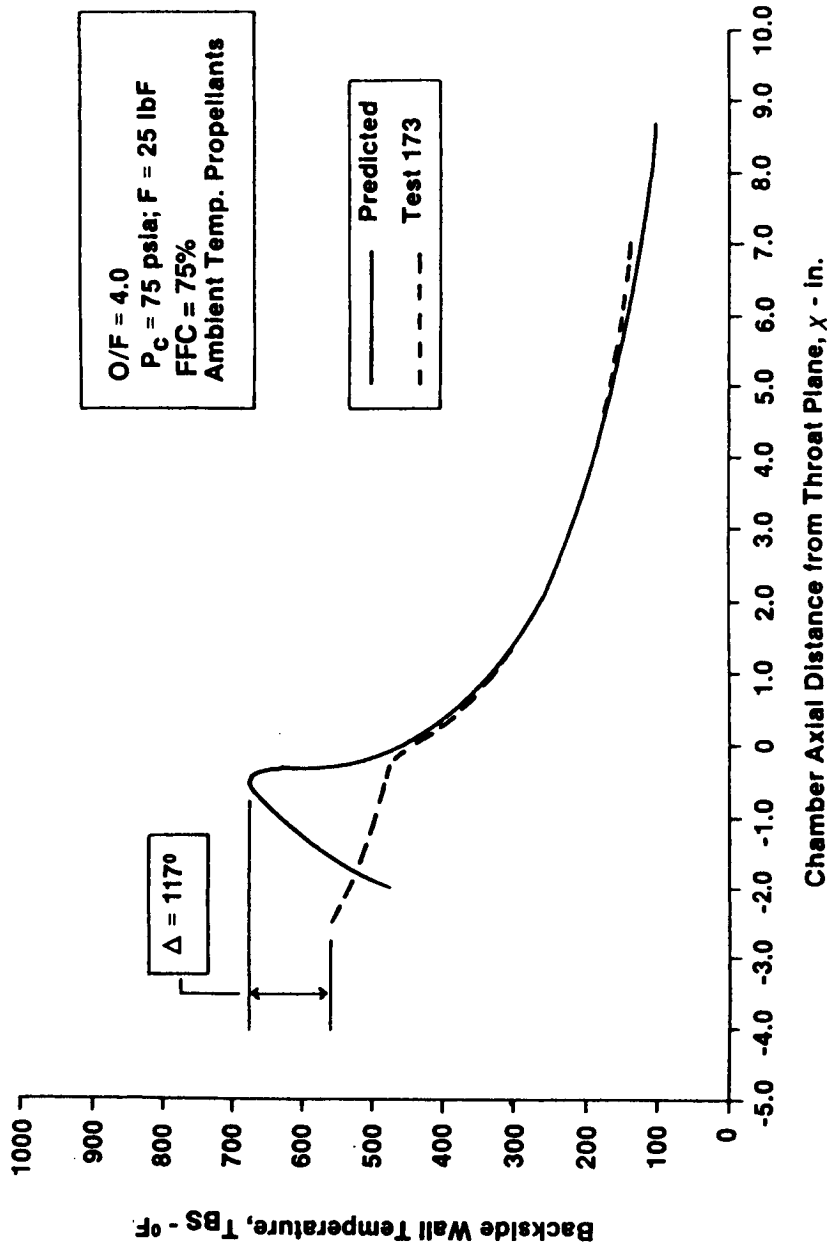


Figure 24. Backside Temperature Profile with 75 Percent FFC

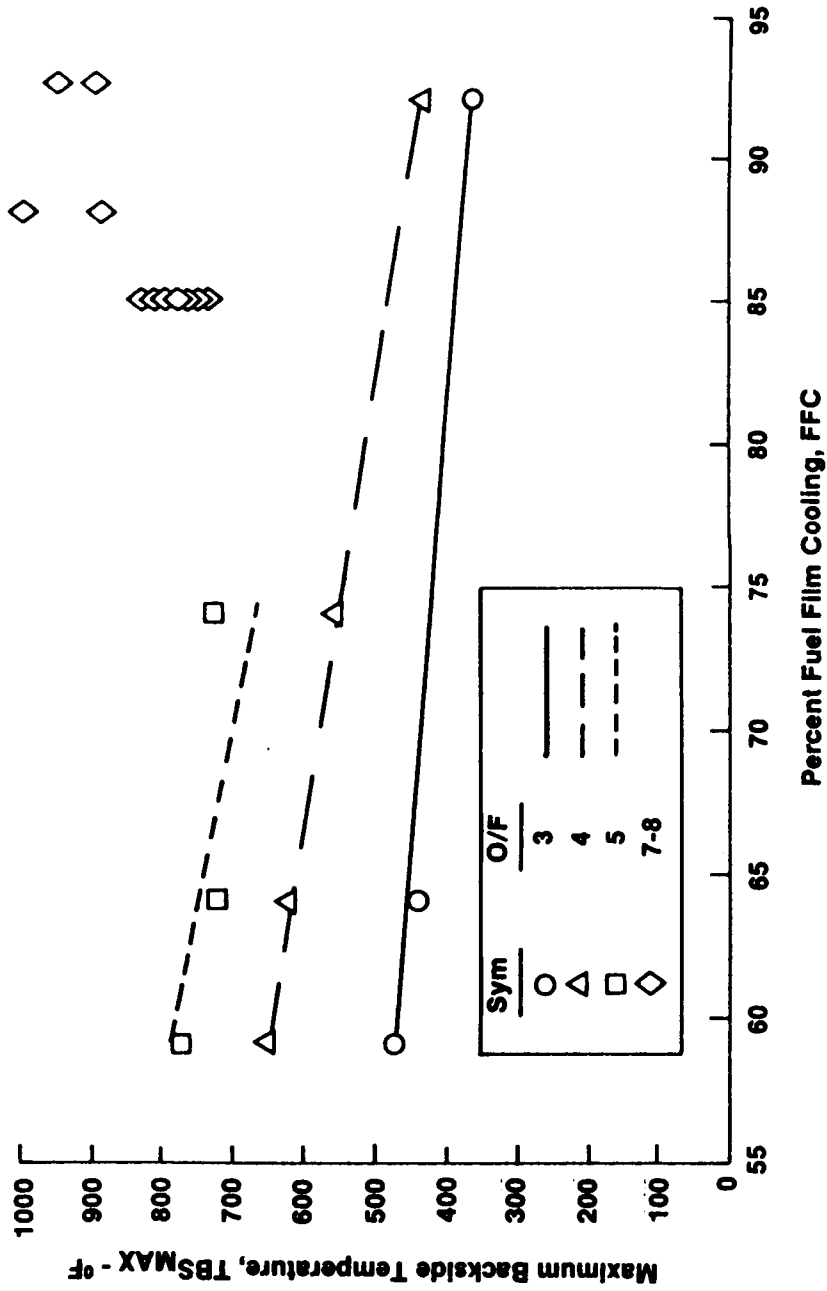


Figure 25. Maximum Backside Temperature Variation with FFC

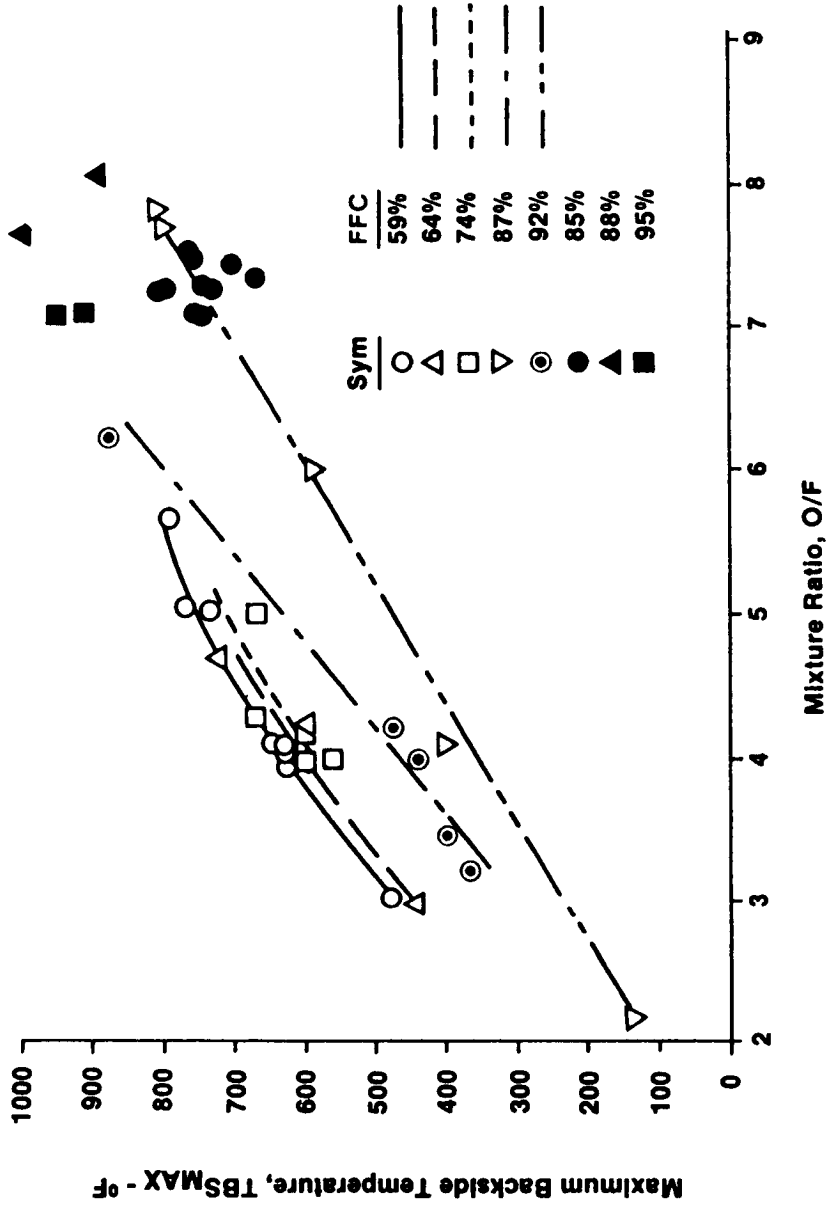


Figure 26. Maximum Backside Temperature Variation with Mixture Ratio

III, D, Test (cont.)

2200 second test previously mentioned. Such low temperatures assure minimum heat rejection to the vehicle.

Performance varied widely with film cooling and mixture ratio, as indicated in Figures 27 and 28; however, variations were linear. Predicted and measured values for performance did not agree as well as for temperature, although the trends were predicted correctly. It appeared that the larger the proportion of hydrogen flowing through the injector, the better the prediction. This condition was attributed to a momentum ratio effect in the core and was influenced by the injector hydraulics. The momentum ratio effect was most pronounced at the off-design operating points for mixture ratios of 7.0 to 8.0. At these high mixture ratios, the hydrogen injection momentum was so low that performance was degraded by 10 to 15 percent. This degradation could be recovered by optimizing the injector hydraulics for the higher mixture ratios.

E. EVALUATION OF RESULTS

In reviewing the experimental results of Thruster No. 1, specifically the measured versus predicted performance values of Figures 27 and 28, there was concern expressed over the apparent disparity in these values. To address this concern, a careful evaluation was performed to document the methodology employed to predict performance, as well as to identify the cause(s) of the performance degradation.

As mentioned previously, the performance predictions were based on measured JPL data which provided the basis for defining a mixing efficiency, E_m . This data was previously given in Figure 8, and was used in determining the percent FFC for the thermal analysis. The E_m values indicated were overall mixing efficiencies, which were influenced by two distinct mixing zones, as shown in Figure 29. The first zone was comprised of 100 percent of the GO_2 and 40 percent (for 60 percent FFC) or perhaps 25 percent (for 75 percent FFC) of the GH_2 . The GH_2 impinged normal to the GO_2 flowing through the annulus formed between the spark plug tip and the inner diameter of the platelet stack. These core gases mixed as they flowed along the inner diameter of the sleeve. At the end of the sleeve, the core gases began to be entrained into the FFC exiting the end of the sleeve, thus forming the second mixing zone. These two zones were treated with a two stream tube model, one stream tube being oxidizer-rich and the other being fuel-rich, as discussed in Section III, B, 3.

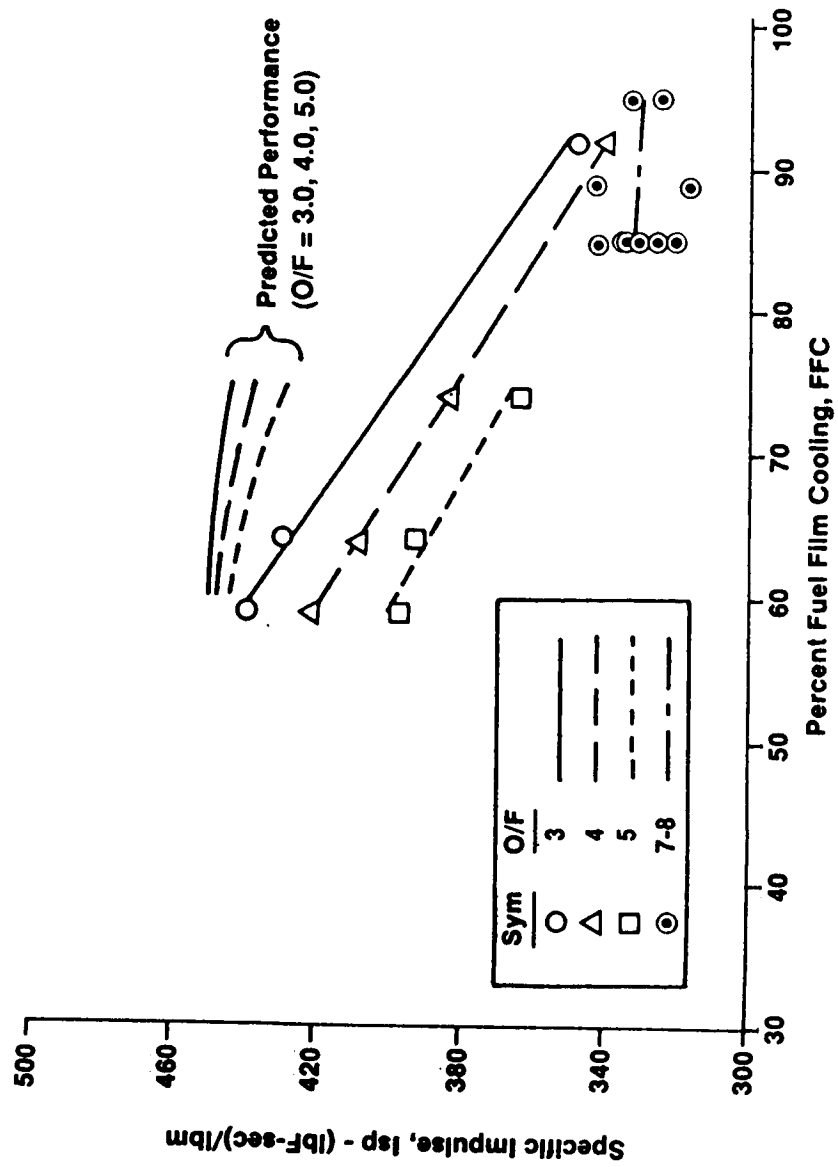


Figure 27. Performance Variation with Percent FFC

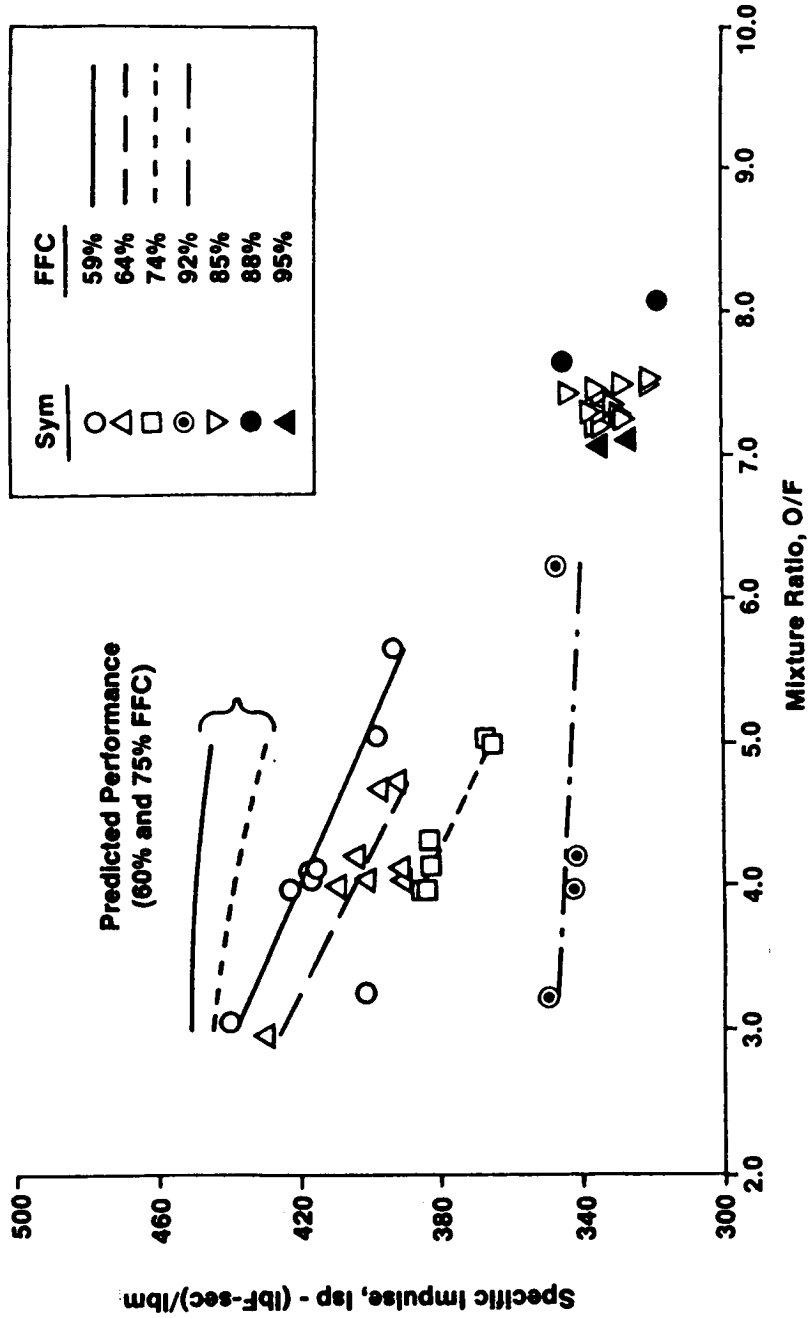


Figure 28. Performance Variation with Mixture Ratio

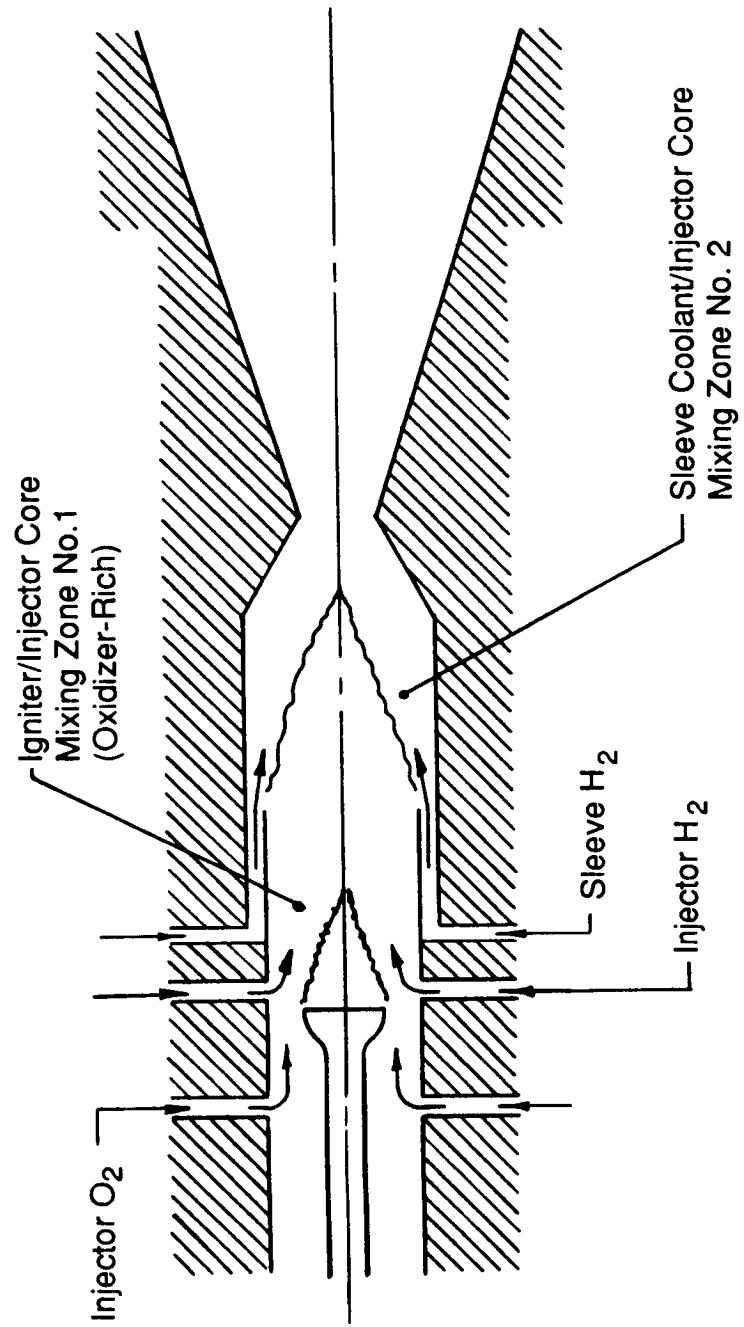


Figure 29. Two Mixing Zones of Thruster Design

III, E, Evaluation of Results (cont.)

The JPL data of Figure 8 defined the trends of combustion efficiency with percent FFC. At an O/F of three (3.0), reasonable combustion efficiencies of approximately 95 percent ($E_m \approx 0.5$) were attained at 60 percent FFC. Even at 90 percent FFC, where the combustion efficiency decreased to approximately 85 percent ($E_m \approx 0.25$), the delivered specific impulse was still 390 to 400 lbf-sec/lbm for the JPL thruster. This performance reduction associated with increased percentage FFC could be caused by either a decrease in the core mixing efficiency or in the core-to-coolant mixing efficiency.

In reviewing Figures 27 and 28 for the performance of the NASA LeRC Thruster No. 1, it is apparent that there was a significant decrease in I_{sp} with increasing FFC and O/F, respectively. Actually, the performance decrease associated with increasing FFC on Thruster No. 1 was greater than observed with the JPL data and greater than predicted. Also, the performance decrease with respect to increasing mixture ratio was dependent upon the percent FFC and was worse than predicted. At high percentages of FFC (~92%), performance was essentially constant for mixture ratios varying from 3.0 to 6.0. The first consideration in understanding these unexpected performance trends was to evaluate the methodology employed in the predictions.

Aerojet has used both the simplified and the rigorous JANNAF methodology for predicting engine performance, these two approaches being outlined in Appendix C. In the case of Thruster No. 1, the pretest performance predictions were based on the simplified JANNAF methodology and the previous JPL design. The performance losses considered included the following:

- Kinetics Efficiency (η_{KN}) - One-Dimensional Kinetics (ODK) Program - tabulated data from 15 degree cones and corrected for throat size.
- Boundary Layer Loss (ΔFBL) - Boundary layer charts from the Turbulent Boundary Layer (TBL) code.
- Divergence Efficiency (η_{DIV}) - Rao nozzle design charts.
- Energy Release Efficiency (η_{ERE}) - Combustion inefficiency due to incomplete mixing before reaching the chamber throat.

III, E, Evaluation of Results (cont.)

Of these losses, the Energy Release Efficiency (ERE) was the least well-characterized for it must account for the intra-core mixing efficiency as well as the core-to-coolant mixing efficiency. Subsequent to Thruster No. 1 testing, analyses were run using test data which determined ERE with respect to O/F. Figure 30 shows ERE plotted as a function of O/F for 59 percent FFC. In addition, curves for ODE, ODK and a perfect injector (ERE = 100 percent) are included in Figure 30. ERE declines significantly with increasing O/F for a fixed FFC of 59 percent, indicating that incomplete propellant mixing was the major cause in the decline of performance at the higher mixture ratios.

The cause(s) of the significant decrease in ERE with increasing O/F was from a decrease in either the core mixing efficiency or the core-to-coolant mixing efficiency. The core to coolant mixing efficiency was determined not to be a contributing factor based on Figure 31. In this figure, ERE was independent of the percentage of FFC and the coolant-to-core velocity ratio, the latter being the significant factor in the mixing efficiency of the core and FFC flows. ERE was highly dependent on O/F, or on the amount of GH_2 flow into the core, i.e., the more GH_2 into the core (lower mixture ratios), the higher the ERE.

Therefore, it was concluded that the mixing efficiency of the core gases was the predominant cause in the degradation of ERE with increasing O/F and that momentum flux ratio ($\rho_F V_F^2 / \rho_{OX} V_{OX}^2$) was the primary factor affecting core mixing efficiency. Previous work performed on the Multiple Jet Study^{12,13} correlated jet penetration and total mixing (E_T) to operating and design parameters. These correlations, when applied to the Space Station Thruster No. 1, indicated the design did not produce good mixing at higher mixture ratios and percentages of FFC, confirming the aforementioned conclusions. Specifically, Thruster No. 1 had inadequate fuel/oxidizer (H_2/O_2) momentum flux ratio and mixing length to achieve a high mixing efficiency (and ERE) at the higher mixture ratios and percentages of FFC, as was evidenced by Figures 32 and 33. The effect of momentum flux ratio and of FFC on ERE was further highlighted by Figure 34. Appropriate design modifications to improve injector hydraulics (H_2/O_2 momentum flux ratio) and effective mixing length would improve the mixing efficiency of the core and thereby improve the ERE (I_{sp}) of the thruster at the higher mixture ratios and percentages of FFC.

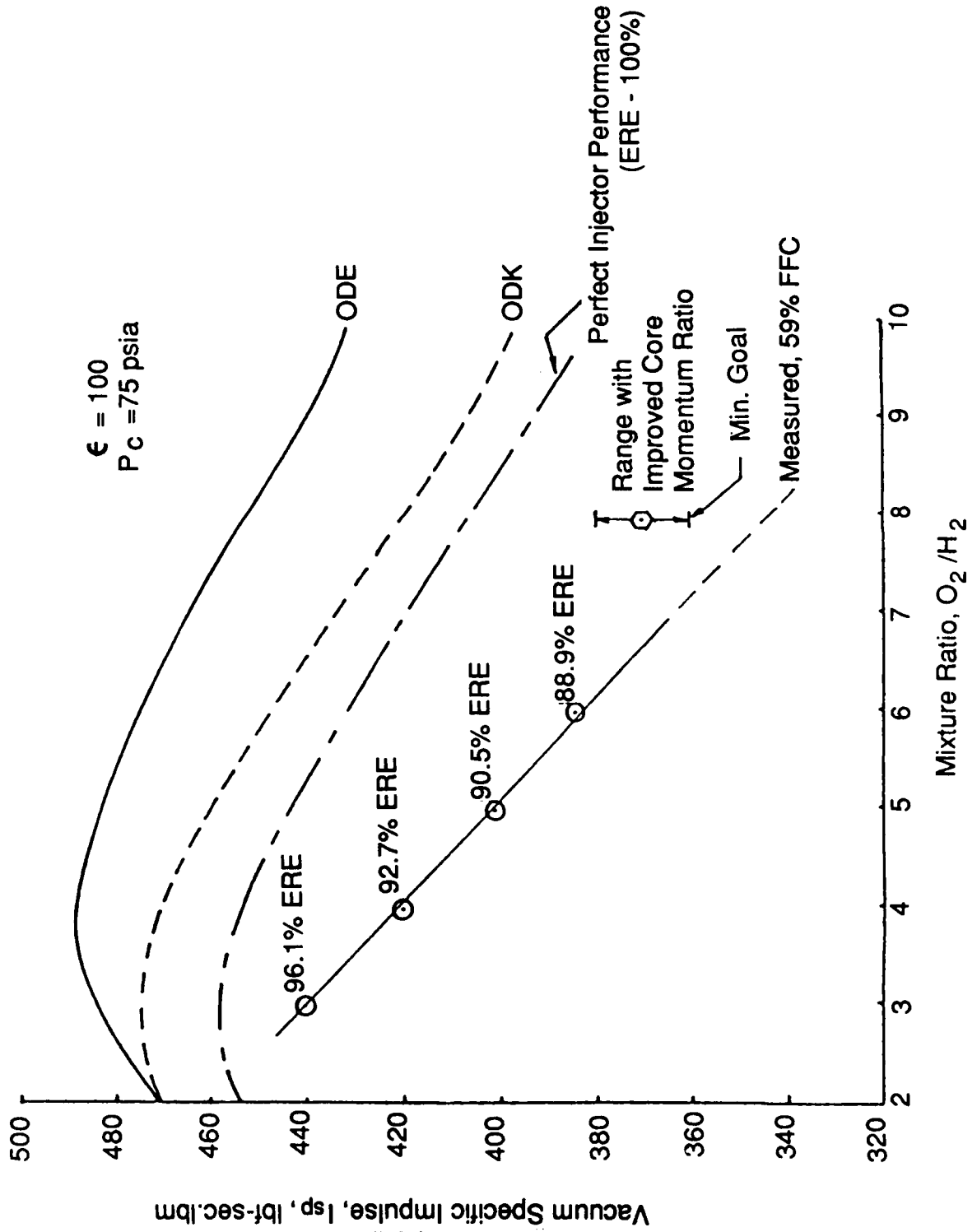


Figure 30. Energy Release Efficiency and Specific Impulse Trends with Increasing O/F

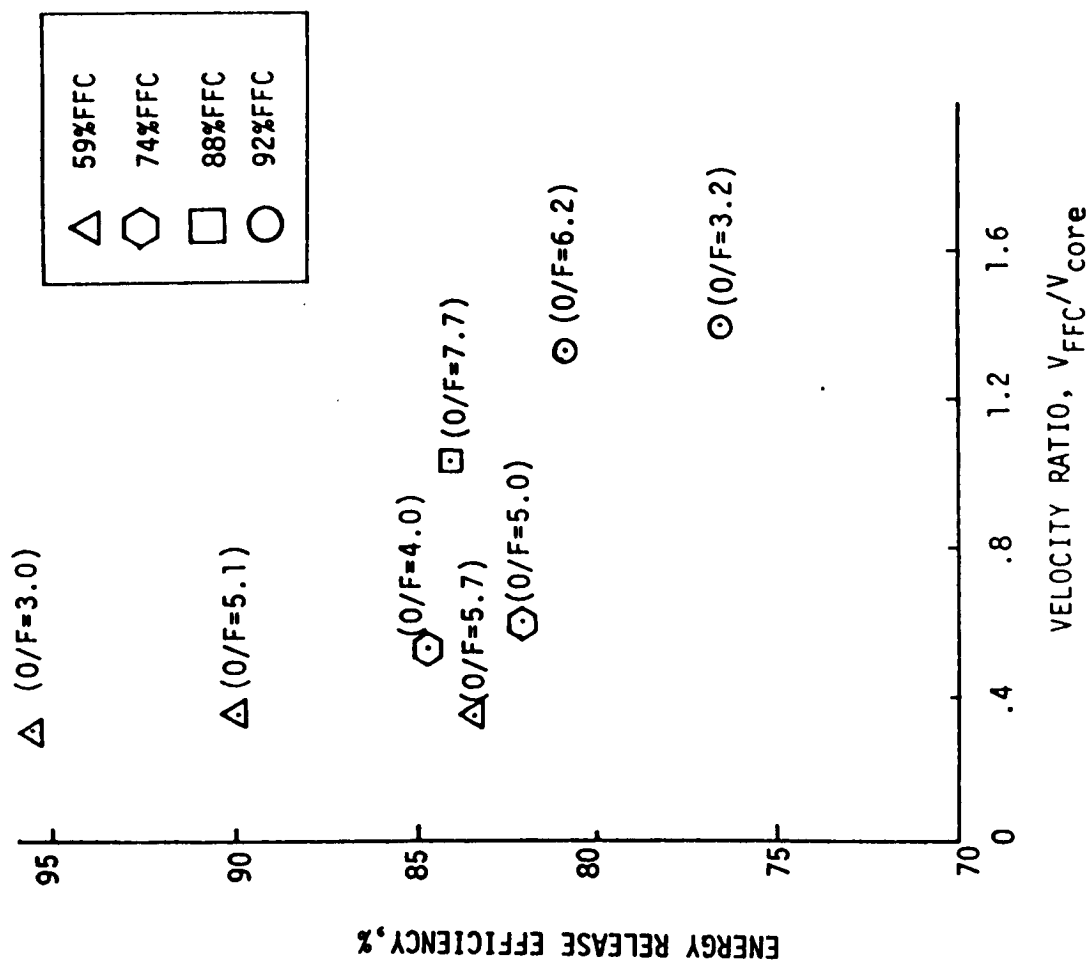
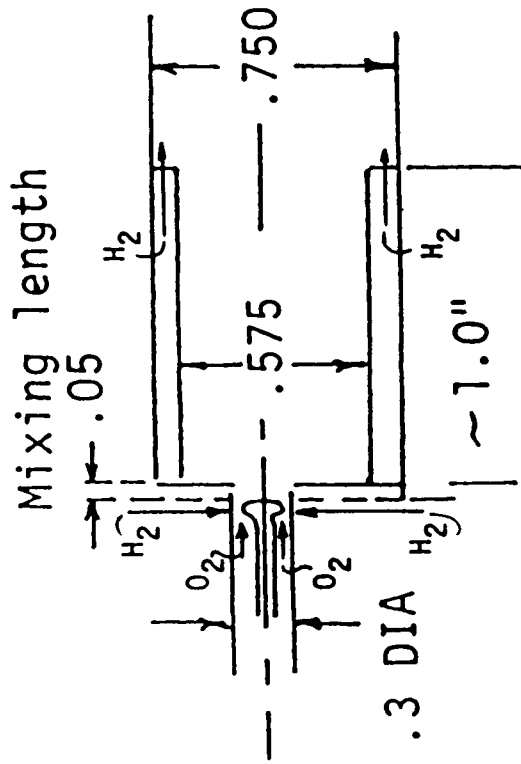


Figure 31. Energy Release Efficiency for Constant %FFC and Velocity Ratio



OPERATING CONDITION

	59% FFC		92% FFC	
	O/F	3.0	6.0	3.0
$\frac{(\rho v^2)_{H_2}}{(\rho v^2)_{O_2}}$	17.0	6.0	1.2	0.3

Figure 32. Current Space Station Thruster has Inadequate H_2/O_2 Momentum Flux Ratio and Mixing Length for Core Flow at High Mixing Ratio

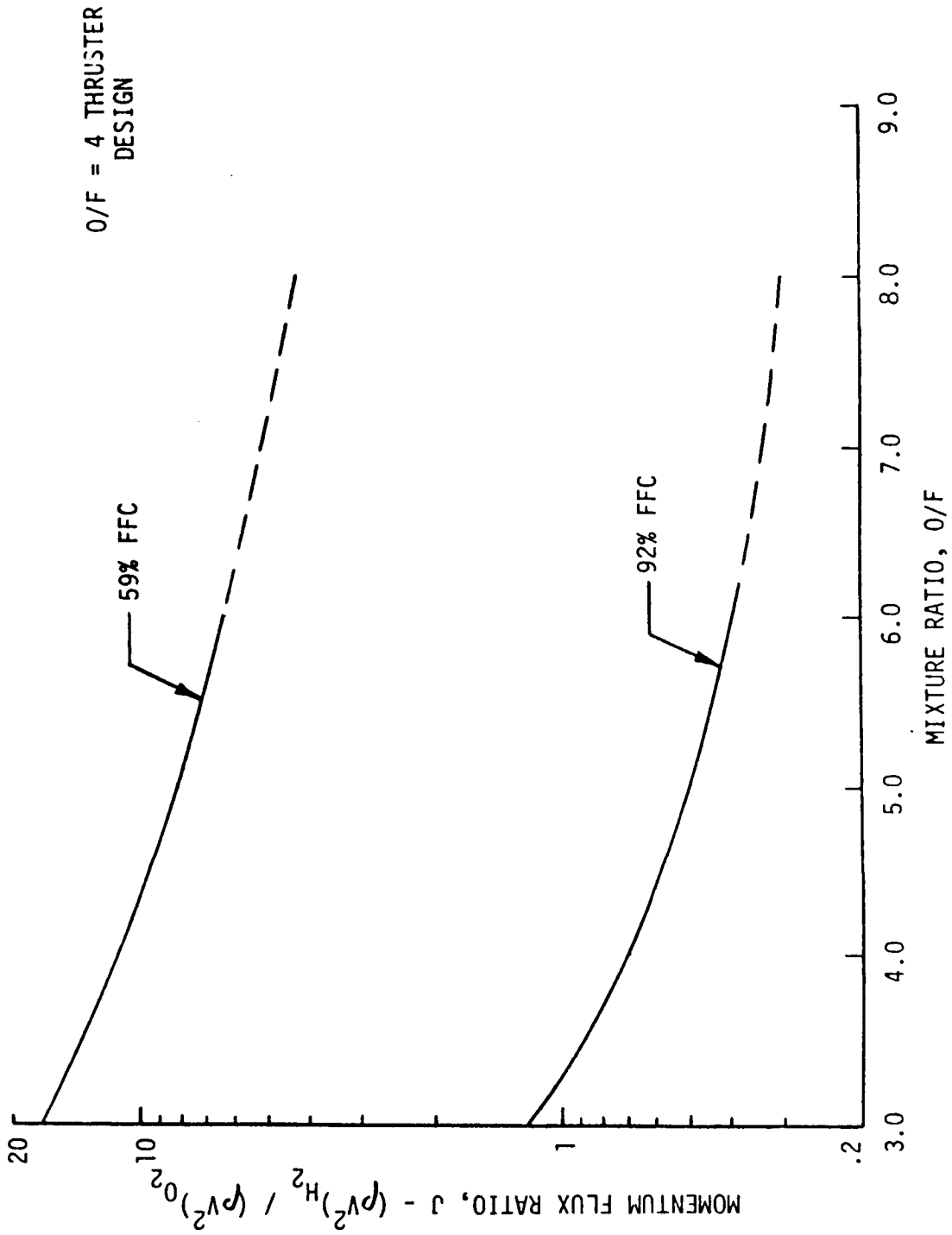


Figure 33. Momentum Flux Ratio for Different %FFC and O/F

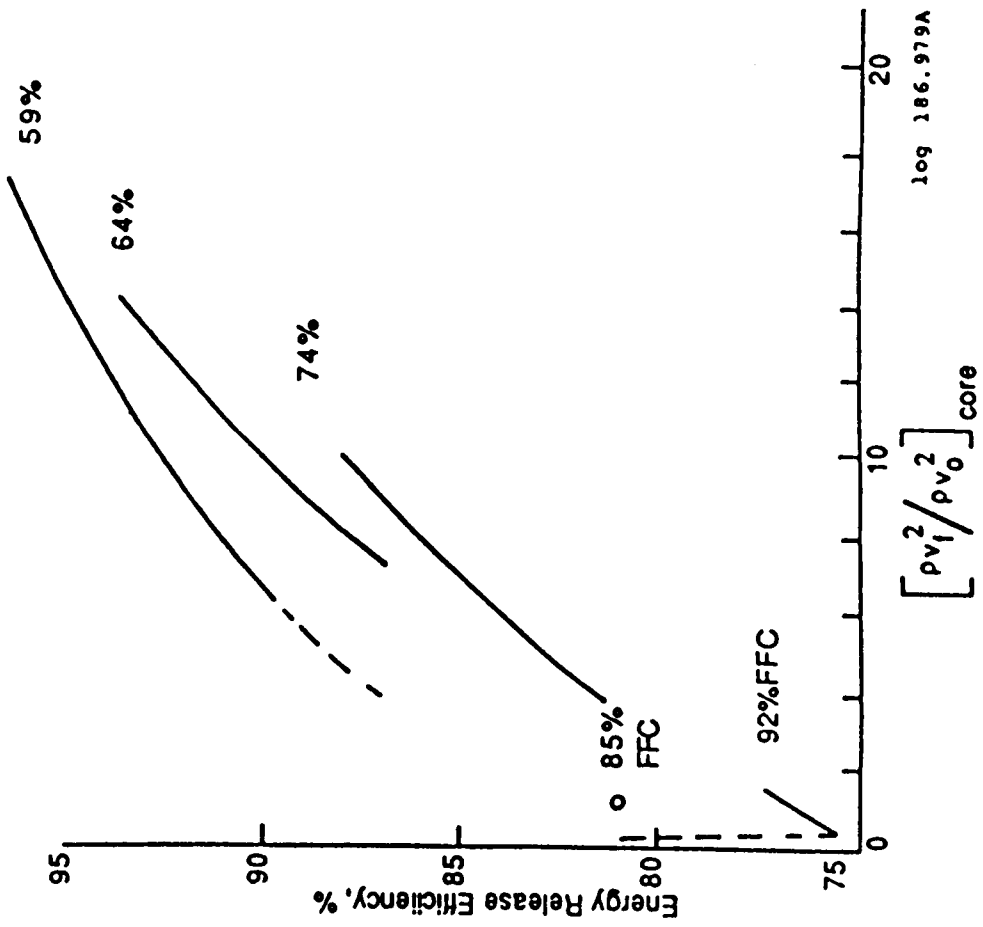


Figure 34. ERE for Increasing %FFC and Momentum Flux Ratio

III, Space Station Thruster No. 1 (cont.)

F. CONCLUSIONS

The technology for a 25 lbf GO_2/GH_2 thruster for Space Station propulsion was successfully demonstrated. Based on a previously proven igniter concept, a good thruster design approach was confirmed through extensive hot-fire testing, which covered mixture ratios from two (2.0) through eight (8.0) and FFC from 59 to 92 percent. The corresponding data base provided a substantial foundation upon which to evaluate the thruster operation and to establish the key design parameters affecting thruster performance. An optimized thruster for successful O/F = 8.0 operation could now be designed.

IV. SPACE STATION THRUSTER NO. 2

A. DESIGN APPROACH

1. Design Background

The design and the test results from Thruster No. 1 formed the basis from which Thruster No. 2 was designed. Figure 30 indicated that a minimum ERE of 96 percent was required to obtain good performance (I_{sp}). In addition, Figures 32, 33, and 34 showed that a momentum flux ratio of 17.0 corresponded to the desired 96 percent ERE ($O/F = 3.0$ and $FFC = 59\%$). Therefore, Figure 35 was prepared to relate the Thruster No. 1 test data with another mixing efficiency parameter, E_T , defined in References 12 and 13. This E_T parameter was directly related to the previously discussed momentum flux ratio, J , within the injector core. An E_T of 60 percent corresponded to an ERE of 96 percent ($O/F = 3.0$ and 59 percent FFC). Therefore, J and E_T became the guiding parameters for the design of the injector hydraulics to assure good core mixing. Specifically, a minimum value of 20 was established for J , and E_T had to surpass 60 at an O/F of 8.0, for design purposes

2. Design Concept

The design concept was not changed for Thruster No. 2, because the concept was believed to be a good one; however, Thruster No. 2 was modified based on Thruster No. 1 test results and optimized for $O/F = 8.0$. For such an overall mixture ratio (8.0), the core mixture ratio was 20.0 for 60 percent FFC. The Thruster No. 2 assembly is shown in Figure 36.

There were seven significant modifications implemented in the design of Thruster No. 2 and these modifications were as follows:

- (1) Decreased potential flow expansion area ratio (ϵ) from 100:1 to 30:1 — lowered coolant bulk temperature rise and lowered fabrication costs;
- (2) Increased the number of chamber coolant channels from 24 to 32 — improved chamber cooling;
- (3) Changed coolant channel geometry to permit variable depth channels so that coolant velocity could be increased at high heat flux locations — improved chamber cooling;

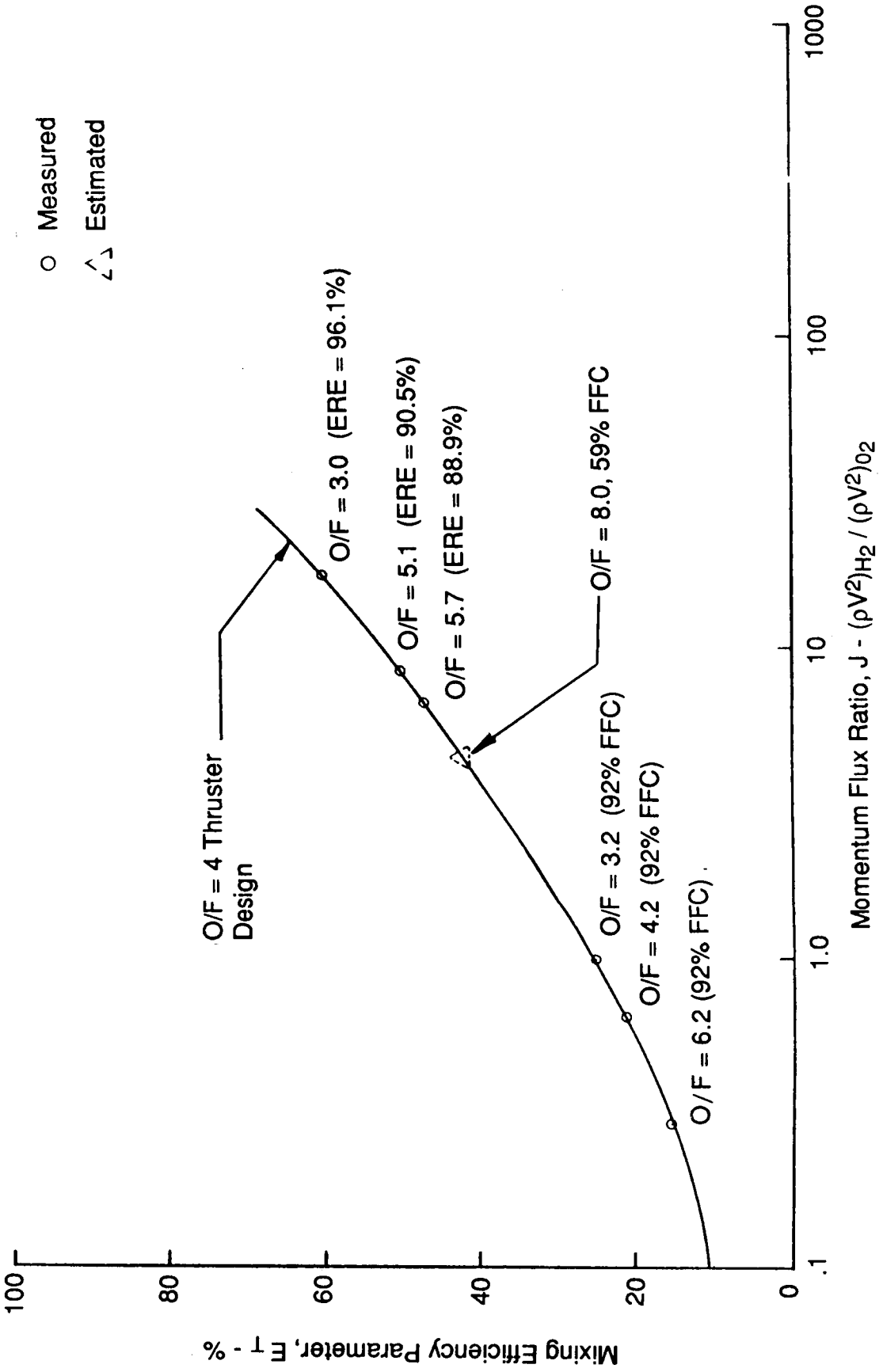


Figure 35. Mixing Efficiency, E_T , for Thruster No.1

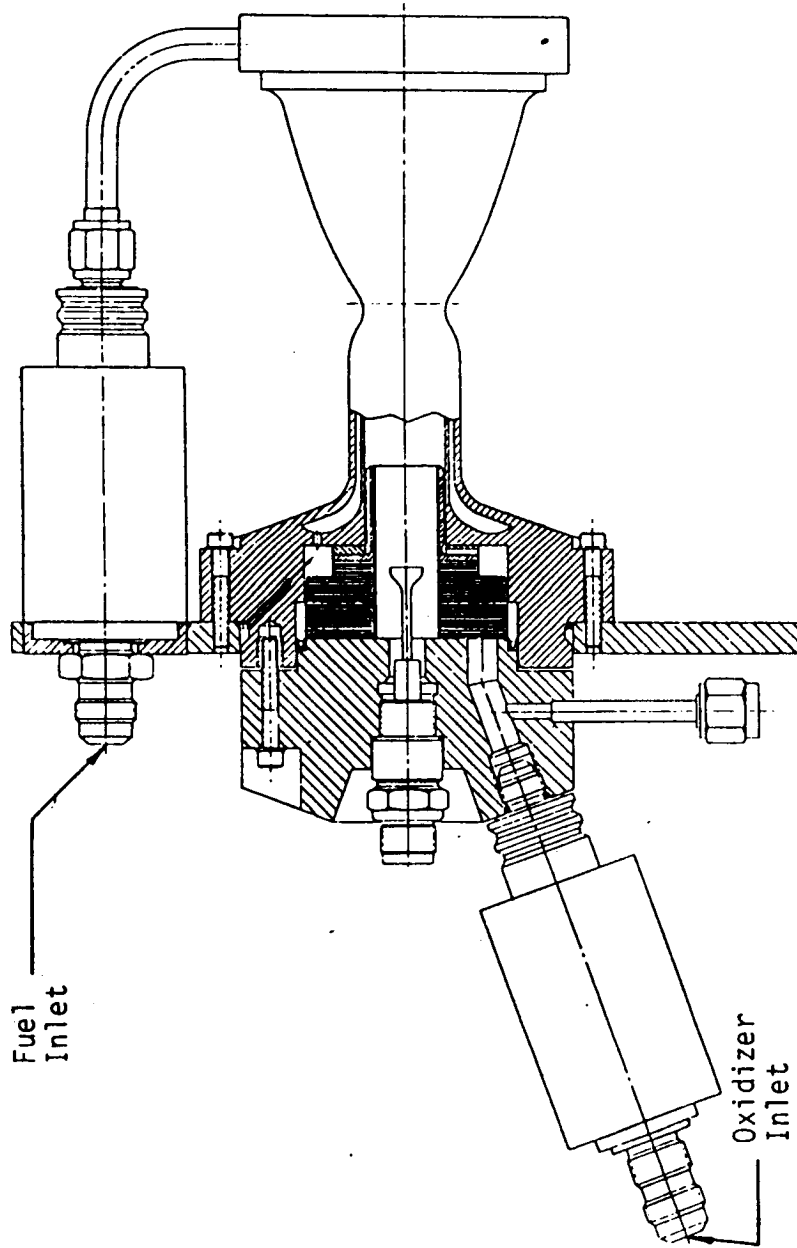


Figure 36. Thruster No.2 Assembly

IV, A, Design Approach (cont.)

- (4) Increased chamber contraction area ratio (ϵ_c) from 2.25 to 4.00 — increased inner surface area, thus lowering effective heat flux;
- (5) Reduced chamber gas-side wall thickness from 0.080 to 0.040 inches — improved chamber cooling;
- (6) Changed injector hydraulics to provide a minimum fuel-to-oxidizer momentum flux ratio of 20 — improved injector core mixing and thruster performance;
- (7) Removed rearward facing step between injector and sleeve — improved injector core mixing and thruster performance.

The initial five modifications were incorporated in the chamber design; the latter two modifications were incorporated into the injector and sleeve designs, with the seventh modification depicted in Figure 37. Based on the design changes implemented, Figures 33 and 35 were updated as Figures 38 and 39, respectively, indicating that the injector hydraulics would provide the desired core mixing.

3. Design Point

The design point for Thruster No. 2, based on the new contract requirements of Table II, were contrasted with the design point of Thruster No. 1 in Table VIII. This design point was compatible with the requirement for water electrolysis generated propellants, namely $O/F = 8.0$ operation.

B. DESIGN ANALYSIS

1. Ignition Analysis

The same type of ignition analysis was performed for Thruster No. 2 as was performed for Thruster No. 1. This analysis resulted in the spark igniter operating characteristics of Table IX.

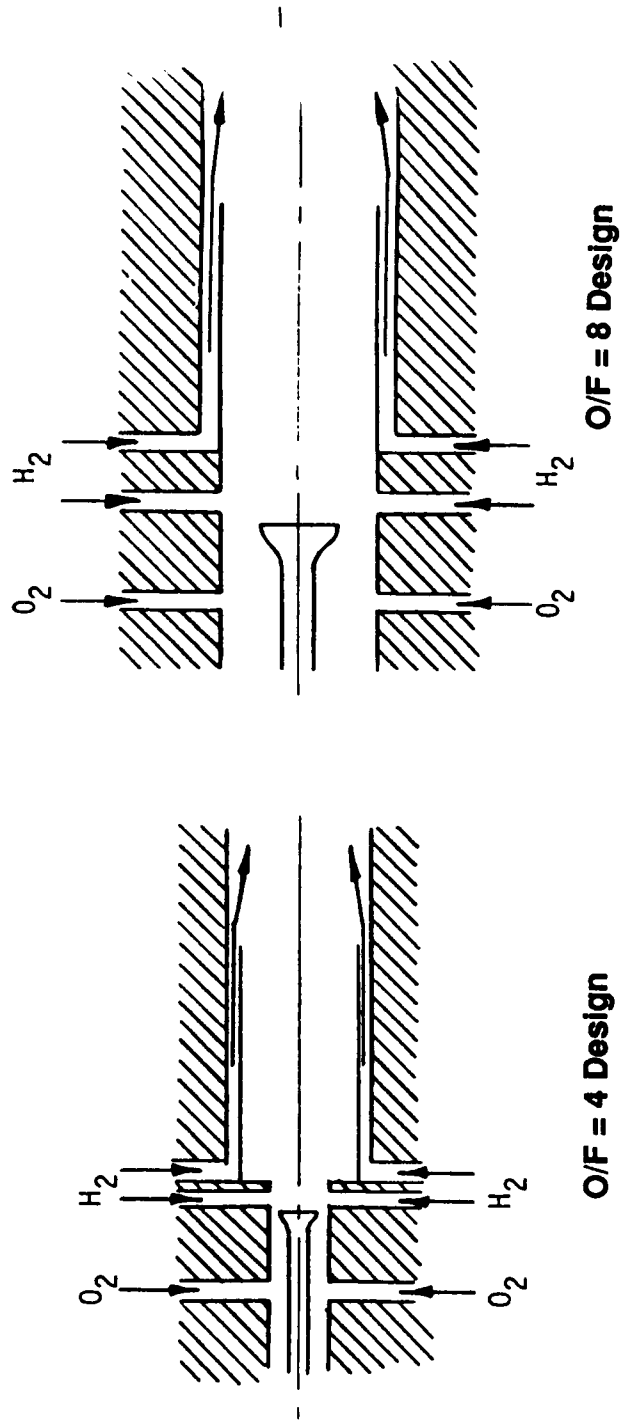


Figure 37. Redesign of Injector / Sleeve Interface

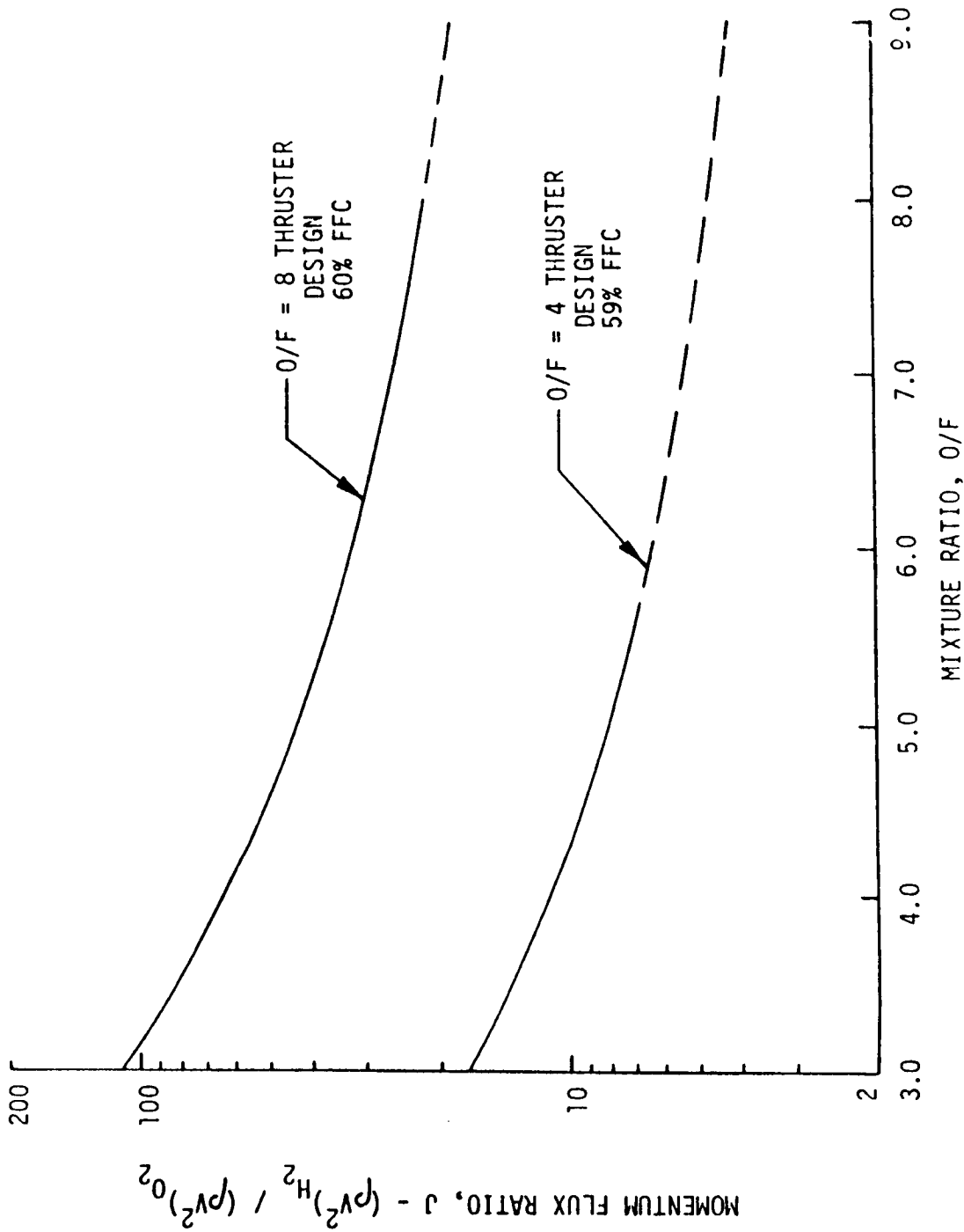


Figure 38. Momentum Flux Ratio Compared for Thruster Nos. 1 and 2

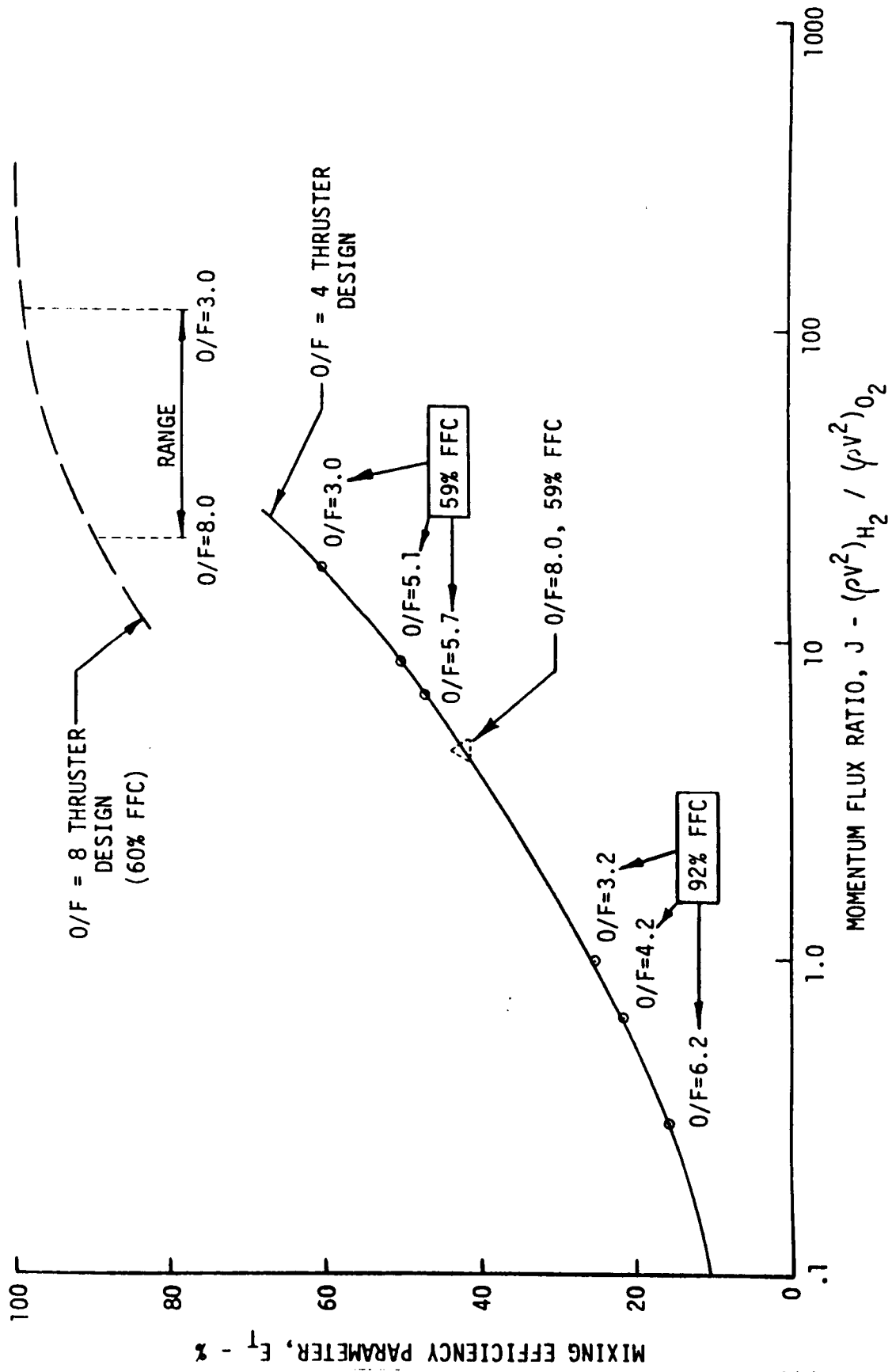


Figure 39. Mixing Efficiency, E_T , Compared for Thruster Nos. 1 and 2

TABLE VIII**DESIGN POINTS, NASA LeRC SPACE STATION THRUSTERS**

<u>Parameter</u>	<u>Thruster No. 1 First Generation</u>	<u>Thruster No. 2 Second Generation</u>
Thrust, F-lbf	25	25
Chamber Pressure, P_c -psia	75	75
% FFC	75	60
Overall Mixture Ratio, MR	4	8
Core Mixture Ratio, MR_{CORE}	16	20
Fuel Inlet Temperature, TFI-°R	200 - 530	200 - 530
Oxidizer Inlet Temperature, TPI-°R	300 - 530	300 - 530
Throat Diameter, D_T -in.	.500	.500
Chamber Diameter, D_C -in.	.750	1.000
Contraction Area Ratio, ϵ_c	2.25	4.00
Expansion Area Ratio, ϵ	100	30
Chamber Length, L' , in.	1.925	2.000

TABLE IX
SPACE STATION THRUSTER NO. 2
SPARK IGNITER OPERATING CHARACTERISTICS

Spark Igniter Energy, mJ	10 min
Spark Rate, SPS (Hz)	60 min.
Spark Gap, in.	0.200
Igniter Sleeve I.D., in.	0.810
Breakdown Potential, Volts	40,000
Minimum Ignition Pressure, psia	3.70
Maximum Ignition Pressure, psia	36.0
Predicted Nominal Cold Flow Pressure, psia	22.4

IV, B, Design Analysis (cont.)

2. Thermal Analysis

The same thermal model was utilized during the design of Thruster No. 2, which required the input of the two empirical constants previously mentioned in Section III, B, 2. These constants, C_{gn} and K_m (formerly KSO), were still based on the aforementioned JPL data. A gas-side temperature profile was predicted for the nominal chamber pressure (75 psia), depicted in Figure 40. In addition, temperature profiles were prepared for 40 percent (30 psia) and 135 percent (101 psia) of nominal chamber pressure (75 psia), presented in Figures 41 and 42, respectively. These three cases were at a mixture ratio of eight (8.0) and 60 percent FFC.

3. Performance Analysis

The output from the thermal mixing model was used to establish the characteristics of the two stream model used in the performance model. The performance analysis accounted for two-dimensional effects, as well as kinetics, divergence and boundary layer losses. The performance prediction was documented in Table X for the design point. Performance predictions for the thruster operating range were made, as displayed in Figure 43. The performance improvement for higher area ratios was determined and presented in Figure 44.

4. Chamber Life Analysis

The temperature differential through the chamber wall was predicted to be about 100°F, which was very small. The associated thermal strain range was predicted to be on the order of 0.2 percent. Such a small thermal strain range gave a low cycle fatigue (LCF) life in excess of 10,000 cycles according to the Manson-Halford method of universal slopes¹¹; therefore, LCF was considered to not be an issue. The design also surpassed the minimum criteria for creep rupture; consequently, the life limiting case would be high cycle fatigue (HCF).

C. DESIGN DESCRIPTION AND FABRICATION

The Thruster No. 2 design was similar to Thruster No. 1 and consisted of three major components: the thrust chamber, the sleeve insert, and the integral igniter injector. The thrust chamber was made of an axially slotted zirconium-copper (ZrCu) liner that had an electroformed nickel (EFNi) outer jacket. This EFNi outer jacket closed out the 32 chamber coolant channels and provided the structural support for the ZrCu liner. The diverging section of the chamber was

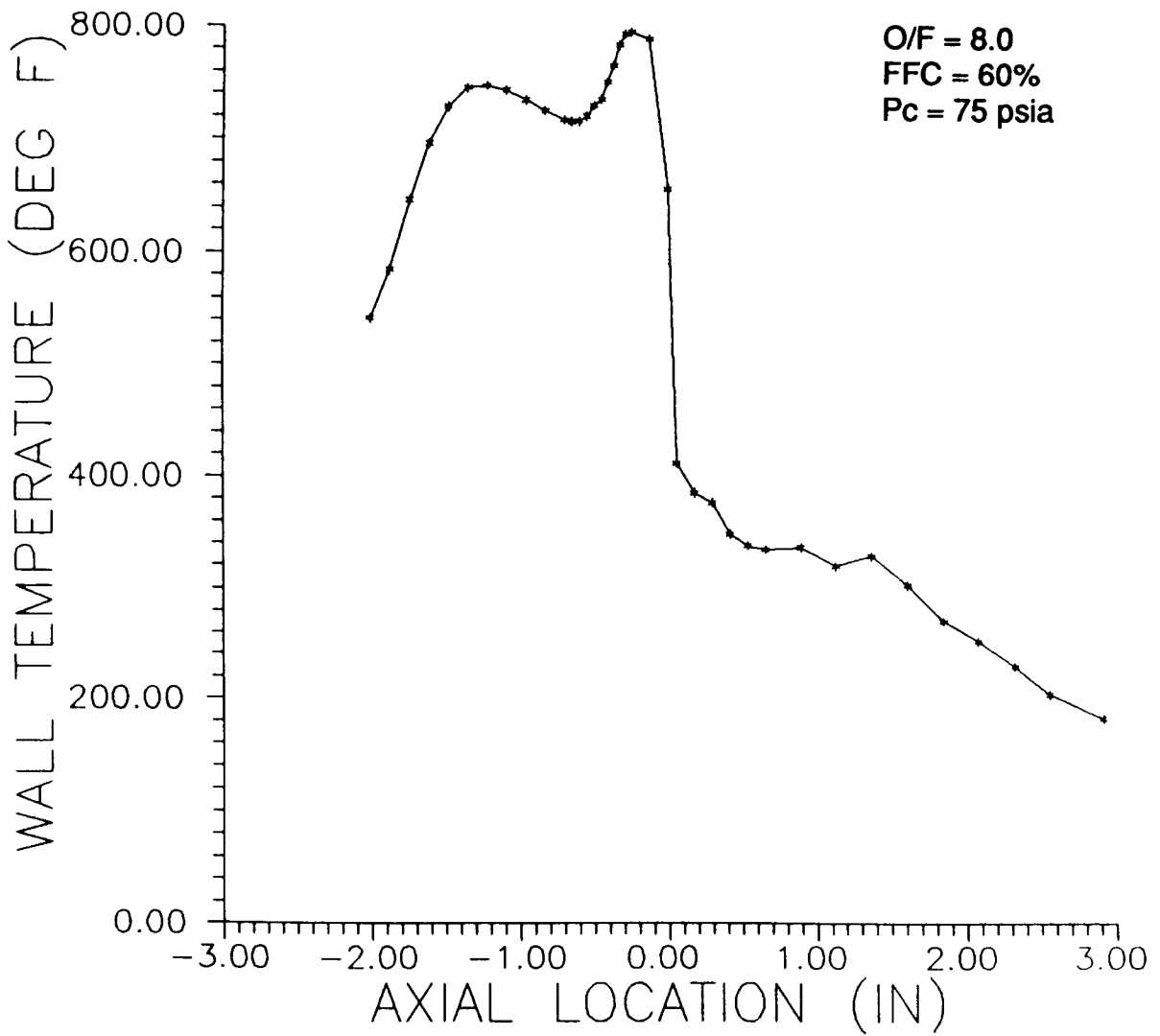


Figure 40. Predicted Gas-Side Wall Temperature Profile for Nominal Chamber Pressure

TABLE X

DESIGN POINT PERFORMANCE PREDICTION FOR THRUSTER NO. 2

- Nozzle contour (potential flow) is optimized at $\epsilon = 30:1$ for 85% bell.
- Boundary layer displacement thickness is accounted for by the geometric nozzle contour.

MR = 8, FFC = 60%

	<u>Turbulent</u>	<u>Laminar</u>
ODK	384.3	
ODE	406.0	
% Kin	94.655	
TDE	404.0	
TDE * % Kin	382.4	
97% ERE	370.9	370.9
BLM Losses	<u>9.9</u>	<u>7.6</u>
Isp*	361.0	363.3

* Isp for a perfect injector is approximately 387.

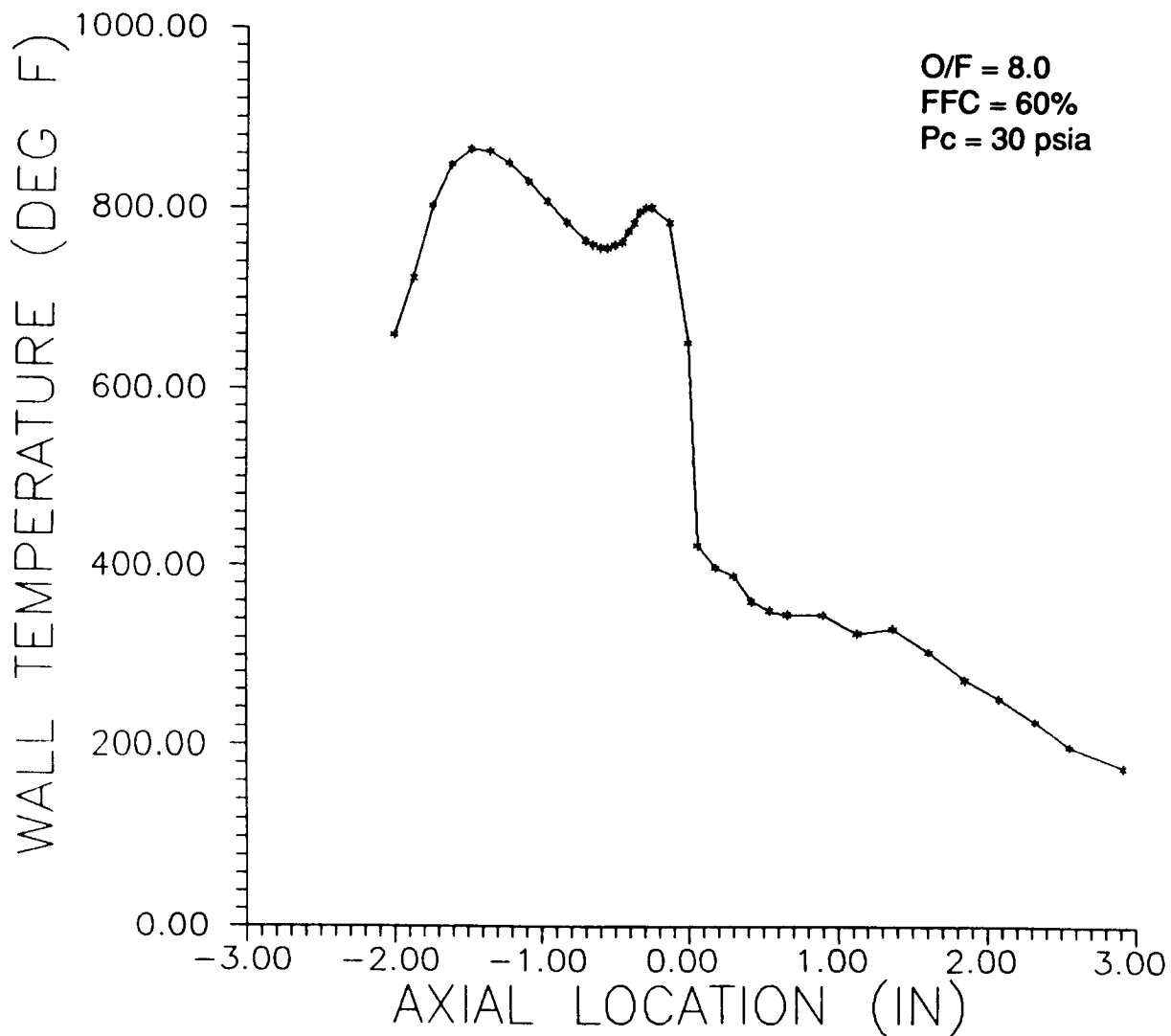


Figure 41. Predicted Gas-Side Wall Temperature Profile for 40 Percent of Nominal Chamber Pressure

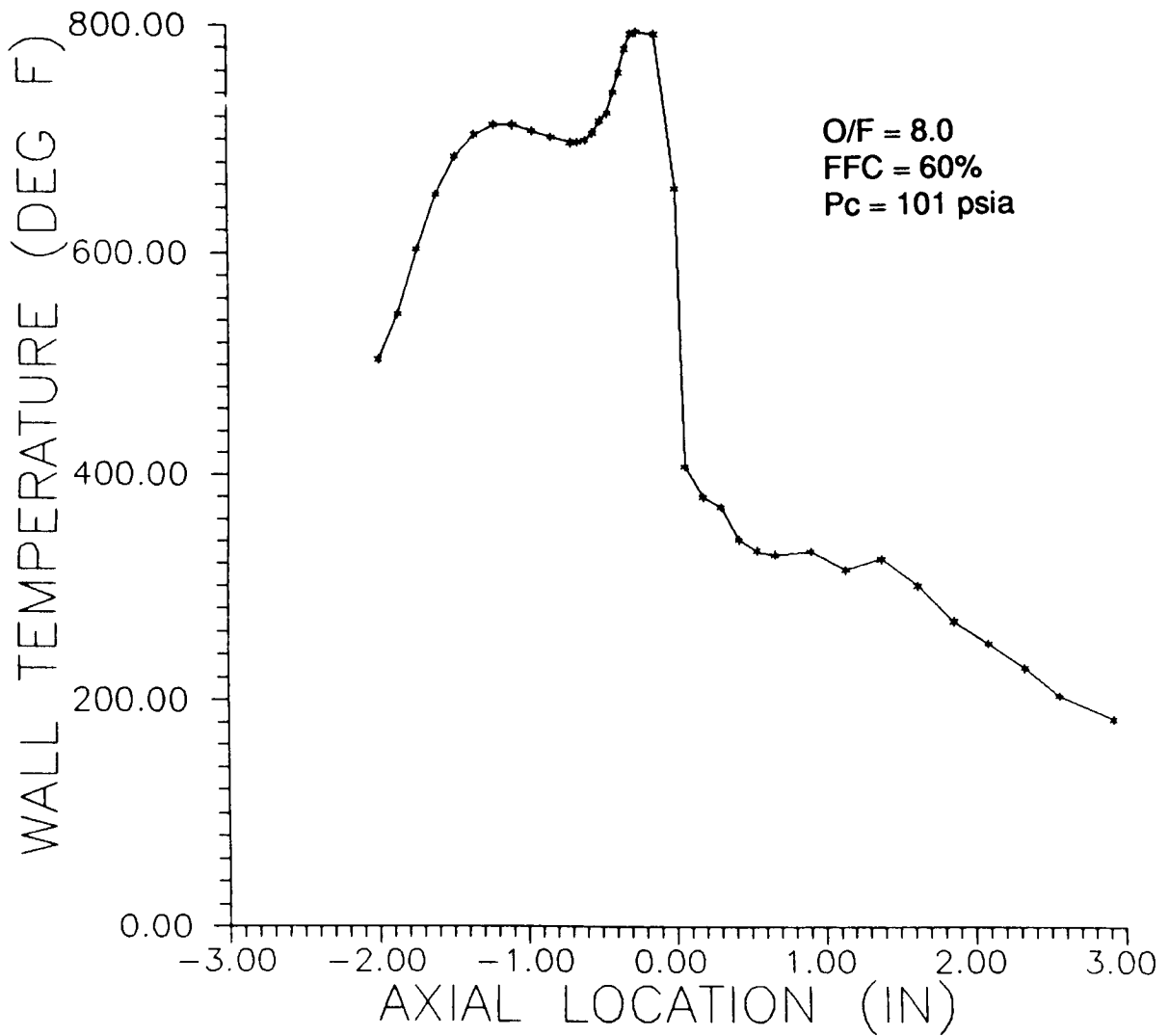


Figure 42. Predicted Gas-Side Wall Temperature Profile for 135 Percent of Nominal Chamber Pressure

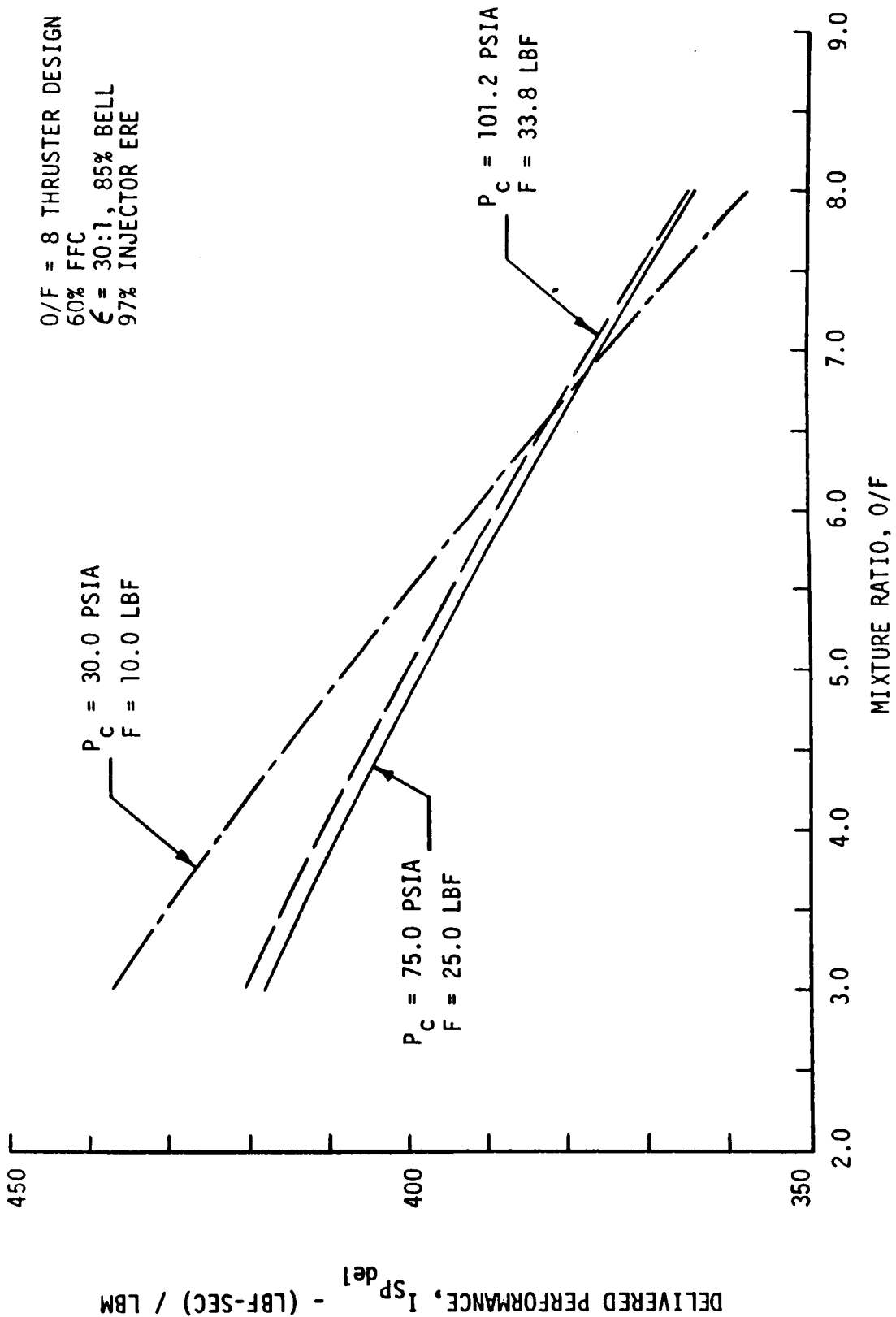


Figure 43. Performance Predictions for Operating Range of Thruster No. 2

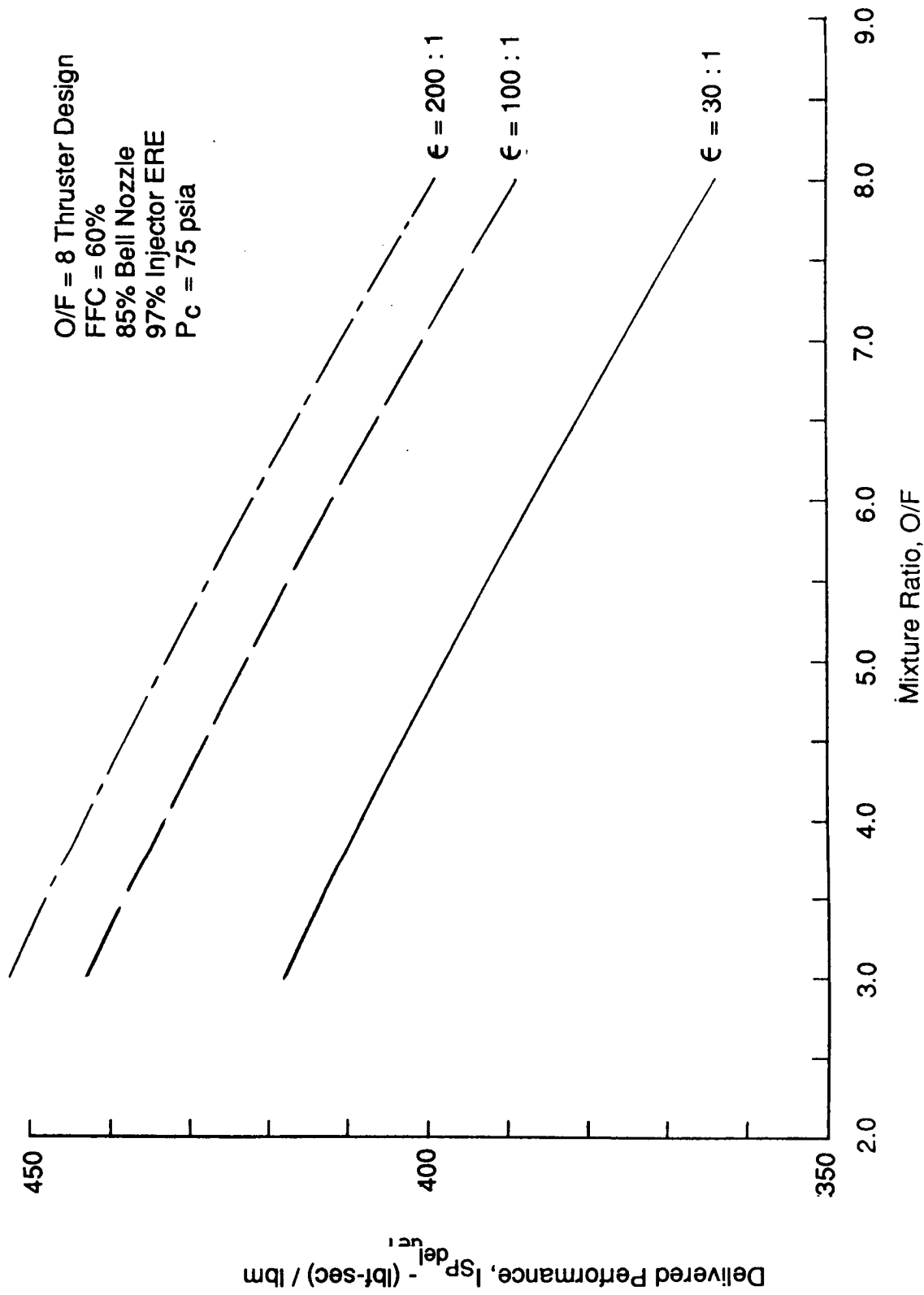


Figure 44. Effects of Nozzle Extensions on Delivered Performance

IV, C, Design Description and Fabrication (cont.)

an optimized Rao contour (85 percent bell) with a potential flow expansion area ratio of 30:1. Figure 45 shows the machined chamber liner.

The sleeve insert was similar to the one for Thruster No. 1 pictured in Figure 18. This insert was designed to fit into the forward end of the thrust chamber. A flow-balancing washer divided the fuel (GH_2) flow that exits the chamber coolant channels between the injector (40 percent) and the sleeve (60 percent). The sleeve was machined from nickel (Ni-200) and had 30 axial slots milled on the outer diameter for regenerative cooling and axial FFC injection.

The integral igniter injector consisted of a machined stainless steel igniter body and a Ni-200 platelet injector. Propellant distribution and metering occurred within the photochemically machined flow passages of the individual injector platelets. These individual platelets were diffusion-bonded to form a homogeneous structure which became the injector. This injector was brazed to the igniter body to complete the assembly. Provisions were made within the igniter body to mount the spark plug, the chamber pressure transducer, the injector fuel and oxidizer manifold pressure transducers, and the oxidizer valve. Both propellant valves mounted directly to the thruster to minimize dribble volume for pulsing duty cycles. The cutaway of Thruster No. 2 was documented in Figure 36, the completed thrust chamber assembly in Figures 46 and 47.

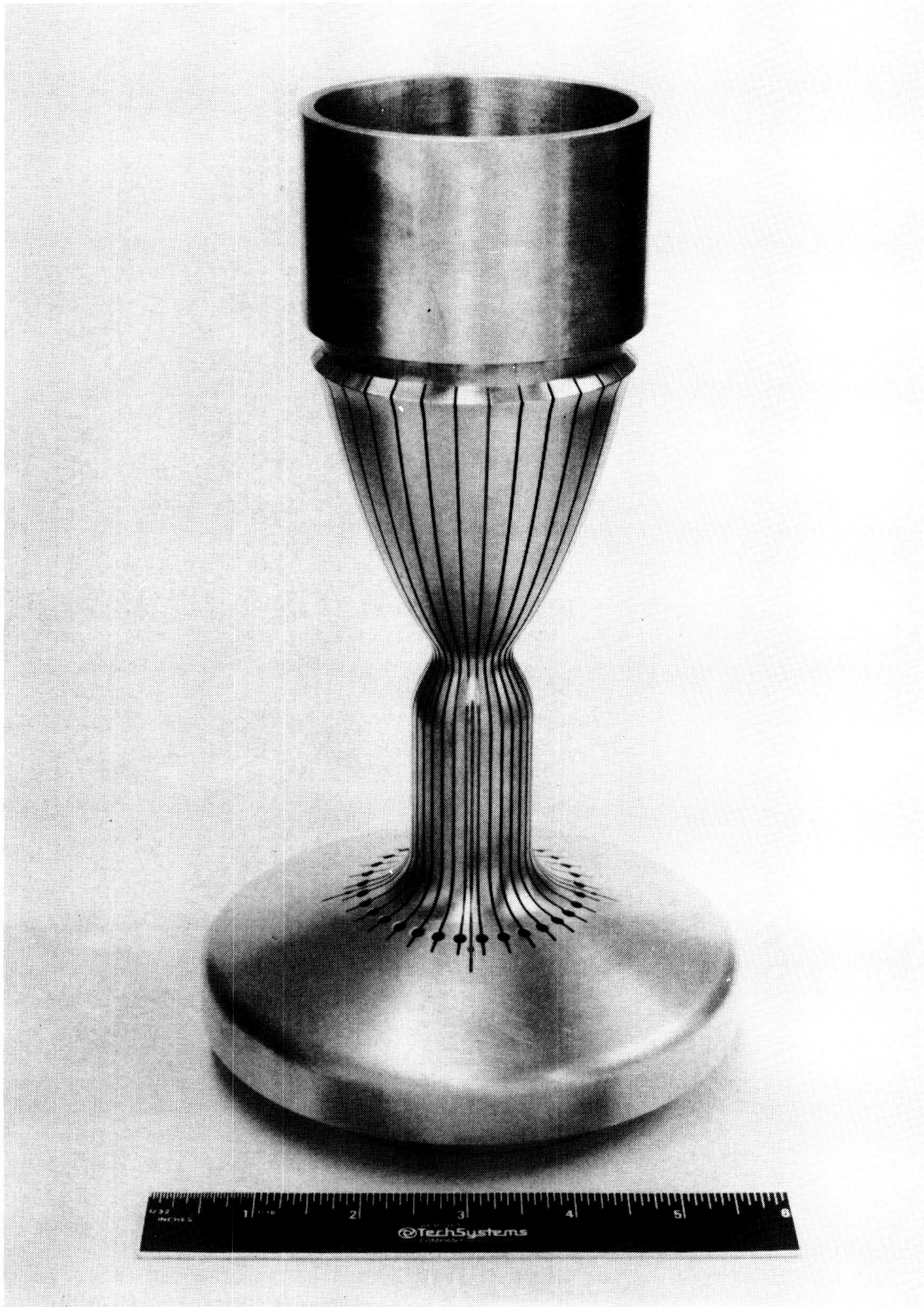
D. TEST

1. Test Setup

The Space Station Thruster No. 2 was assembled at Aerojet and shipped to NASA LeRC for altitude testing in their new low-thrust rocket engine facility. The thruster was mounted to a test stand within the LeRC facility designed to measure thrust. A water-cooled diffuser maintained the required nozzle back pressure to ensure that the thruster nozzle flowed full. Propellants were plumbed to the test cell from standard GH_2 and GO_2 trailers.

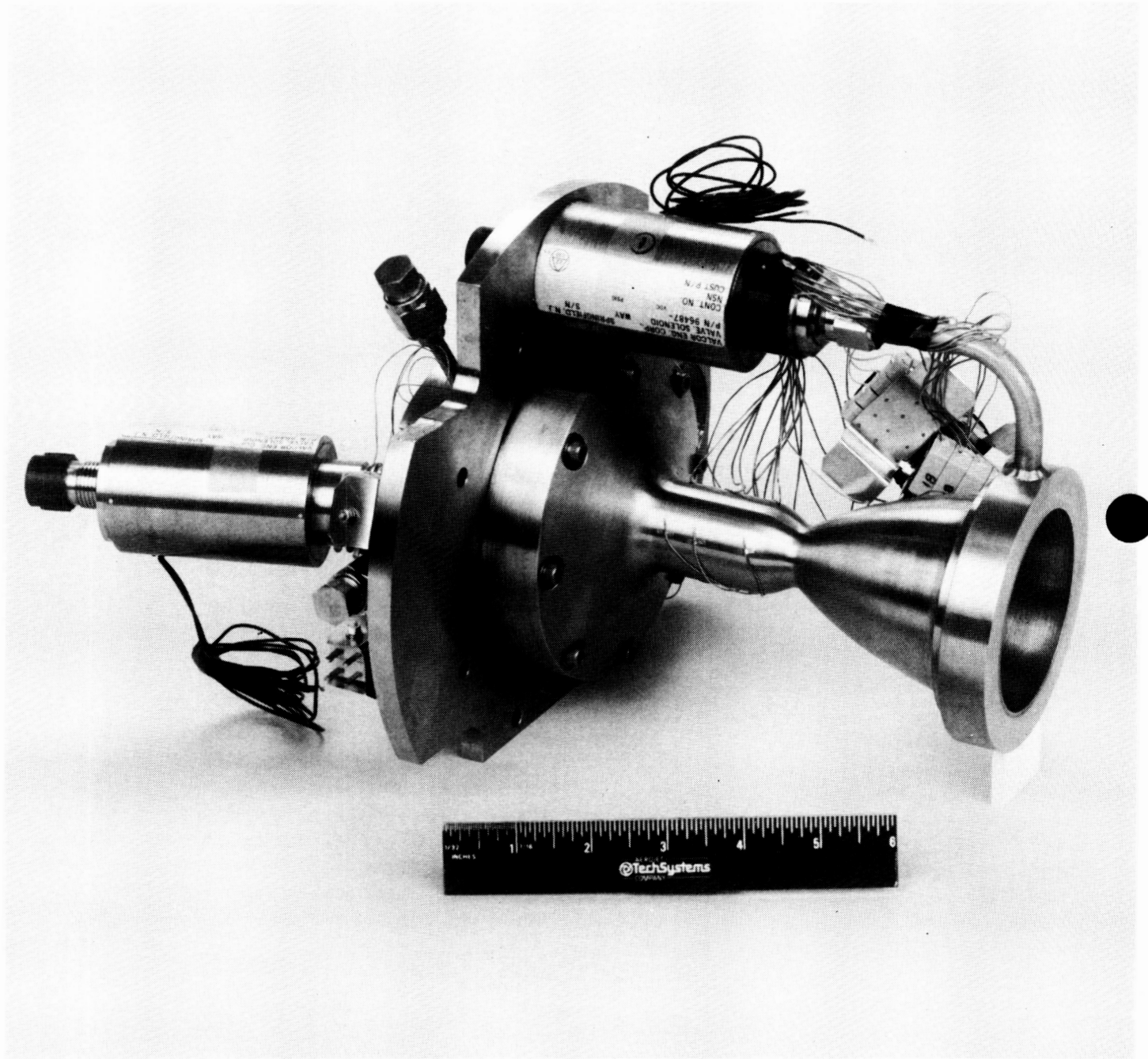
2. Instrumentation

The thruster test assembly was instrumented to measure thrust, propellant flowrates, inlet pressures and temperatures, coolant bulk temperature rise, and chamber internal (gasside) and external (backside) wall temperatures. There were thirty (30) thermocouples integral with the thrust chamber:



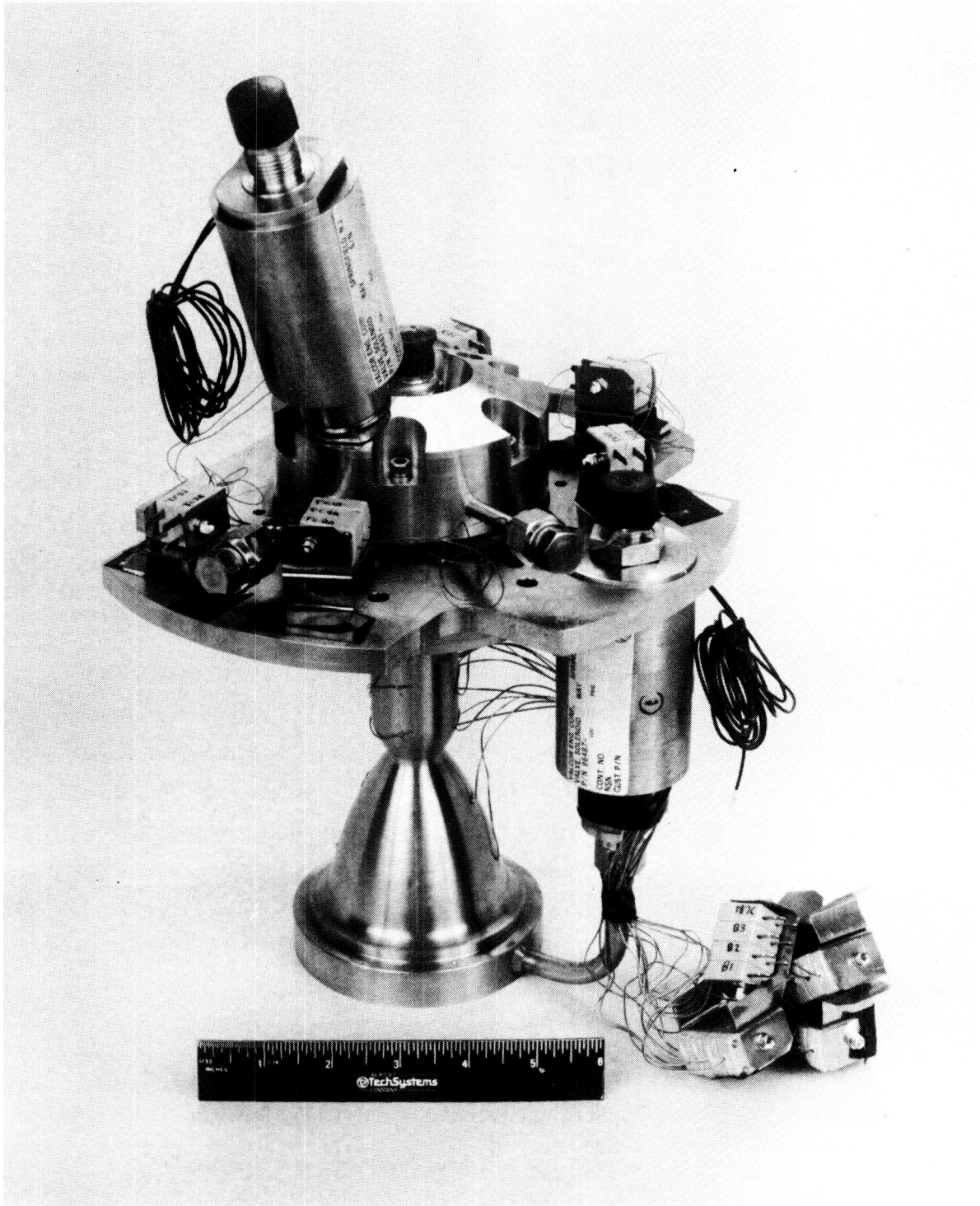
C1287 5153

Figure 45. Machined ZrCu Chamber Liner for Thruster No. 2



C1088 4621

Figure 46. Thrust Chamber Assembly - Aft End



C1088 4620

Figure 47. Thrust Chamber Assembly - Head End

IV, D, Test (cont.)

- four (4) fuel injector manifold (TFJ) thermocouples — one (1) was required, three (3) were redundant;
- twelve (12) chamber internal (gasside) wall (TCI) thermocouples — six (6) were required, six (6) were redundant;
- fourteen (14) chamber external (backside) wall (TCE) thermocouples — seven (7) were required, seven (7) were redundant.

Two additional thermocouples were added to the chamber external wall in the converging and throat regions after Test No. 041. The aforementioned test instrumentation is summarized in Table XI and depicted in the schematic of Figure 48.

Further definition of the thermocouple positions was provided by Figures 49, 50, 51 and 52. Figure 49 defined the axial positions of the thermocouples relative to datum -A-, these positions designated as Station Nos. 1 through 7. The external thermocouples added after Test No. 041, TCE-CNVRG and TCE-THRT, were included for reference. Figure 50 designated the thermocouple row assignments, i.e. Row A, Row B, Row C, and Row D. Rows A and C were identical, as were Rows B and D, thus providing redundancy as well as to guard against attrition during fabrication. The internal thermocouples (TCI) were located in four channels milled in between the cooling channels, as indicated in Figure 50. These four channels (Rows A through D) were documented in Figures 51 and 52. Thermocouples were brazed within these four channels prior to electroforming the nickel (EFNi) closeout. Axial station four (4) was common to all four rows to provide measurement of circumferential temperature variations. The thermocouples were designated by internal or external location (TCI or TCE), by axial station and by row, e.g. TCI-1A, TCE-4C, TCI-3B, etc.

3. Test Summary

Thruster No. 2 was given basic checkout testing at the NASA LeRC test facility during the summer of 1989. This testing covered a broad range of mixture ratio (O/F), but a narrow range of fuel film cooling (FFC), i.e., an O/F range from 3.0 to 9.5, and FFC's of 55.2, 60.9, and 64.2 percent. Tables XII and XIII summarized the tests run with regard to O/F and FFC, respectively.

TABLE XI
TEST INSTRUMENTATION
SPACE STATION THRUSTER NO. 2

<u>Parameter</u>	<u>Mnemonic</u>	<u>Range</u>
<u>Pressure</u>		
Fuel Pressure, Tank	PFT	TBD
Oxid Pressure, Tank	POT	TBD
Fuel Pressure, Venturi Inlet	PFVI	TBD
Oxid Pressure, Venturi Inlet	POVI	TBD
Fuel Pressure, Thrust Chamber Valve Inlet	PFTCVI	50 - 300 psia
Oxid Pressure, Thrust Chamber Valve Inlet	POTCVI	50 - 300 psia
Fuel Pressure, Injector Manifold	PFJ(1)	20 - 200 psia
Oxid Pressure, Injector Manifold	POJ(1)	20 - 200 psia
Chamber Pressure	PC(1)	15 - 150 psia
<u>Thrust</u>		
Thrust,	F1	5 - 50 lbf
Redundant Thrust	F2	5 - 50 lbf
<u>Temperature</u>		
Fuel Temp., Venturi Inlet	TFVI	TBD
Oxid Temp., Venturi Inlet	TOVI	TBD
Fuel Temp., Thrust Chamber Valve Inlet	TFTCVI	-260° - 70°F(2)
Oxid Temp., Thrust Chamber Valve Inlet	TOTCVI	-160° - 70°F(2)
Fuel Temp., Injector Manifold	TFJ(3)	250° - 600°F(6)
Internal Chamber Wall Temp.	TCI(4)	40° - 1000°F(6)
External Chamber Wall Temp.	TCE(5)	40° - 1000°F(6)

TABLE XI
TEST INSTRUMENTATION
SPACE STATION THRUSTER NO. 2
(Continued)

Parameter	Mnemonic	Range
Electrical		
Current Trace, Fuel Thrust Chamber Valve	IFTCV	TBD
Current Trace, Oxid Thrust Chamber Valve	IOTCV	TBD
Voltage Trace, Fuel Thrust Chamber Valve	VFTCV	0 - 32 Volts
Voltage Trace, Oxid Thrust Chamber Valve	VOTCV	0 - 32 Volts

- (1) Ports for indicated pressures are integral with the thruster.
- (2) Indicated temperature range is the design range; however, actual temperature range is facility dependent and will probably be limited to perhaps 40° to 70°F.
- (3) Four TFJ thermocouples are integral with the thruster; however, only one is required (three are redundant).
- (4) Twelve TCI thermocouples are integral with the chamber outside wall; however, only seven are required (seven are redundant).
- (6) Indicated temperature ranges are estimates only.

Additional instrumentation may be required to monitor test cell pressure and temperature, load cell temperature, and other facility parameters. All thermocouples that are integral with the thruster are ANSI Type K (Chromel/Alumel) with a range of 32 to 2300°F.

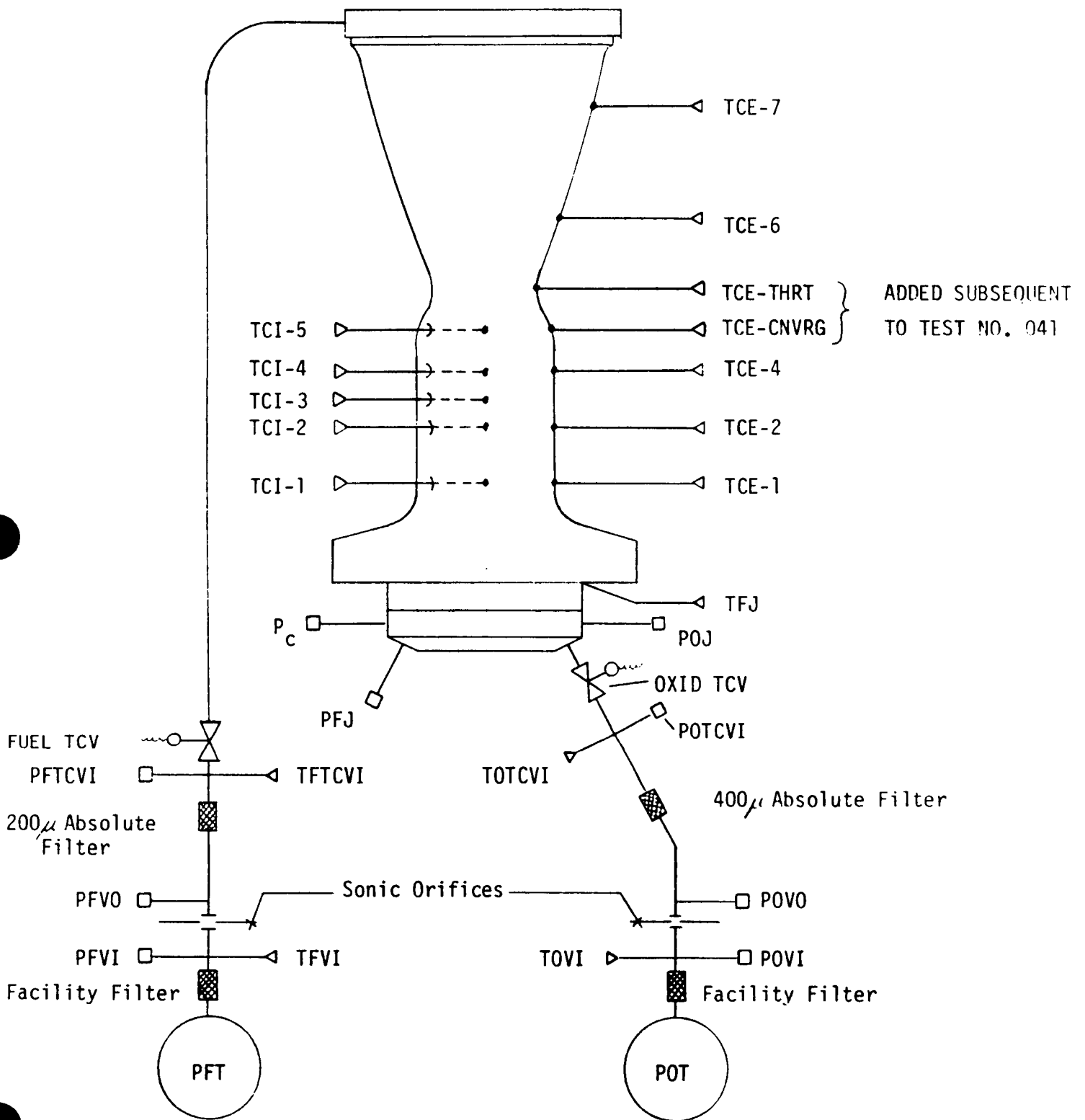
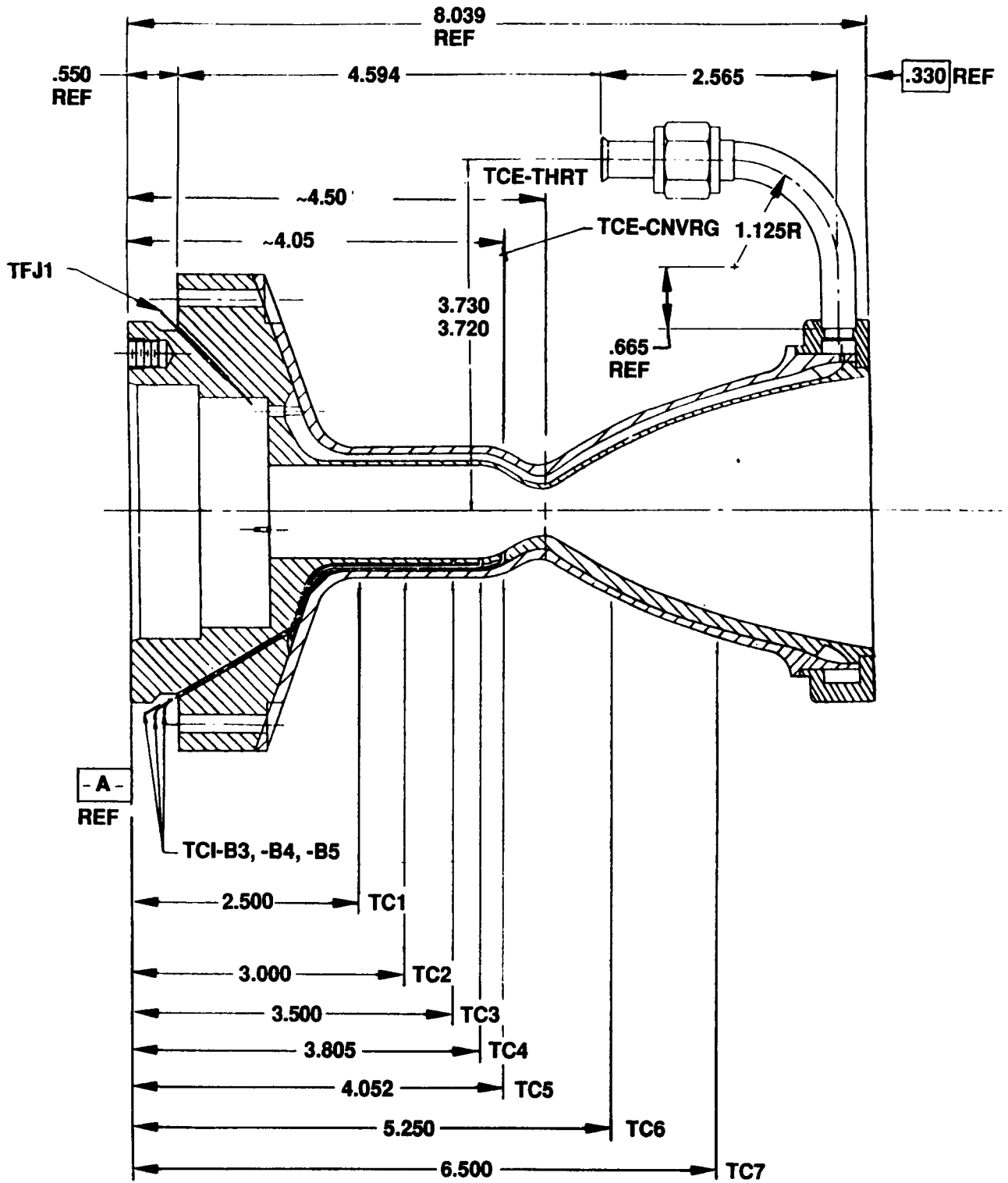


Figure 48. Instrumentation Schematic for Space Station Thruster No. 2



Thermocouple Axial Positions
Stations Nos. 1 Through 7

Figure 49. Axial Positions of Thermocouples

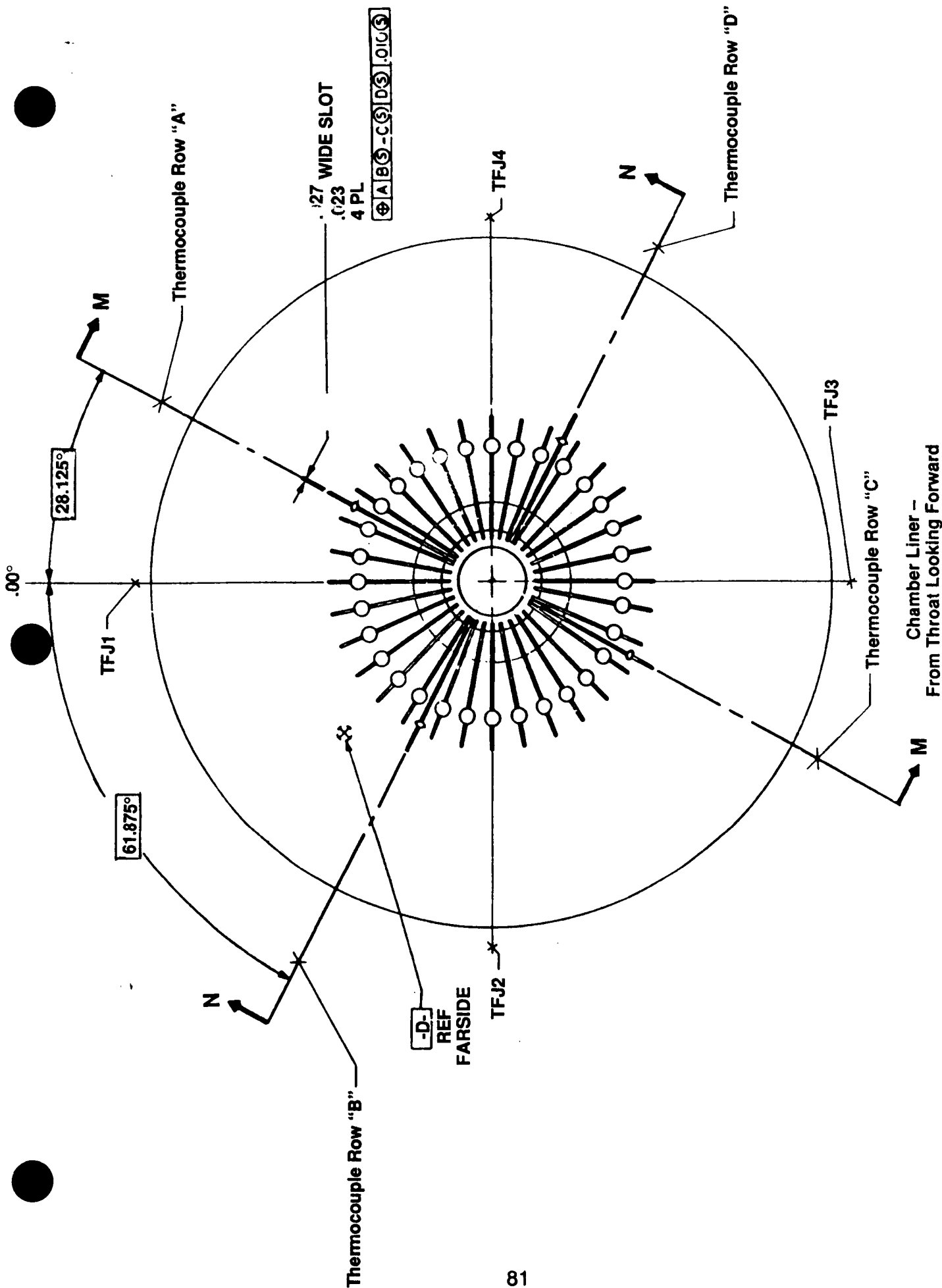


Figure 50. Internal Thermocouple (TC) Row Designations

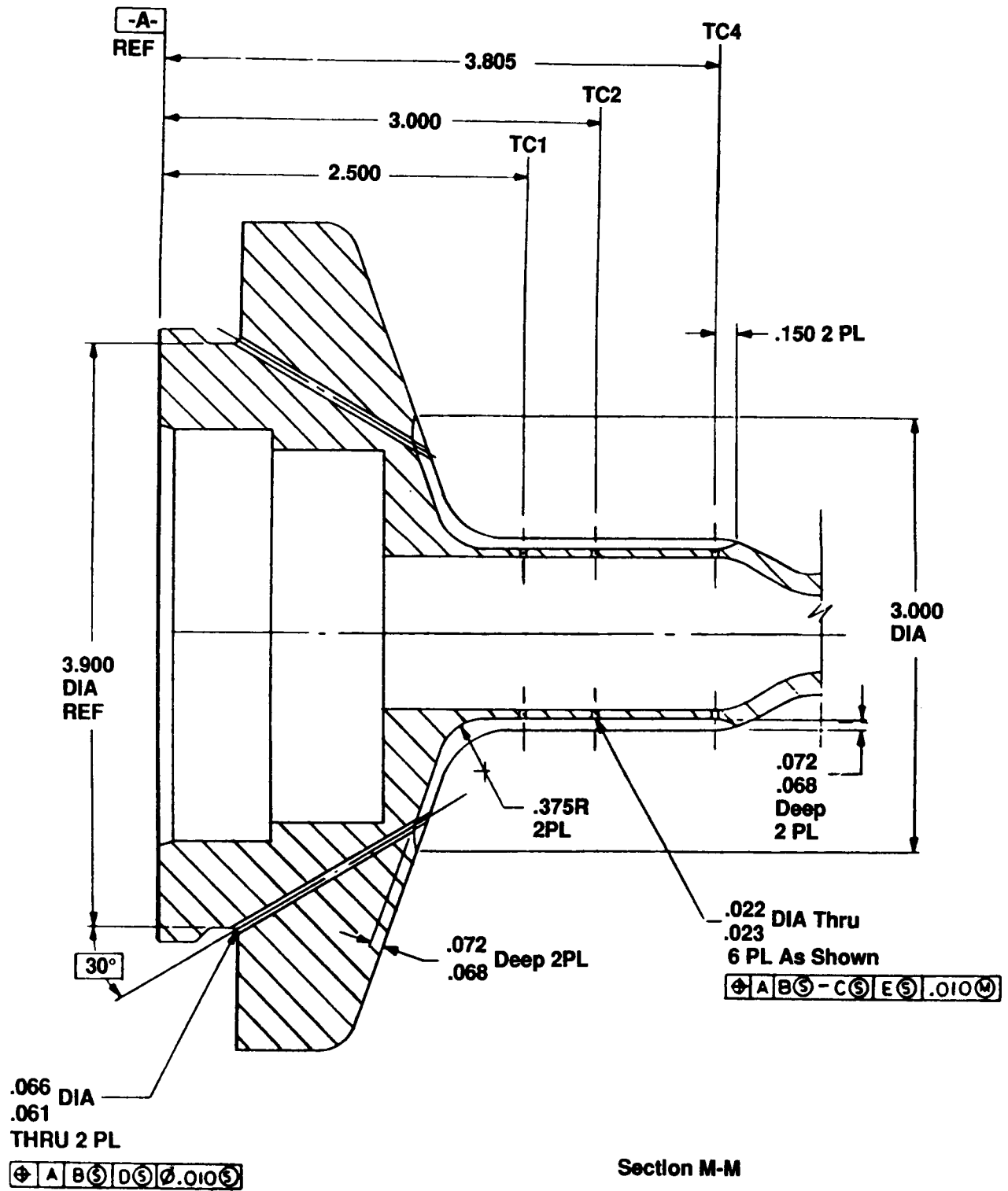


Figure 51. Row A and Row C Thermocouples

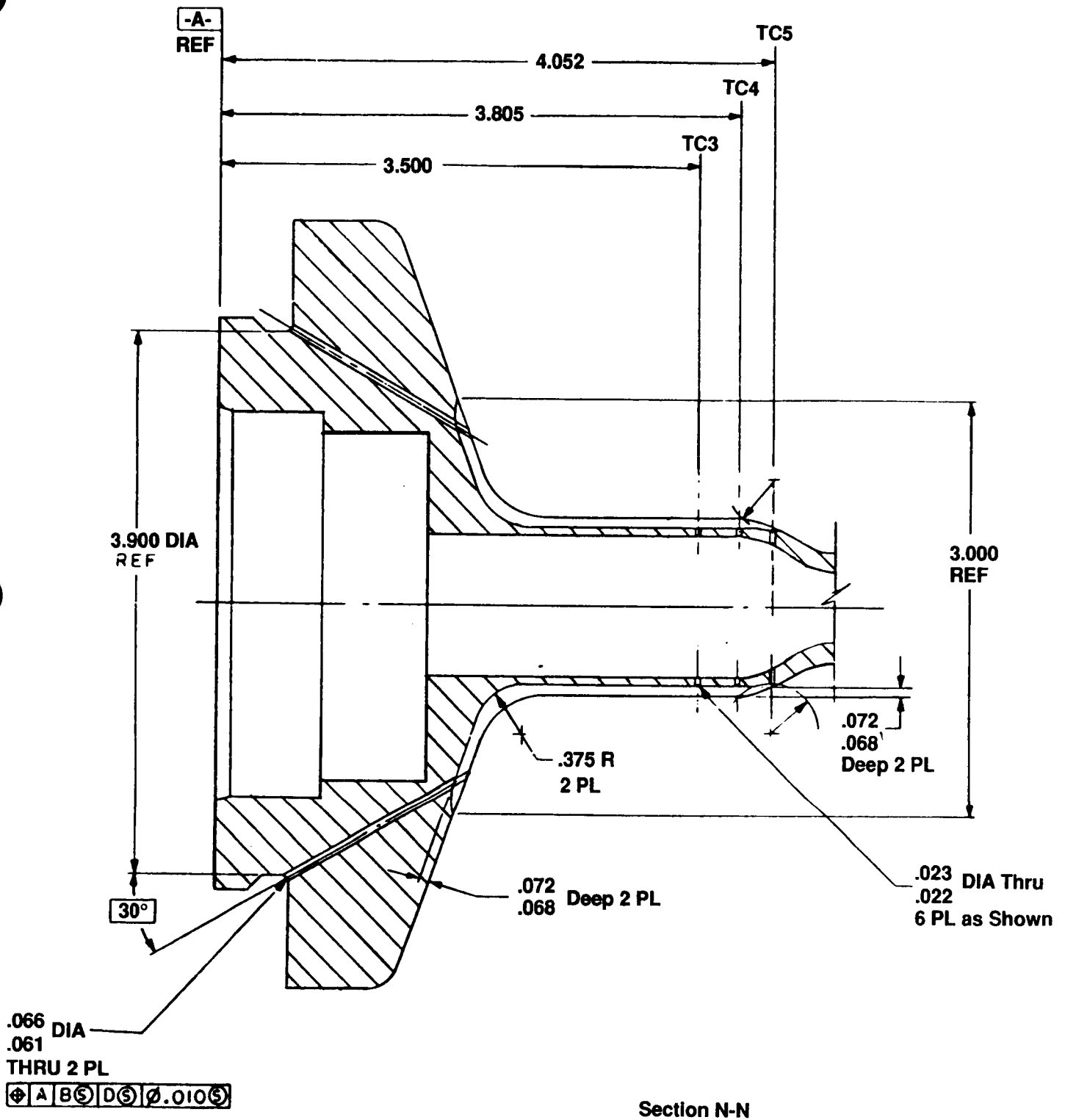


Figure 52. Row B and Row D Thermocouples

TABLE XII
THRUSTER NO. 2 TEST SUMMARY
FOR
MIXTURE RATIO RANGE

Mixture Ratio O/F	Total Duration (sec)	Total Impulse (lbf-sec)
3.0	105	2,265
3.5	230	5,880
4.0	629	15,960
4.5	20	507
5.0	666	18,232
5.5	10	249
6.0	534	14,718
6.5	5	131
7.0	295	7,714
7.5	9	216
8.0	328	8,433
8.5	14	338
9.0	—	—
9.5	<u>37</u>	<u>926</u>
Total:	2,882	75,569

TABLE XIII

**THRUSTER NO. 2 TEST SUMMARY
FOR
PERCENT FUEL FILM COOLING RANGE**

<u>Fuel Film Cooling, FFC - (%)</u>	<u>Mixture Ratio O/F</u>	<u>Total Duration, t-(sec)</u>	<u>Total Impulse, I_t-(lbf-sec)</u>
55.2	3.0	5	124
	3.5	85	2,106
	4.0	154	3,664
	5.0	148	4,234
	6.0	135	3,917
	7.0	65	1,802
	7.5	4	91
	8.0	84	2,014
	8.5	9	216
	60.9	3.0	95
3.5		140	3,644
4.0		405	10,479
4.5		15	381
5.0		448	12,276
5.5		10	249
6.0		334	9,181
6.5		5	131
7.0		168	4,320
7.5		5	125
8.0		235	6,204
8.5		5	122
9.5		37	926
64.2		3.0	5
	3.5	5	130
	4.0	70	1,817
	4.5	5	126
	5.0	70	1,722
	6.0	65	1,620
	7.0	62	1,592
	8.0	<u>9</u>	<u>215</u>
	Total:	2,882	75,569

IV, D, Test (cont.)

4. Experimental Results

The testing performed at NASA LeRC during the summer of 1989 consisted solely of limited checkout testing. Some initial ignition problems were caused by an improperly insulated high voltage cable, but these were ultimately resolved. In addition, the sealing surface at the injector/chamber interface was scratched while resolving the ignition problem, resulting in below normal performance measurements due to slight GH_2 leakage during a number of tests, occurred. As a result, the number of tests providing a true view of the Thruster No. 2 operation were fewer than desired, but sufficient to determine its operating characteristics. Tests were conducted over mixture ratios ranging from 2.86 to 9.47 at fuel film cooling (FFC) percentages of 55.2, 64.2 and 60.9. Due to the aforementioned GH_2 leakage, the tests for FFC's of 55.2 and 64.2 percent were suspect as performance measurements were too low. Tests at 60.9 percent FFC with and without GH_2 leakage showed a consistent trend.

The measured thruster performance for 60.9 percent FFC at a nominal chamber pressure of 75.0 psia followed the predicted performance within 1 to 2 percent from a mixture ratio of 3.0 to 8.0, as shown in Figure 53. The line for the predicted values was for an assumed injector energy release efficiency (ERE) of 97 percent. The maximum ERE determined for Thruster No. 1 was 96.1 percent. Using this ERE value for predicting performance resulted in Figure 54, where the predicted and the measured performance coincided over the range of mixture ratio from 3.0 to 8.0.

Unlike the performance data, the measured thermal data did not closely follow the prediction. The trend was right, but the magnitude was high by about 200°F for the gas-side wall. In addition, the ΔT through the chamber wall appeared to be less than the predicted 100°F . These comparisons were depicted in Figure 55. Although the wall temperature was higher, the fact that the ΔT was lower indicated an even greater low cycle fatigue (LCF) life available; however, the LCF was already in excess of 10,000 cycles for a predicted ΔT of 100°F .

E. EVALUATION OF RESULTS

Since Space Station Thruster No. 2 had a significant number of thermocouples (T/C) for taking gas-side and back-side wall temperature data, as well as coolant bulk temperature rise, calibration of the thermal model was performed. The thruster was instrumented with 12 gas-side

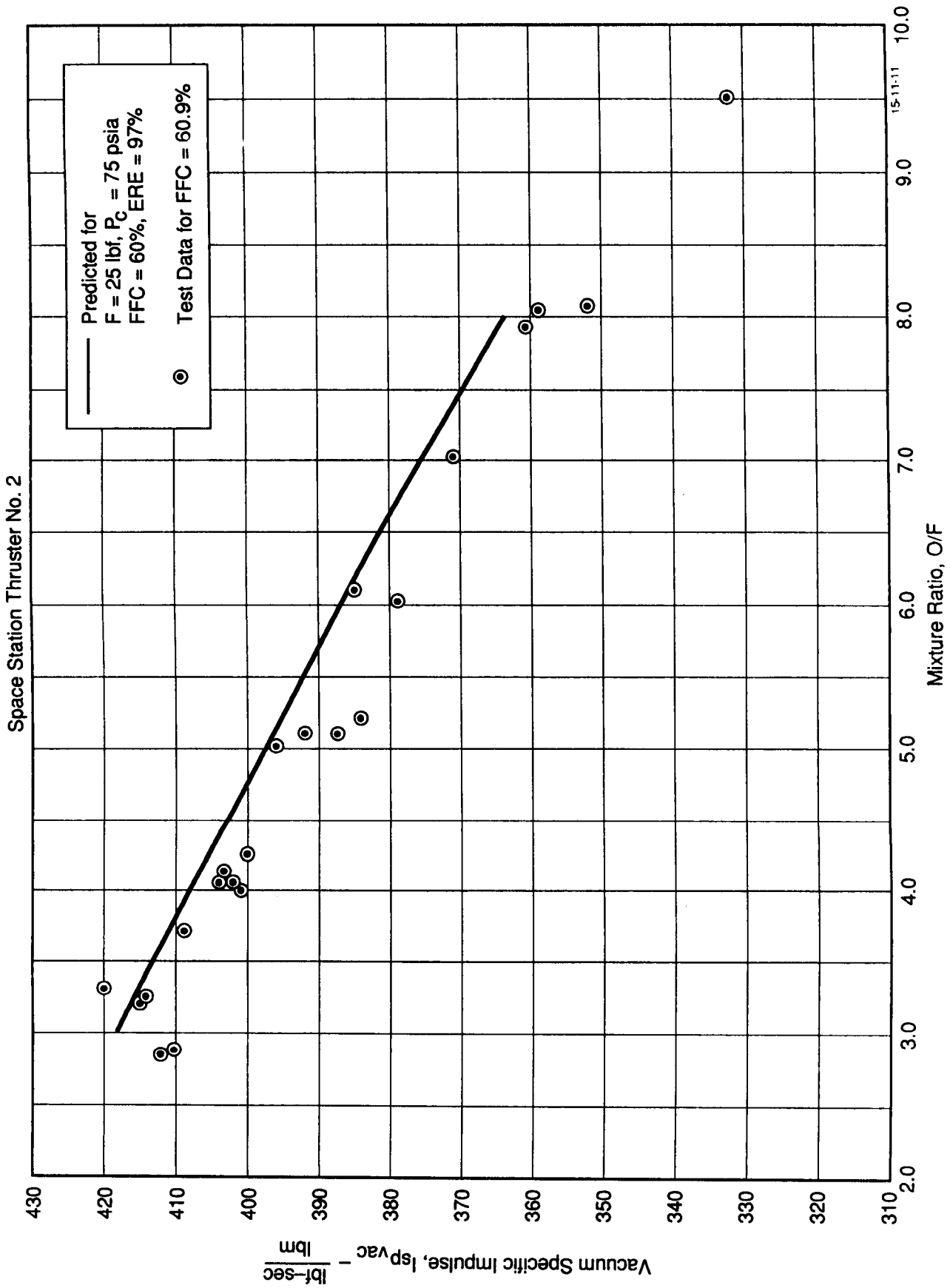


Figure 53. Predicted Vs. Measured Performance for an Assumed Injector ERE of 97.0%

Space Station Thruster No. 2

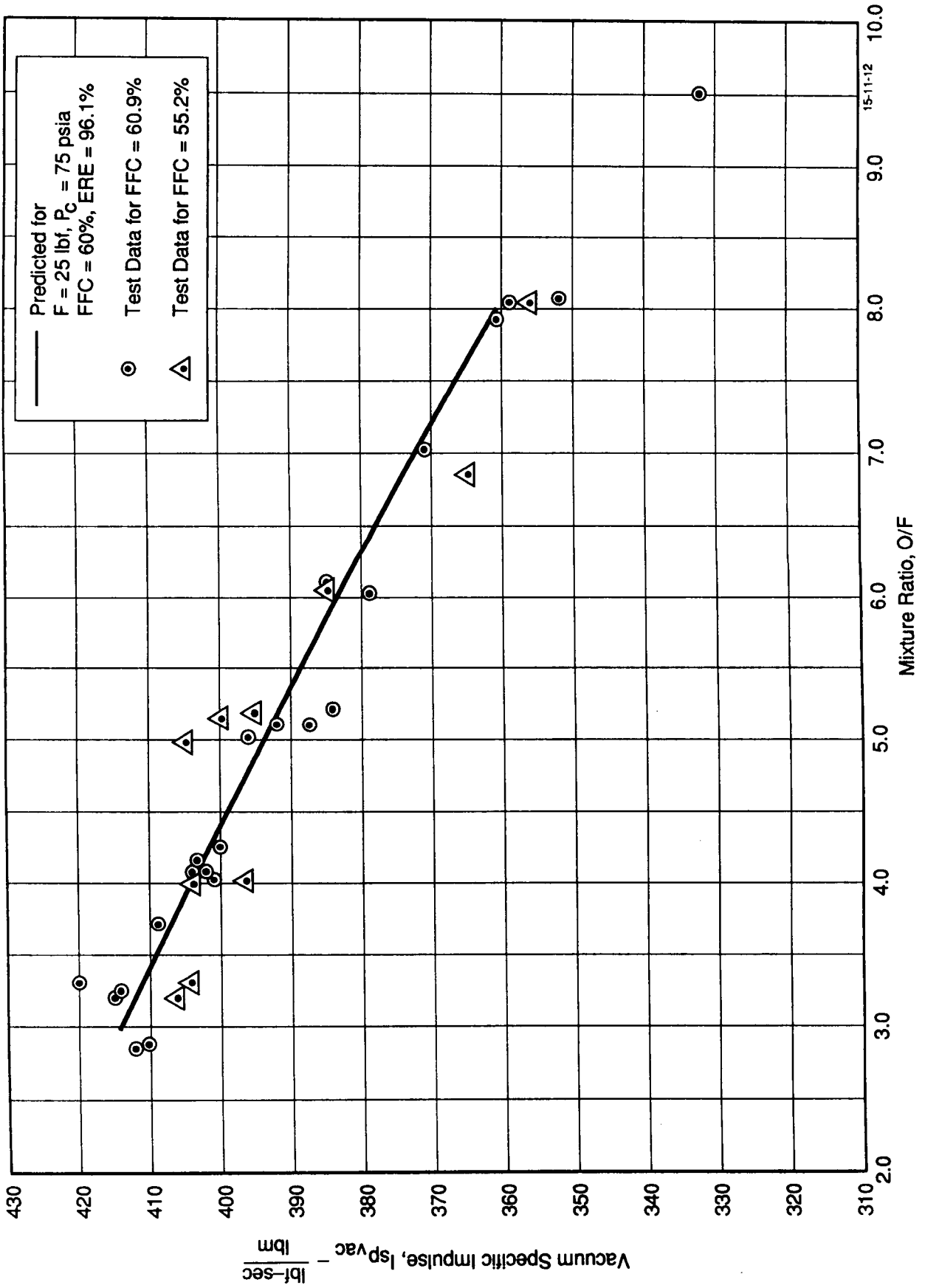


Figure 54. Predicted Vs. Measured Performance for an Assumed Injector ERE of 96.1%

**Pretest Predicted vs Measured Wall Temperatures
(Earlier Model @ Nominal Conditions)
Pretest Thermal Model @ Nominal (Design Point) Conditions**

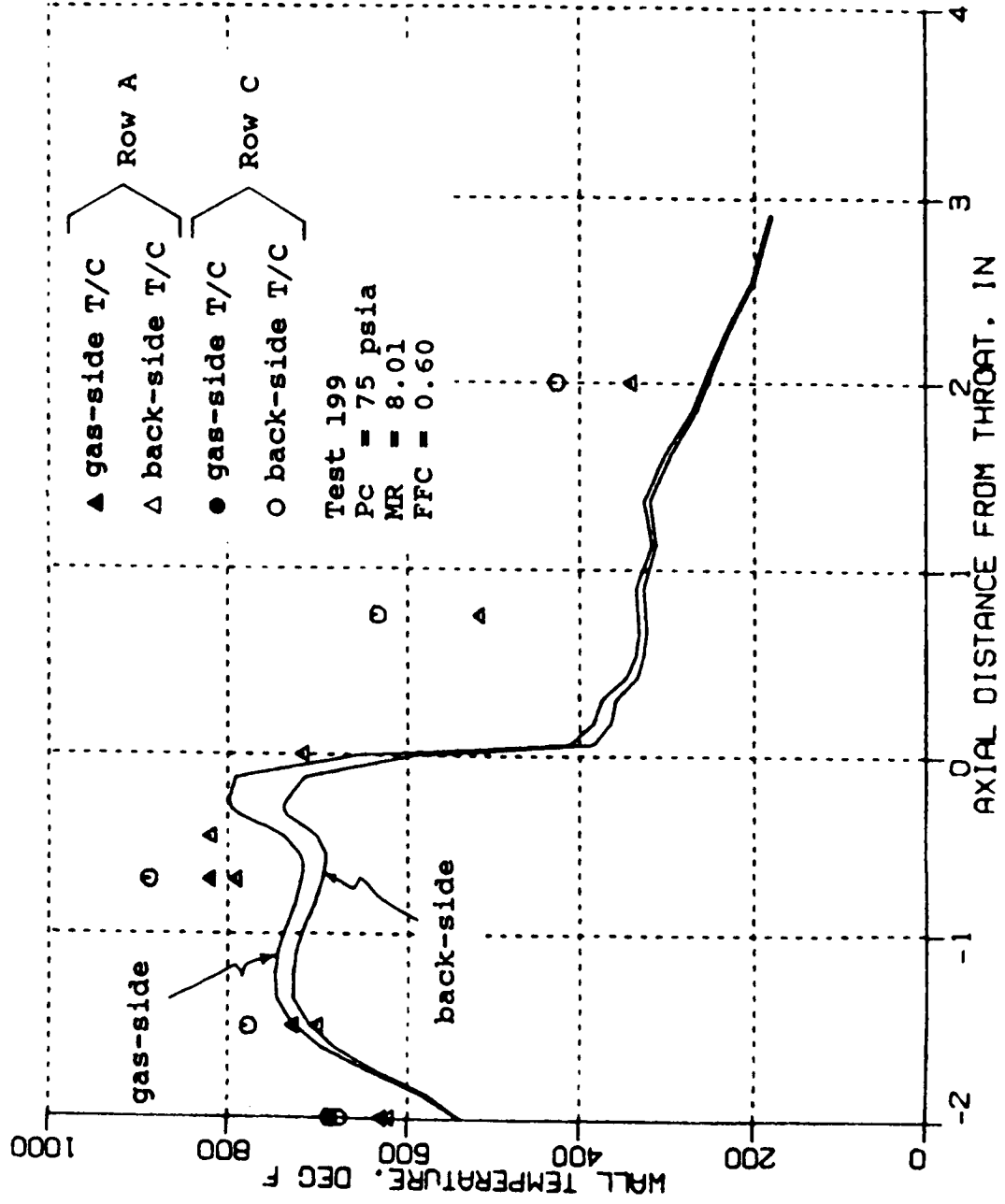


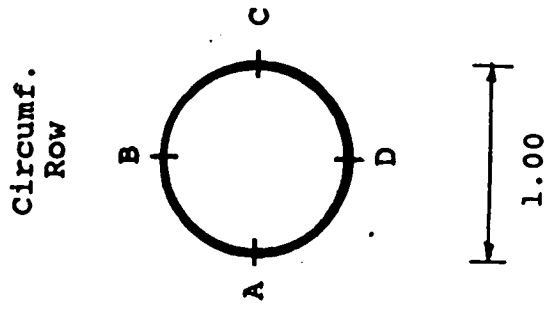
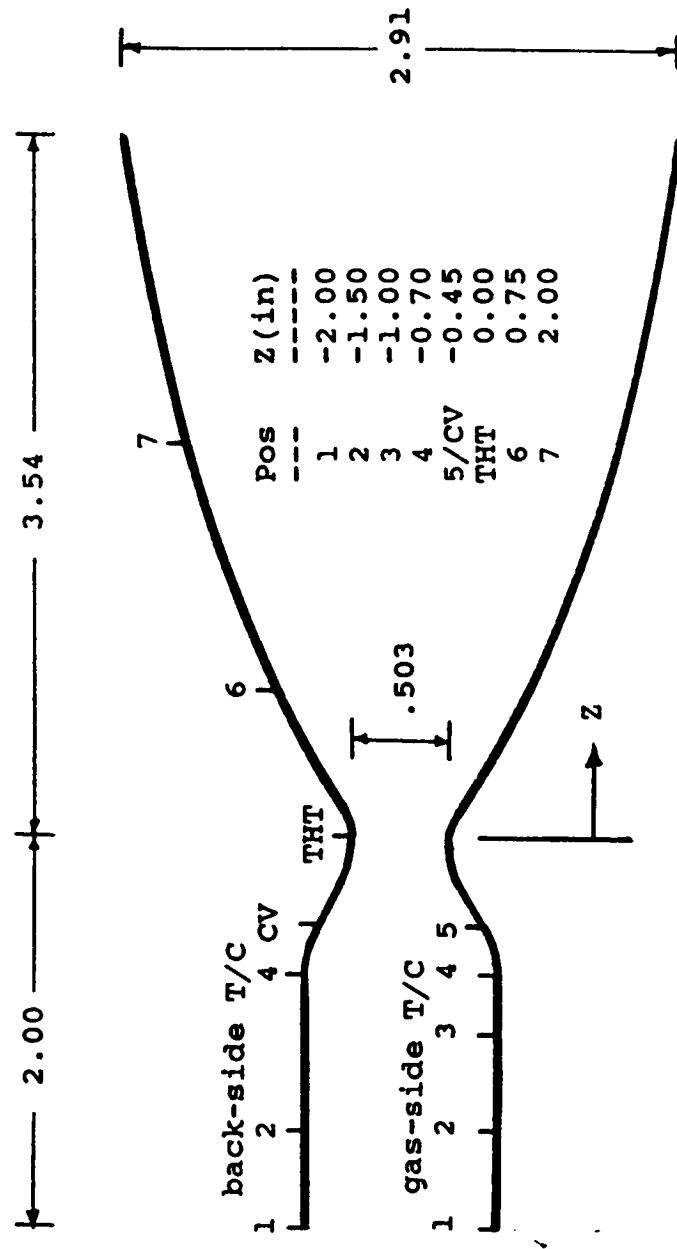
Figure 55. Measured vs Predicted Wall Temperatures at the Design Point

IV, E, Evaluation of Results (cont.)

thermocouples and 18 back-side thermocouples scattered over a grid of 7 axial stations and 4 circumferential positions, as shown in Figure 56, where axial station 1 corresponds to the end of the film coolant sleeve insert. Steady state data from five tests (Test No. 166, 193, 199, 207, and 227) were chosen to define representative wall temperatures over a wide range of mixture ratio. Tables XIV to XVIII present the test data summary for these five tests. Due to the scarcity of gas-side thermocouples, the back-side thermocouple data was used to calibrate and validate the model. Since the heat flux is low and the wall is made of copper, the difference in temperature between the gas-side and back-side is also low. The highest back-side temperatures were recorded along row C and the lowest along row A, which is on the other side. Row A has a back-side thermocouple measurement on all 7 axial positions, while row C has all but the convergent section and throat measurements. Since it was desirable to calibrate to the hottest row, the two missing measurements in row C were estimated from row A, as graphically illustrated in Figures 57 to 61 for the five tests.

Back-side wall temperature measurements from row C were used to calibrate the thermal model. The model was calibrated to the nominal conditions of 75 psia chamber pressure, a mixture ratio of 8 and 60% fuel film cooling, which were the conditions achieved in Test 199. The calibration was first performed for an entrainment multiplier, K_m , of 5.0, which was used for pretest predictions in an earlier model. This K_m value is based on the test data correlation of the JPL thruster. However, it was found that a K_m of 2.2 gave a better fit of the head end data, as shown in Figure 62. The C_{gn} profile for the calibrated model at both K_m values is shown in Figure 63. The C_{gn} value is 0.9 in the barrel, 0.6 in the throat, and 1.1 in the nozzle for the K_m of 5.0 model. The C_{gn} value is 1.3 in the barrel, 0.8 in the throat, and 1.1 in the nozzle for the K_m of 2.2 model. The slower mixing model, K_m of 2.2, requires higher C_{gn} values upstream of the throat to account for the lower wall mixture ratio. However, downstream of the throat, the wall mixture ratio for both K_m values is high enough as to produce similar heat fluxes, thus giving the same C_{gn} value. The predicted stream tube mixture ratios are shown in Figure 64 for both K_m values. The corresponding adiabatic wall temperatures are shown in Figure 65.

Four tests were used to validate the calibrated model at off-nominal conditions. Three tests (Test Nos. 193, 207, and 227) were at off-nominal mixture ratio conditions ($MR = 3 - 10$) and one test (Test No. 166) was at an off-nominal fuel film cooling condition (55% FFC). Figures 66 to 69 show that the slower mixing model, K_m of 2.2, predicts the measured back-side wall temperatures much better than the faster mixing model, K_m of 5.0, for all three off-mixture ratio tests. The slower mixing model also predicts the slope of wall temperature profile in the



Pos	Z (in)
1	-2.00
2	-1.50
3	-1.00
4	-0.70
5/CV	-0.45
THT	0.00
6	0.75
7	2.00

Figure 56. Thermocouple Grid Position

TABLE XIV
TEST DATA SUMMARY FOR TEST NO. 166

Test 166

t = 47.4 sec
 F = 26.66 lb
 Pc = 75 psia
 MR = 8.02
 Isp = 355.9 sec
 Wt = .0749 lb/sec
 Pcool = 105 psia (inlet)
 80 psia (outlet)
 Tcool = 78 deg F (inlet)
 599 deg F (outlet)
 FFC=.55

ΔT_{s1} = 297 deg F (Est.)
 T_{s1} = 599 + 297 = 896 deg F
 RHOC = .0104 lb/ft³
 RHOE = .0285 lb/ft³
 UCUE = 1.11
 MUSC = .918E-06 lb/in-sec

GAS-SIDE T/C

Axial Pos	Circumferential Pos			
	A	B	C	D
---	---	---	---	---
1	687	-	736	-
2	808	-	-	-
3	-	929	-	932
4	919	713	-	945
5	-	995	-	1005

BACK-SIDE T/C

Axial Pos	Circumferential Pos			
	A	B	C	D
---	---	---	---	---
1	676	698	705	717
2	775	805	839	817
4	882	914	954	922
CV	910	-	-	-
THT	856	-	-	-
6	566	-	616	-
7	368	-	437	-

Row C Estimate from Row A T/C

CV = 984 deg F
 THT = 926 deg F

TABLE XV
TEST DATA SUMMARY FOR TEST NO. 193

Test 193

t = 59.9 sec
F = 28.54 lb
Pc = 79 psia
MR = 5.12
Isp = 392.0 sec
Wt = .0728 lb/sec
Pcool = 129 psia (inlet)
 86 psia (outlet)
Tcool = 85 deg F (inlet)
 382 deg F (outlet)
FFC=.60

ΔT_{s1} = 234 deg F (Est.)
T_{s1} = 382 + 234 = 616 deg F
RHOC = .0138 lb/ft³
RHOE = .0248 lb/ft³
UCUE = 1.22
MUSC = .785E-06 lb/in-sec

GAS-SIDE T/C

Axial Pos	Circumferential Pos			
	A	B	C	D
1	412	-	442	-
2	490	-	-	-
3	-	561	-	574
4	529	539	-	567
5	-	573	-	590

BACK-SIDE T/C

Axial Pos	Circumferential Pos			
	A	B	C	D
1	404	423	436	438
2	460	481	510	496
4	503	527	577	543
CV	515	-	-	-
THT	477	-	-	-
6	333	-	378	-
7	233	-	320	-

Row C Estimate from Row A T/C

CV = 596 deg F
THT = 550 deg F

TABLE XVI
TEST DATA SUMMARY FOR TEST NO. 199

Test 199

t = 59.5 sec
F = 27.81 lb
Pc = 75 psia
MR = 8.01
Isp = 358.8 sec
Wt = .0775 lb/sec
Pcool = 105 psia (inlet)
 79 psia (outlet)
Tcool = 86 deg F (inlet)
 580 deg F (outlet)
FFC=.60

ΔTsl = 258 deg F (Est.)
Tsl = 580 + 258 = 838 deg F
RHOC = .0109 lb/ft³
RHOE = .0304 lb/ft³
UCUE = 1.24
MUSC = .890E-06 lb/in-sec

GAS-SIDE T/C

Axial Pos	Circumferential			Pos
	A	B	C	
1	631	-	687	-
2	728	-	-	-
3	-	834	-	861
4	819	663	-	868
5	-	893	-	922

BACK-SIDE T/C

Axial Pos	Circumferential			Pos
	A	B	C	
1	622	643	677	671
2	701	728	777	759
4	790	819	884	848
CV	818	-	-	-
THT	717	-	-	-
6	517	-	634	-
7	342	-	427	-

Row C Estimate from Row A T/C

CV = 918 deg F
THT = 822 deg F

TABLE XVII
TEST DATA SUMMARY FOR TEST NO. 207

Test 207

t = 59.6 sec
 F = 25.40 lb
 Pc = 72 psia
 MR = 3.26
 Isp = 414.3 sec
 Wt = .0613 lb/sec
 Pcool = 145 psia (inlet)
 82 psia (outlet)
 Tcool = 89 deg F (inlet)
 294 deg F (outlet)
 FFC=.60

$\Delta T_{s1} = 211$ deg F (Est.)
 $T_{s1} = 294 + 211 = 505$ deg F
 RHOC = .0140 lb/ft³
 RHOE = .0174 lb/ft³
 UCUE = 1.27
 MUSC = .730E-06 lb/in-sec

GAS-SIDE T/C

Axial Pos	Circumferential Pos			
	A	B	C	D
---	---	---	---	---
1	304	-	323	-
2	379	-	-	-
3	-	460	-	459
4	433	426	-	427
5	-	423	-	426

BACK-SIDE T/C

Axial Pos	Circumferential Pos			
	A	B	C	D
---	---	---	---	---
1	299	311	313	317
2	336	350	360	353
4	368	383	397	390
CV	367	-	-	-
THT	327	-	-	-
6	234	-	266	-
7	180	-	233	-

Row C Estimate from Row A T/C

CV = 396 deg F
 THT = 357 deg F

TABLE XVIII
TEST DATA SUMMARY FOR TEST NO. 227

Test 227

 t = 31.6 sec
 F = 25.34 lb
 Pc = 71 psia
 MR = 9.47
 Isp = 331.6 sec
 Wt = .0764 lb/sec
 Pcool = 95 psia (inlet)
 73 psia (outlet)
 Tcool = 88 deg F (inlet)
 595 deg F (outlet)
 FFC=.60

ΔTsl = 266 deg F (Est.)
 Tsl = 595 + 266 = 861 deg F
 RHOC = .0101 lb/ft³
 RHOE = .0314 lb/ft³
 UCUE = 1.18
 MUSC = .901E-06 lb/in-sec

GAS-SIDE T/C

Axial Pos	Circumferential Pos			
	A	B	C	D
1	704	-	754	-
2	825	-	-	-
3	-	934	-	975
4	937	805	-	986
5	-	1002	-	1044

BACK-SIDE T/C

Axial Pos	Circumferential Pos			
	A	B	C	D
1	693	708	726	746
2	799	817	868	858
4	907	925	996	964
CV	934	-	-	-
THT	885	-	-	-
6	593	-	665	-
7	388	-	488	-

Row C Estimate from Row A T/C

 CV = 1028 deg F
 THT = 976 deg F

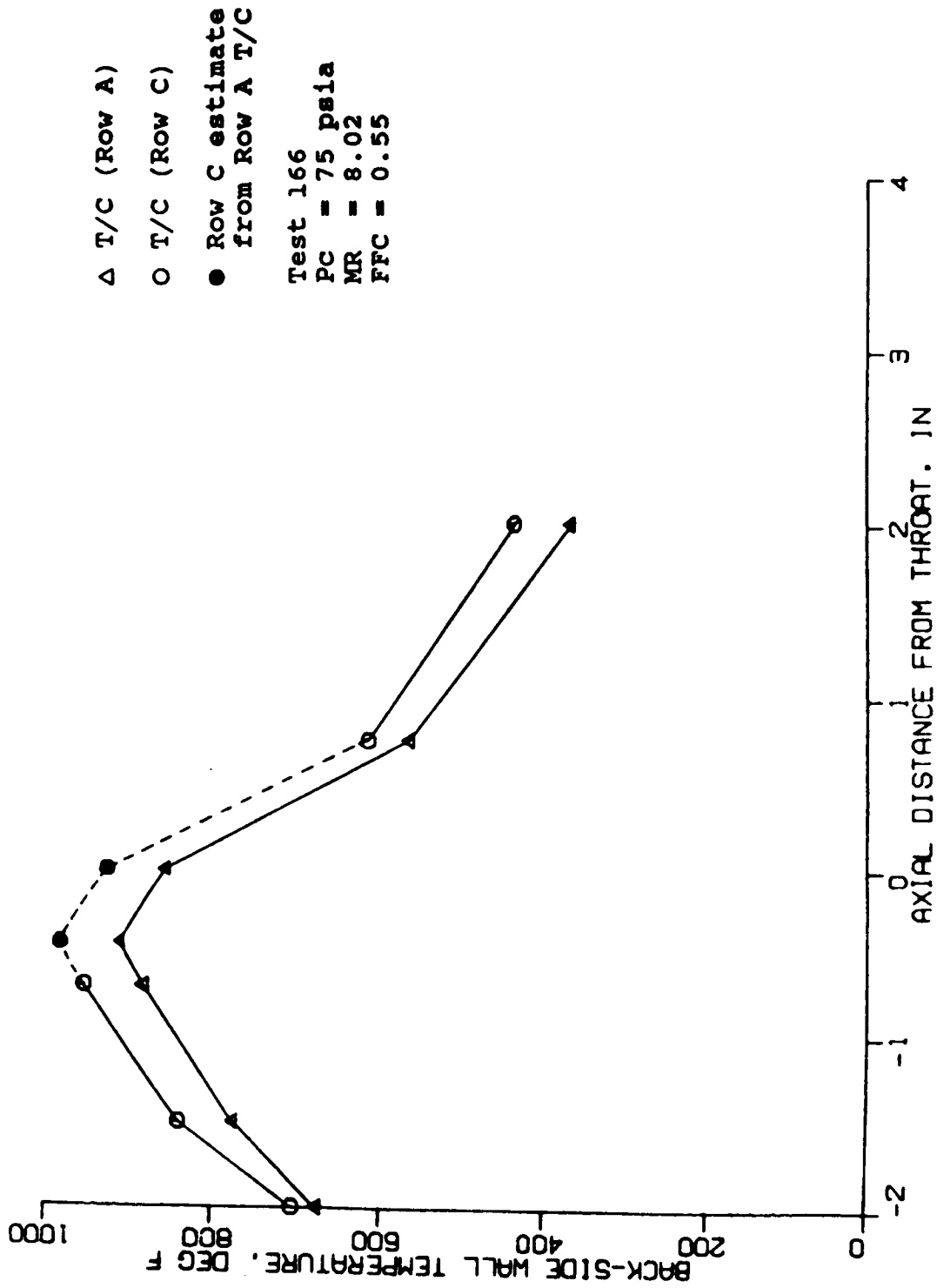


Figure 57. Measured Back-Side Wall Temperatures for Test No. 166

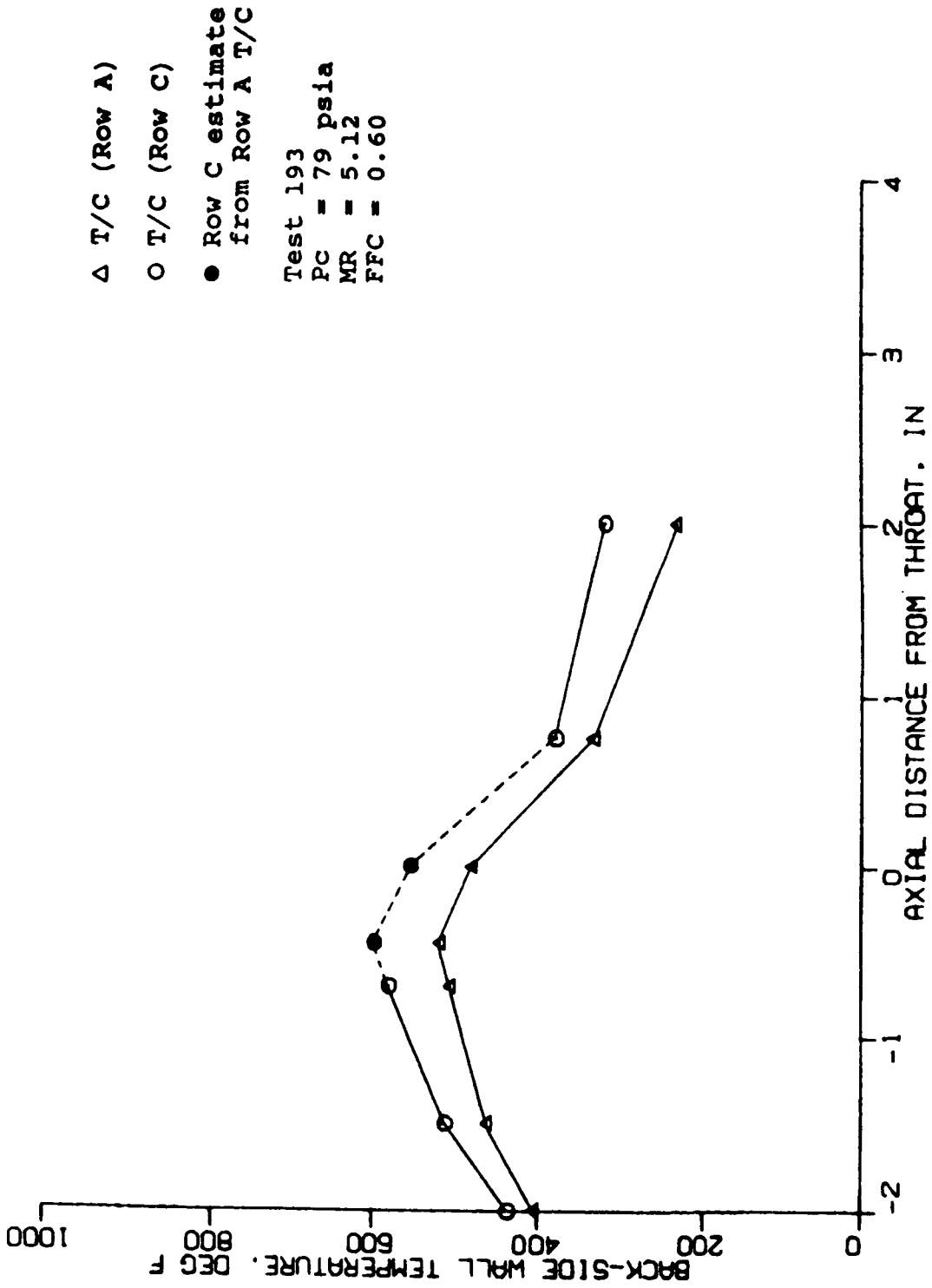


Figure 58. Measured Back-Side Wall Temperatures for Test No. 193

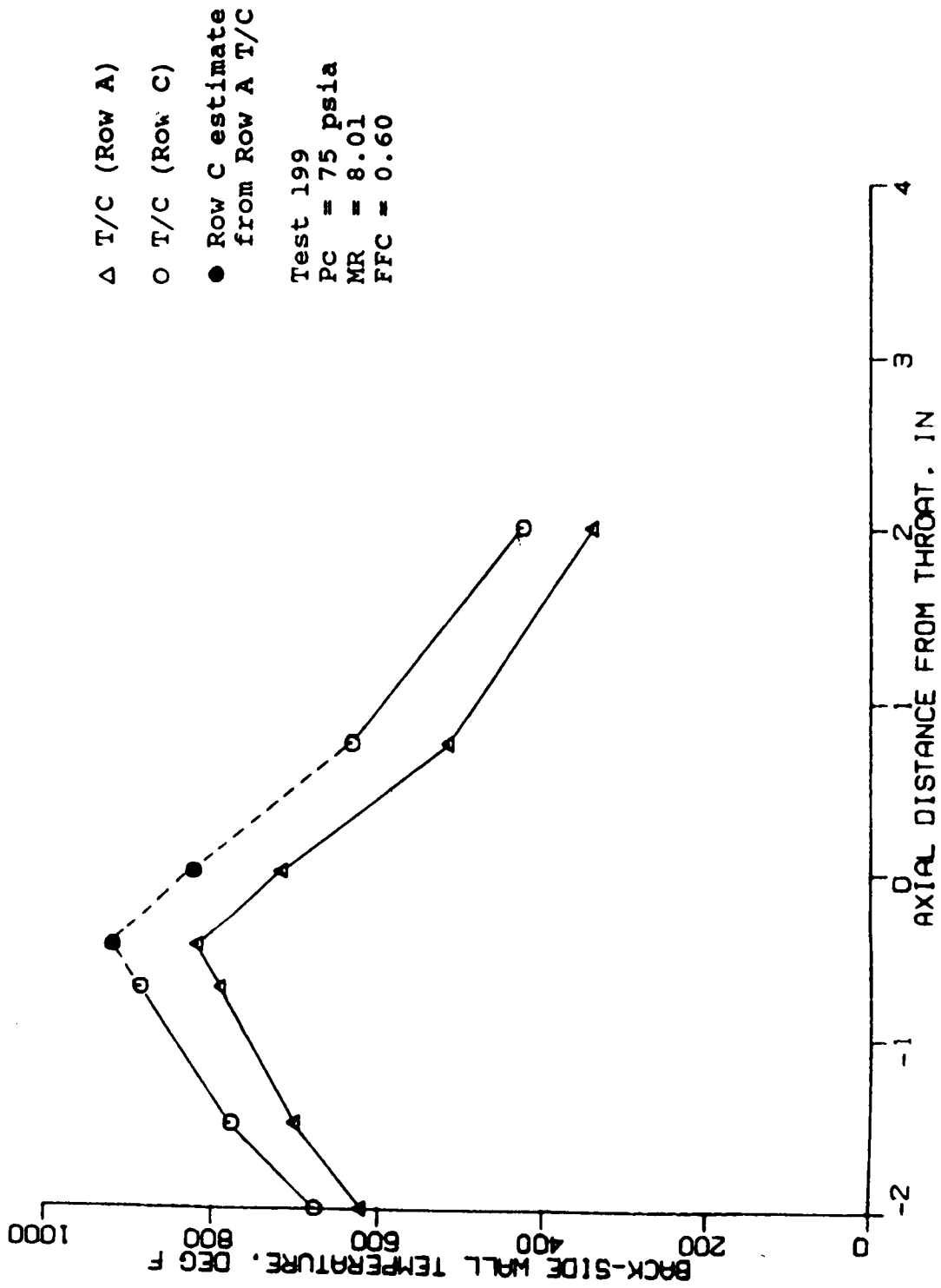


Figure 59. Measured Back-Side Wall Temperatures for Test No. 199

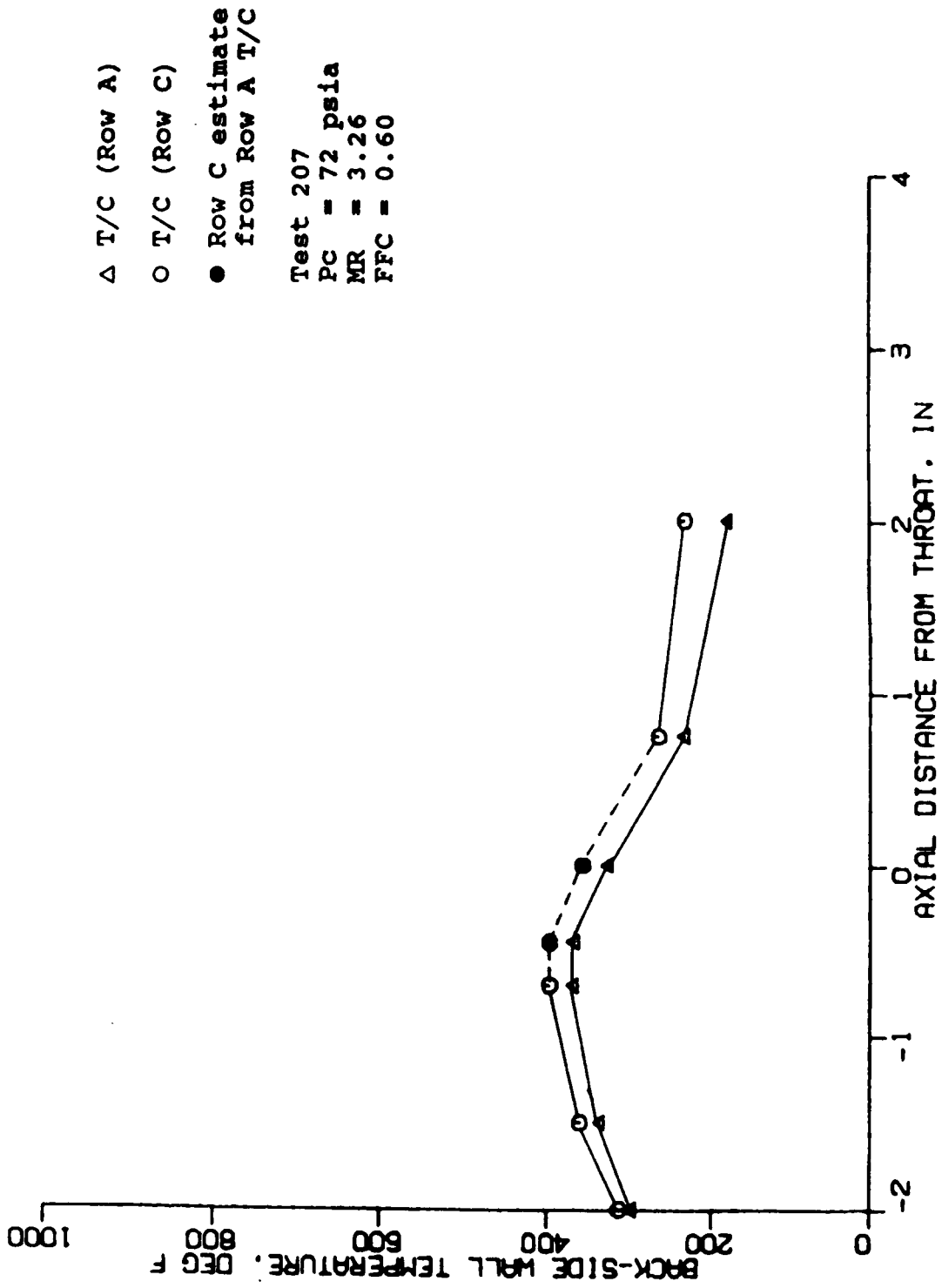


Figure 60. Measured Back-Side Wall Temperatures for Test No. 207

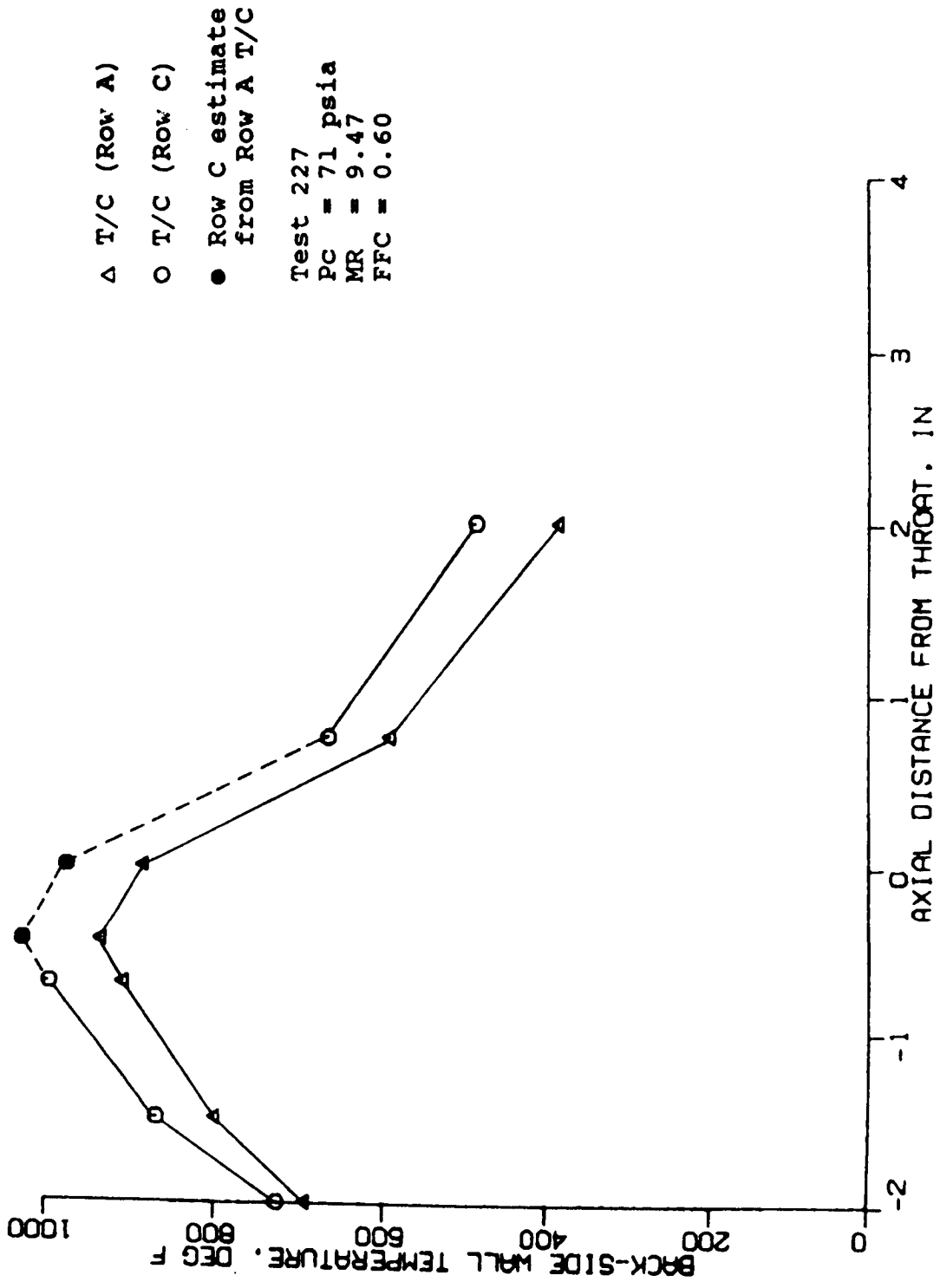


Figure 61. Measured Back-Side Wall Temperatures for Test No. 227

(Model Calibration Test @ Nominal Conditions)

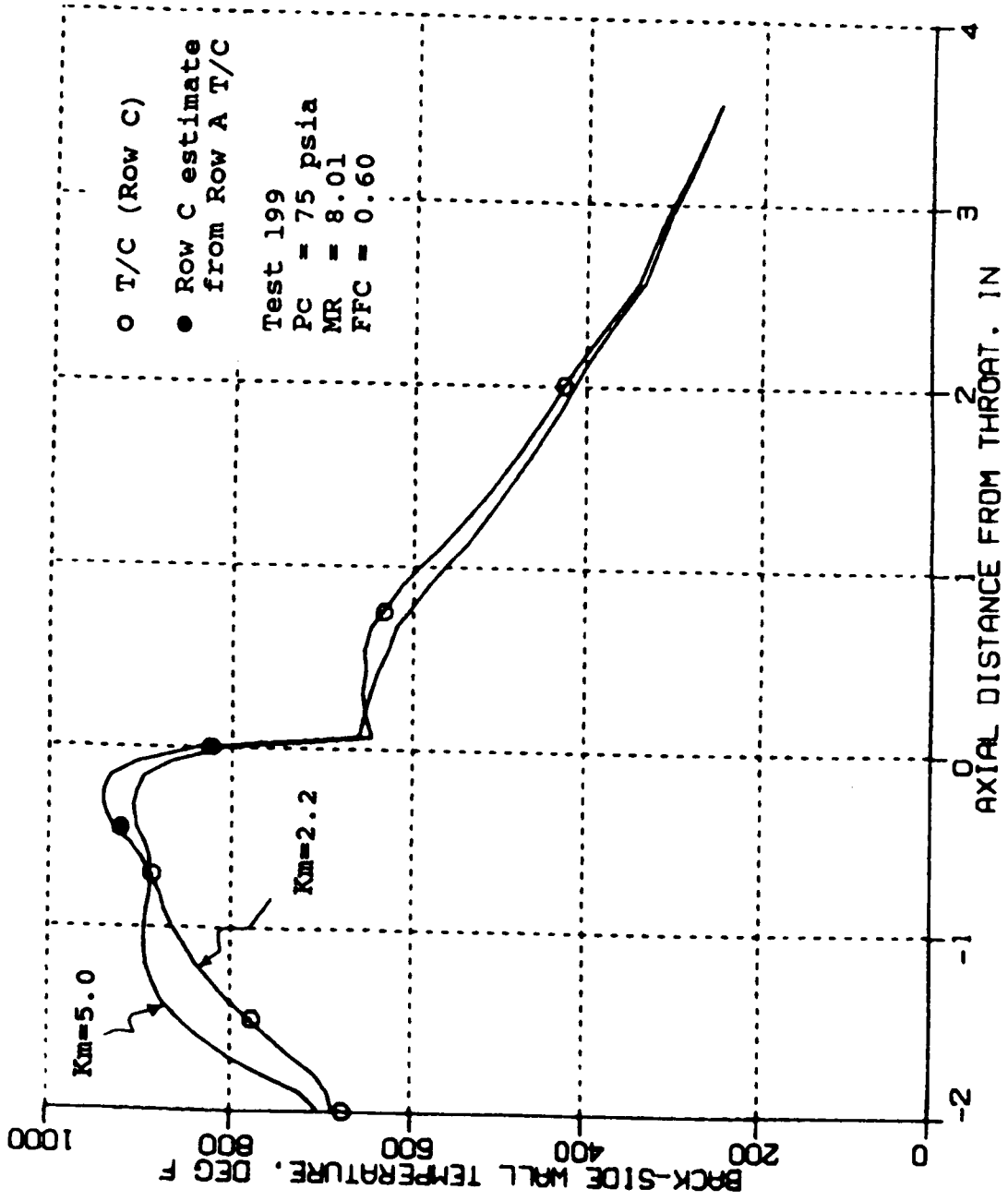


Figure 62. Predicted vs Measured Back-Side Wall Temperatures for the Thruster Design Point

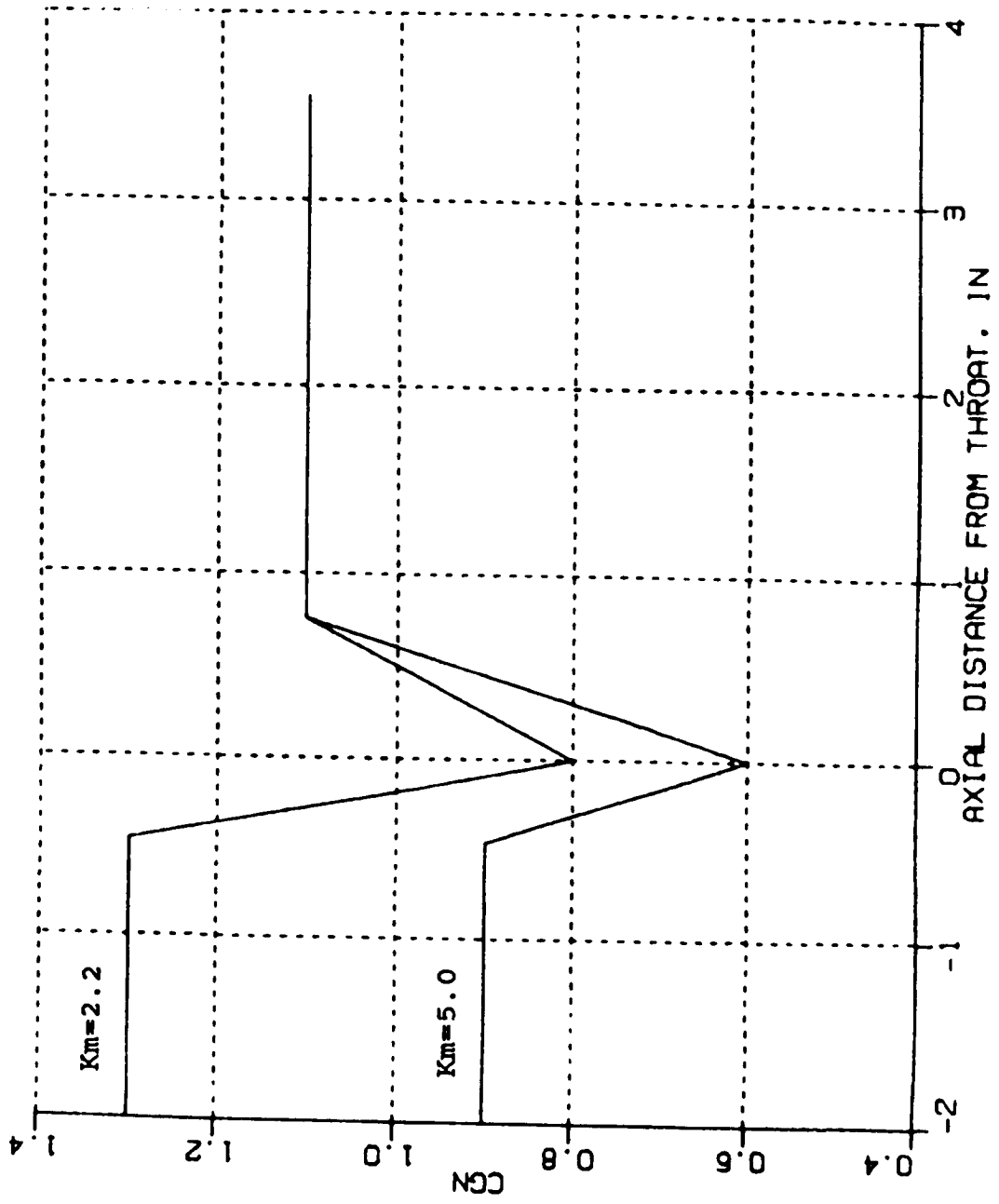


Figure 63. Cgn Profile for Calibrated Model

(Nominal Conditions)

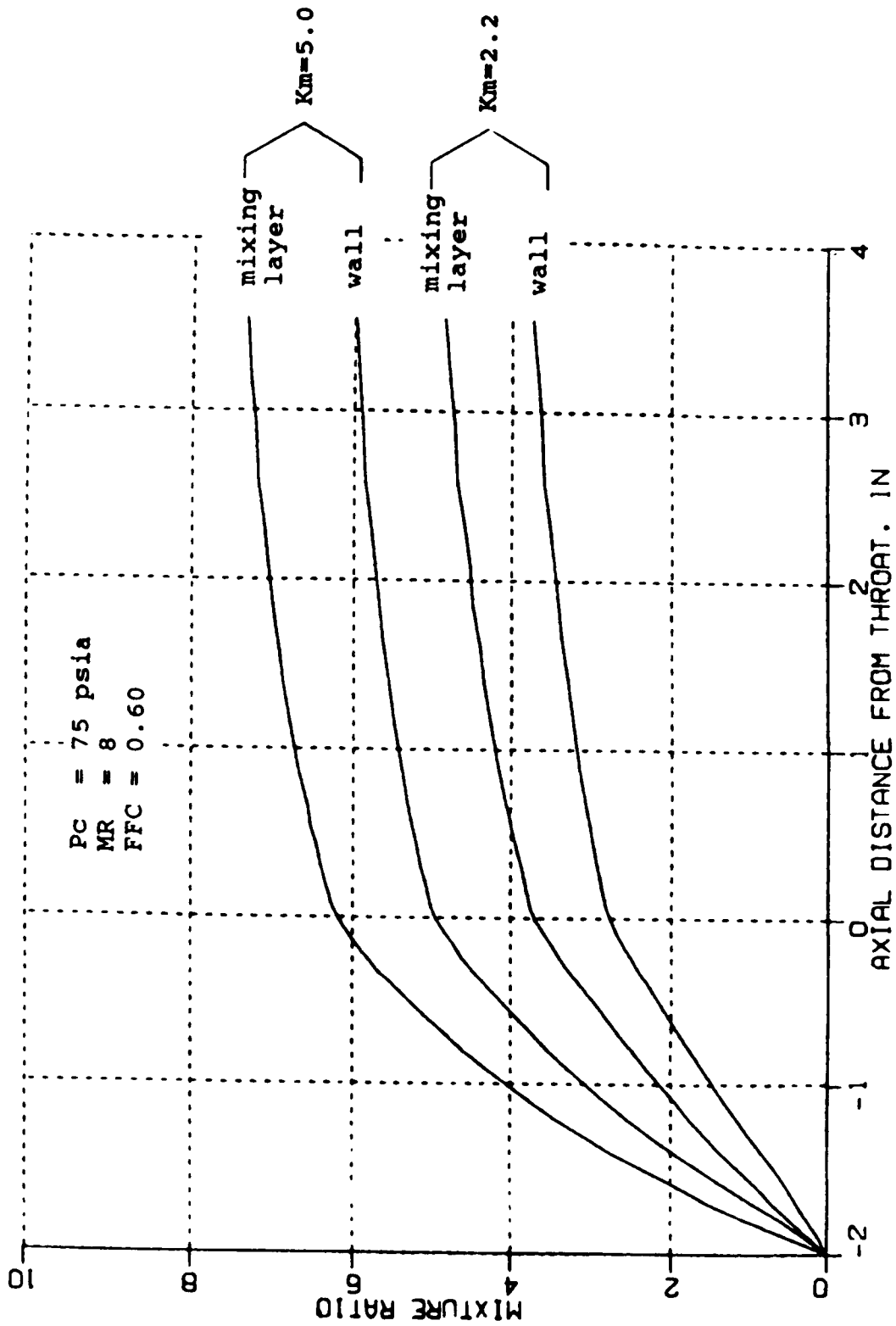


Figure 64. Predicted Stream Tube Mixture Ratios

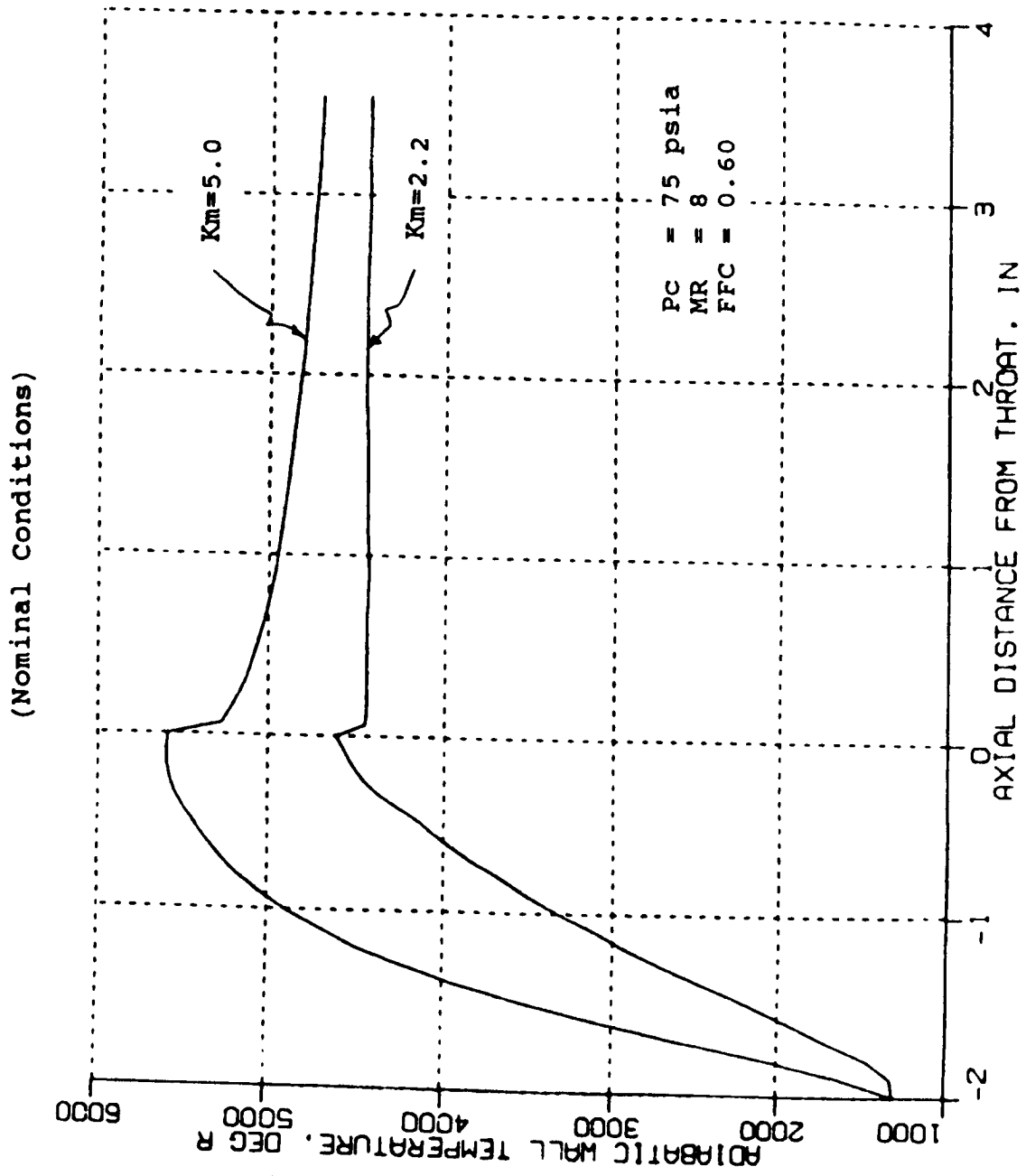


Figure 65. Predicted Adiabatic Wall Temperatures

(Off-Nominal Mixture Ratio)

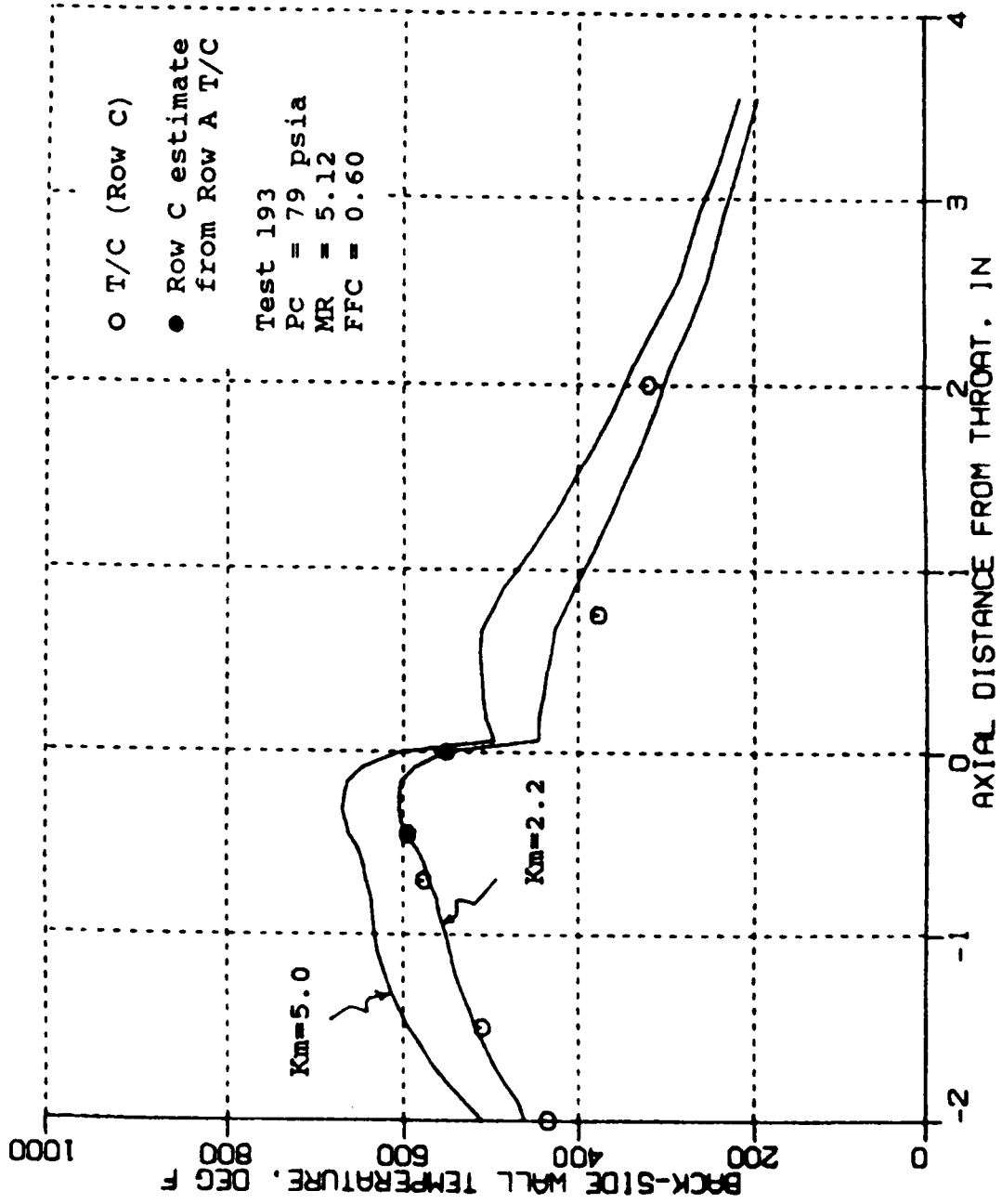


Figure 66. Predicted vs Measured Back-Side Wall Temperatures for Test No. 193

(Off-Nominal Mixture Ratio)

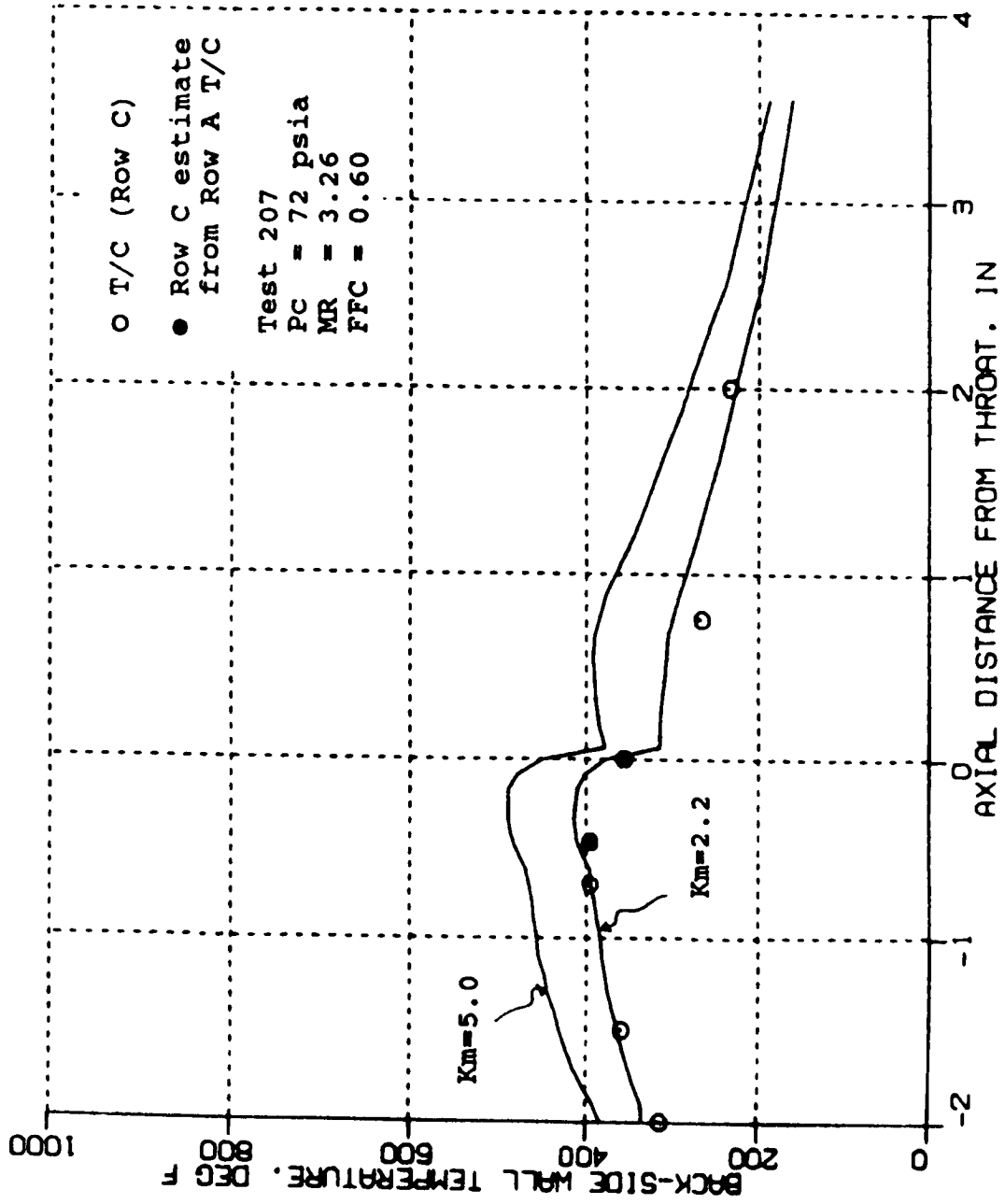


Figure 67. Predicted vs Measured Back-Side Wall Temperatures for Test No. 207

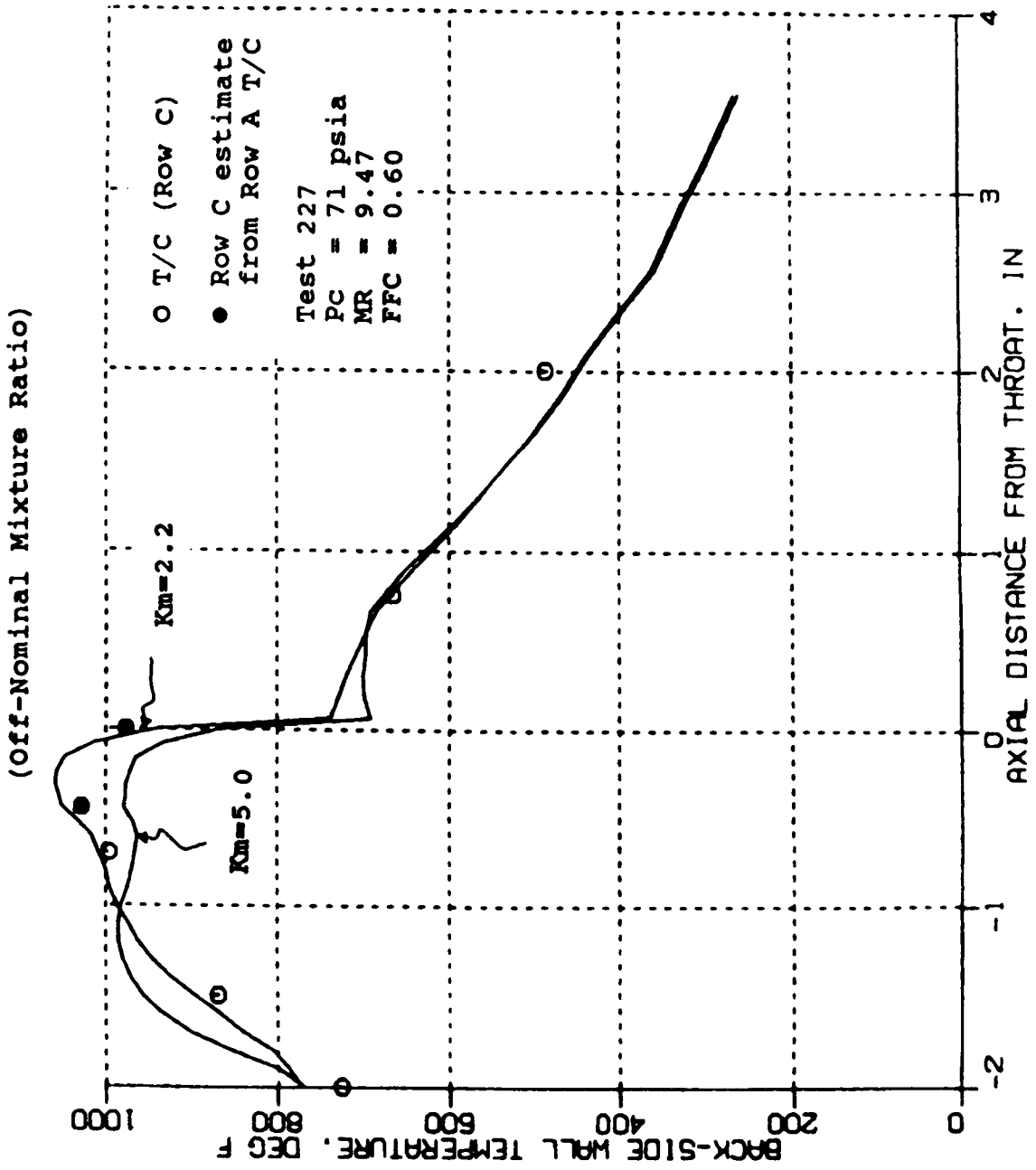


Figure 68. Predicted vs Measured Back-Side Wall Temperatures for Test No. 227

(Off-Nominal Fuel Film Cooling)

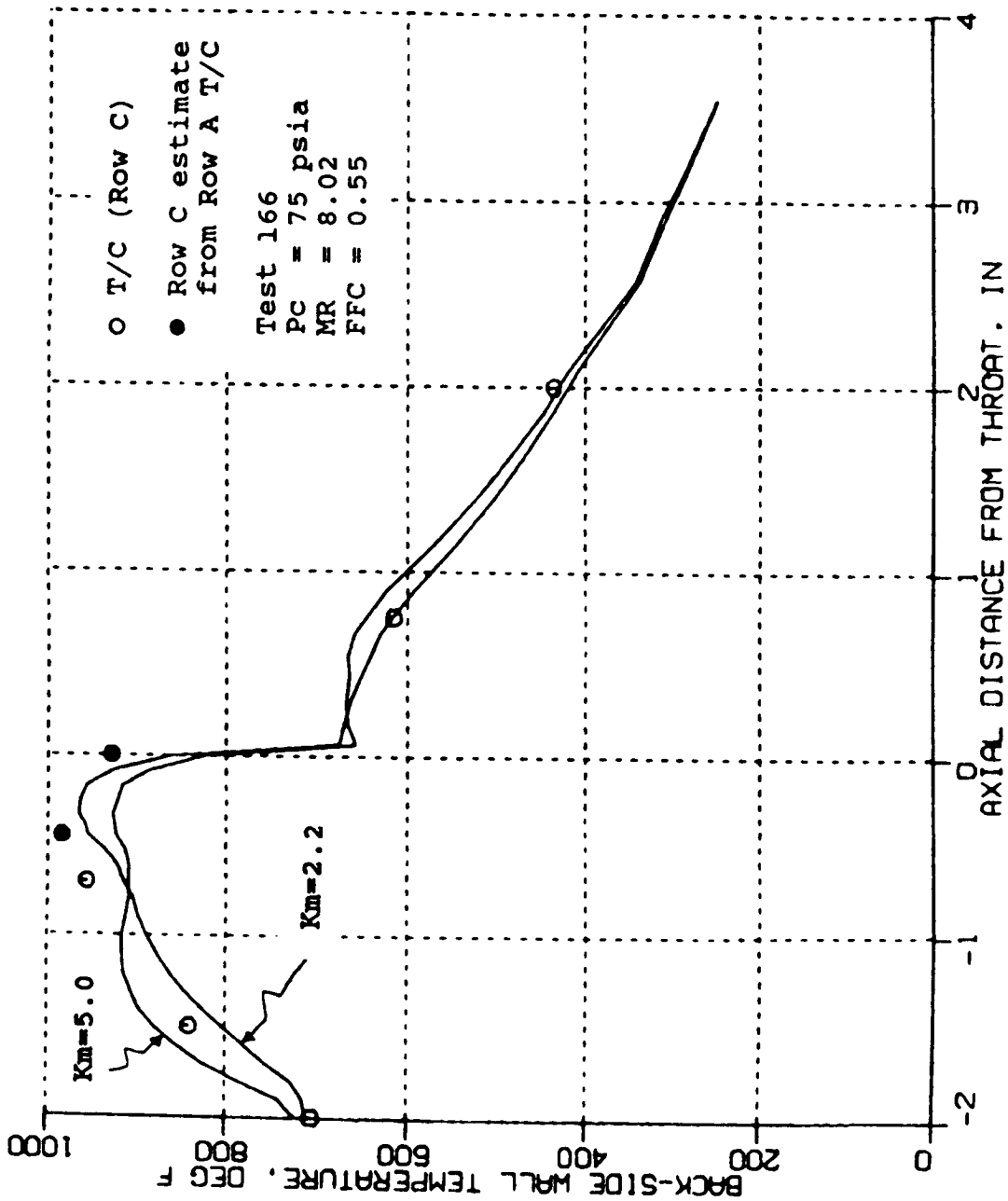


Figure 69. Predicted vs Measured Back-Side Wall Temperatures for Test No. 166

IV, E, Evaluation of Results (cont.)

barrel, especially at higher mixture ratios. The faster mixing model tends to overpredict at lower than nominal mixture ratio and underpredict at higher than nominal mixture ratio. Both models under predicted the lower fuel film cooling test, although the slower mixing model matched the slope of the temperatures in the barrel. This indicates that a slightly higher K_m value in the slower mixing model is necessary to match the 55% fuel film cooling condition.

Figure 70 shows the updated predictions of maximum gas-side and back-side wall temperatures for nominal conditions using the slower mixing (K_m of 2.2) model. A maximum gas-side wall temperature of 1010 deg F is predicted just upstream of the throat. A maximum temperature difference between the gas-side and back-side of 89 deg F is also predicted just upstream of the throat. As previously discussed, such a low ΔT through the chamber wall resulted in a LCF life well in excess of 10,000 cycles due to the extremely small thermal strain range. In addition, the thruster surpassed the minimum criteria for creep rupture; therefore, the life limiting case would be high cycle fatigue (HCF).

Even though the performance data fit very well with predicted values, the former predictions were based on the old thermal model with its entrainment multiplier, K_m , of 5.0. Therefore, performance predictions were made from the thermal model using the new K_m of 2.2. Initially the mixing was assumed to be complete by the throat plane, as the previous predictions used this assumption with good results; however, the new predictions for a perfect injector (ERE = 100 percent) were too low, i.e., lower than the measured performance data. It was then assumed that some mixing did in fact occur downstream of the throat and the thermal mixing model determined mixing up to the nozzle exit plane. This output from the thermal model was used as input to the performance model, with the resulting performance predictions for a perfect injector forming effectively an upper limit on performance. These two sets of predictions were plotted in Figure 71 along with the same measured data that was plotted in Figures 53 and 54. The majority of the data lies just under the upper limit, thus substantiating the assumption that some mixing does in fact occur downstream of the throat plane. Furthermore, the effective injector ERE appears to range from 99.7 percent at an O/F of 3.0 to 98.5 percent at an O/F of 8.0, relative to the upper limit. This value of ERE is more consistent with the earlier ERE assumption of 97 percent, i.e., an improvement over the 96.1 percent ERE of Thruster No. 1.

To gain a better appreciation for the performance increase in going from the Thruster No. 1 design to the Thruster No. 2 design, Figure 72 was prepared. In this figure, the performance of Thruster No. 1 was plotted as a function of mixture ratio. A performance prediction

(Calibrated Model [Km=2.2] @ Nominal Conditions)

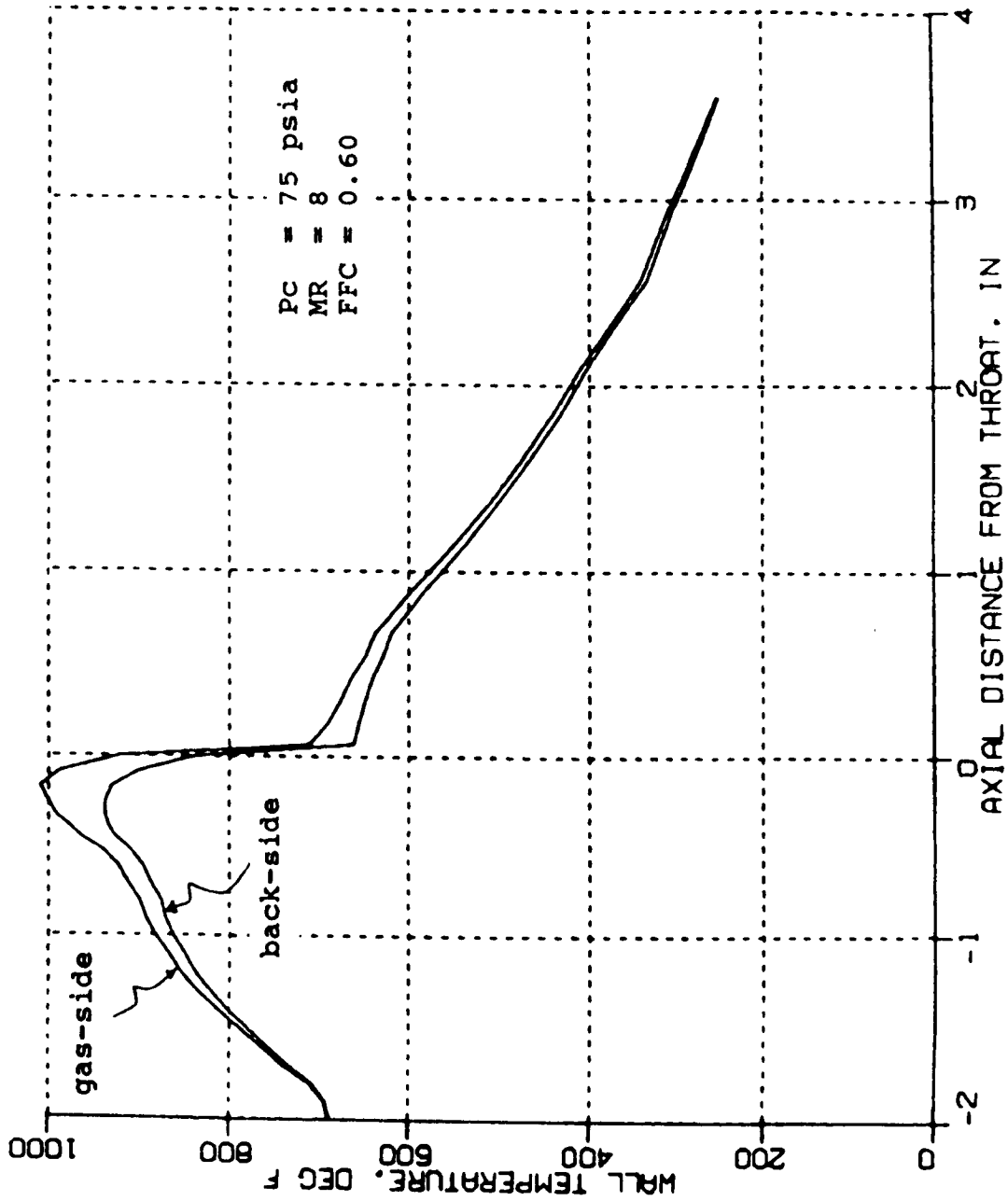


Figure 70. Predicted Maximum Wall Temperatures for Design Point

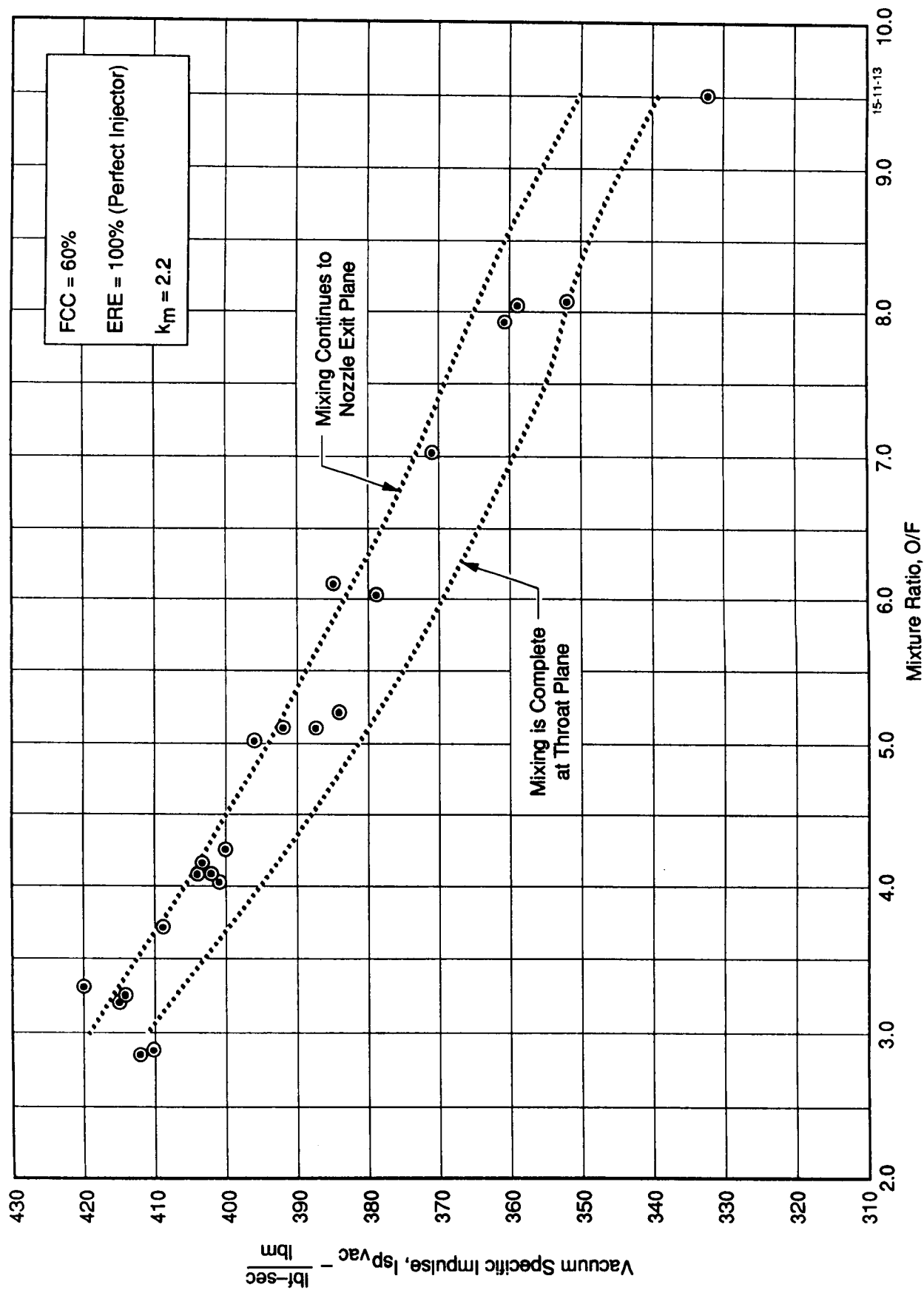


Figure 71. Revised Space Station Thruster Performance Predictions for Calibrated Thermal Model

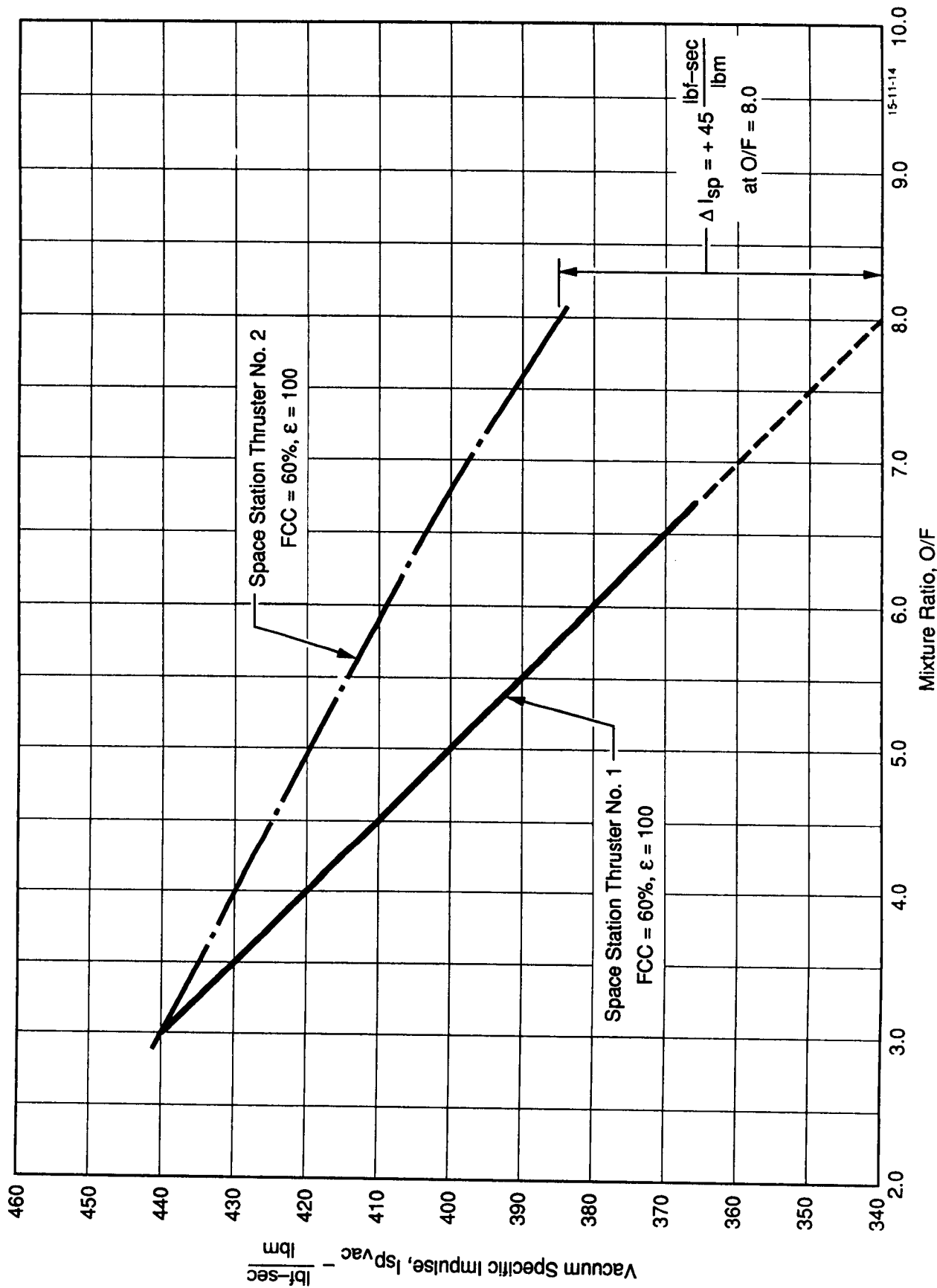


Figure 72. Performance Improvement for Space Station Thruster No. 2

IV, E, Evaluation of Results (cont.)

was made for Thruster No. 2 using the revised thermal and performance models for an optimized 100:1 nozzle contour. This prediction for Thruster No. 2 was also plotted on Figure 72. The net result was an increase of specific impulse of 45 lbF-sec/lbM at an O/F of 8.0, a 13.2 percent increase. Therefore, the post test performance and hydraulic evaluations performed on Thruster No. 1, and used to guide the design of Thruster No. 2, were entirely correct.

F. CONCLUSIONS

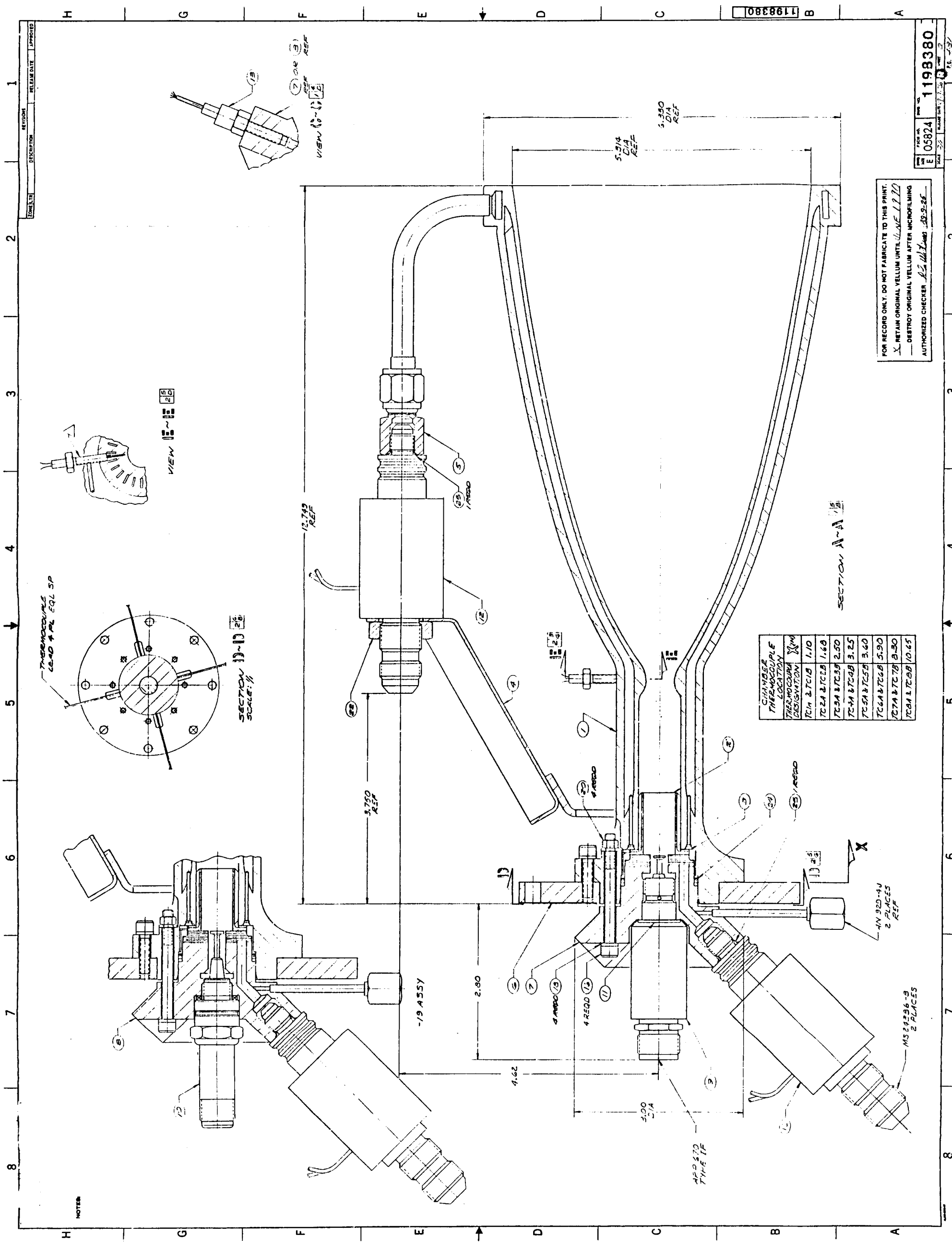
The objective of the program funded by the NASA LeRC under Contract NAS 3-24398 was to establish a technical data base to support future development of GO₂/GH₂ flight thrusters for a Space Station Auxiliary Propulsion System (APS). Specific issues of concern were thruster performance and thrust chamber life. Through the design, fabrication and testing of the two 25 lbF GO₂/GH₂ thrusters described in this final report, it is clear that a significant technical data base has been established to guide future development of the flight thrusters for the Space Station APS. Furthermore excellent specific impulse values over a mixture ratio range of 3.0 to 8.0 were achieved, along with very small temperature gradients through the thrust chamber wall. This low ΔT (89°F) results in an insignificant thermal strain range (0.2 percent), yielding a predicted low cycle fatigue life well in excess of 10,000 cycles. With creep rupture not an issue, the life limiting mechanism is high cycle fatigue, which means that the thrust chamber itself would not be the life limiting component. This conclusion is further supported by the absence of any streaking on the chamber walls which could cause premature failure. The technical development of the GO₂/GH₂ thrusters has been successful and flight development can be initiated.

V. REFERENCES

1. Rosenberg, S.D., Aitken, A.J., Jassowski, D.M., and Royer, K.F., "Ignition Systems for Space Shuttle Auxiliary Propulsion System," NASA CR-72890, 1972. NASA Contract NAS 3-14348.
2. Schoenman, L., "Hydrogen-Oxygen Auxiliary Propulsion for Space Shuttle," NASA CR-120895, Aerojet Liquid Rocket Co., Sacramento, CA, January 1973.
3. Blubaugh, A.L. and Schoenman, L., "Extended Temperature Range ACPS Thruster Investigation," NASA CR-134655, Aerojet Liquid Rocket Co., August 1974. NASA Contract NAS 3-16775.
4. Berkman, D.K. and Schoenman, L., "Oxygen/Hydrogen Thrusters for Space Station Auxiliary Propulsion Systems," Final Report 956457-F-1, Aerojet TechSystems Company, August 1984. JPL Contract 956457.
5. Dowdy, M.W. and Appel, M.A., "High Temperature Gaseous Oxygen/Hydrogen Thrusters for Space Station," Jet Propulsion Laboratory, CIT, Pasadena, CA.
6. Ewen, R.L., et al, "Combustion Effects on Film Cooling," HOCOOL Users Manual, Contract NAS 3-17813, Aerojet Liquid Rocket Co., 15 July 1975.
7. Rousar, D.C. and Ewen, R.L., "Combustion Effects on Film Cooling," NASA CR-135052, Aerojet Liquid Rocket Co., 24 February 1977.
8. Nickerson, G.R., Coats, E.E., and Bartz, J.L., "Two-Dimensional Kinetic Reference Computer Program-TDK," NAS 9-12652, December 1973.
9. Weigold, H.D. and Zupnik, T.F., "Turbulent Boundary Layer Nozzle Analysis Computer Program-TBL," Prepared for the ICRPG Performance Standardization Working Group, AD841202, Aerojet, July 1968.
10. Calhoon, D.F., Ito, J.I., and Kors, D.L., "Investigation of Gaseous Propellant Combustion and Associated Injector/Chamber Design Guidelines," Final Report, NASA CR 121234, Aerojet Liquid Rocket Company, Sacramento, CA, July 1973. NASA Contract 3-14379.
11. Manson, S.S. and Halford, G., "A Method of Estimating High-Temperature Low-Cycle Fatigue Behavior of Materials," Prepared for the International Conference on Thermal and High-Strain Fatigue, Monograph and Report Series No. 32, The Metals and Metallurgy Trust, London, England, 1967.
12. Walker, R.E. and Kors, D.L., "Multiple Jet Study Final Report," NASA CR 121217, Aerojet Liquid Rocket Company, Sacramento, CA, June 1973. NASA Contract NAS 3-15703.
13. Walker, R.E. and Eberhardt, R.G., "Multiple Jet Study Data Correlations," NASA CR 134795, Aerojet Liquid Rocket Company, Sacramento, CA, April 1975. NASA Contract NAS 3-18026.

APPENDIX A
DETAILED DRAWINGS
SPACE STATION THRUSTER NO. 1

<u>Drawing No.</u>	<u>Title</u>
1198364	Bracket Valve
1198369	Spark Igniter
1198380	Engine Assembly, Space Station
1198381	Platelet, Flow Balancing
1198382	Chamber Assembly
1198383	Body, Igniter
1198384	Chamber Sleeve Assembly
1198385	Igniter Body and Platelet Assembly
1198558	Body, Igniter
1198559	Igniter Body and Platelet Assembly
1198674	Fitting
1198675	Plate, Thrust
1198692	Spark Igniter
1198832	Gasket, Spark Igniter



REVISIONS
 DESCRIPTION
 RELEASE DATE
 APPROVED

1198380
 E 05824
 1198380
 AUTHORIZED CHECKER: [Signature]
 28-9-25

FOR RECORD ONLY. DO NOT FABRICATE TO THIS PRINT.
 X RETAIN ORIGINAL YELLOW UNTIL UAXE 1110
 DESTROY ORIGINAL YELLOW AFTER MICROFILMING
 AUTHORIZED CHECKER: [Signature] 28-9-25

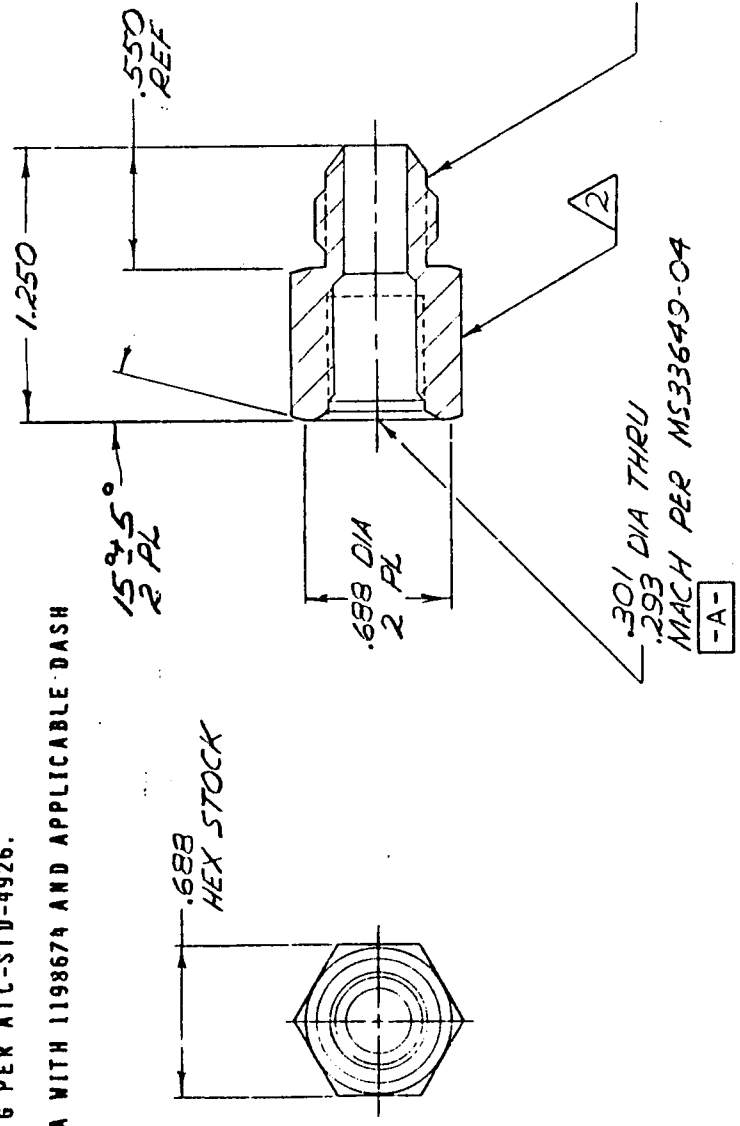
NOTES

4 3 2 1

D C B A

NOTES:

- 1 INTERPRET DRAWING PER ATC-STD-4926.
- 2 MARK PER AS478-7A WITH 1198674 AND APPLICABLE DASH NUMBER.



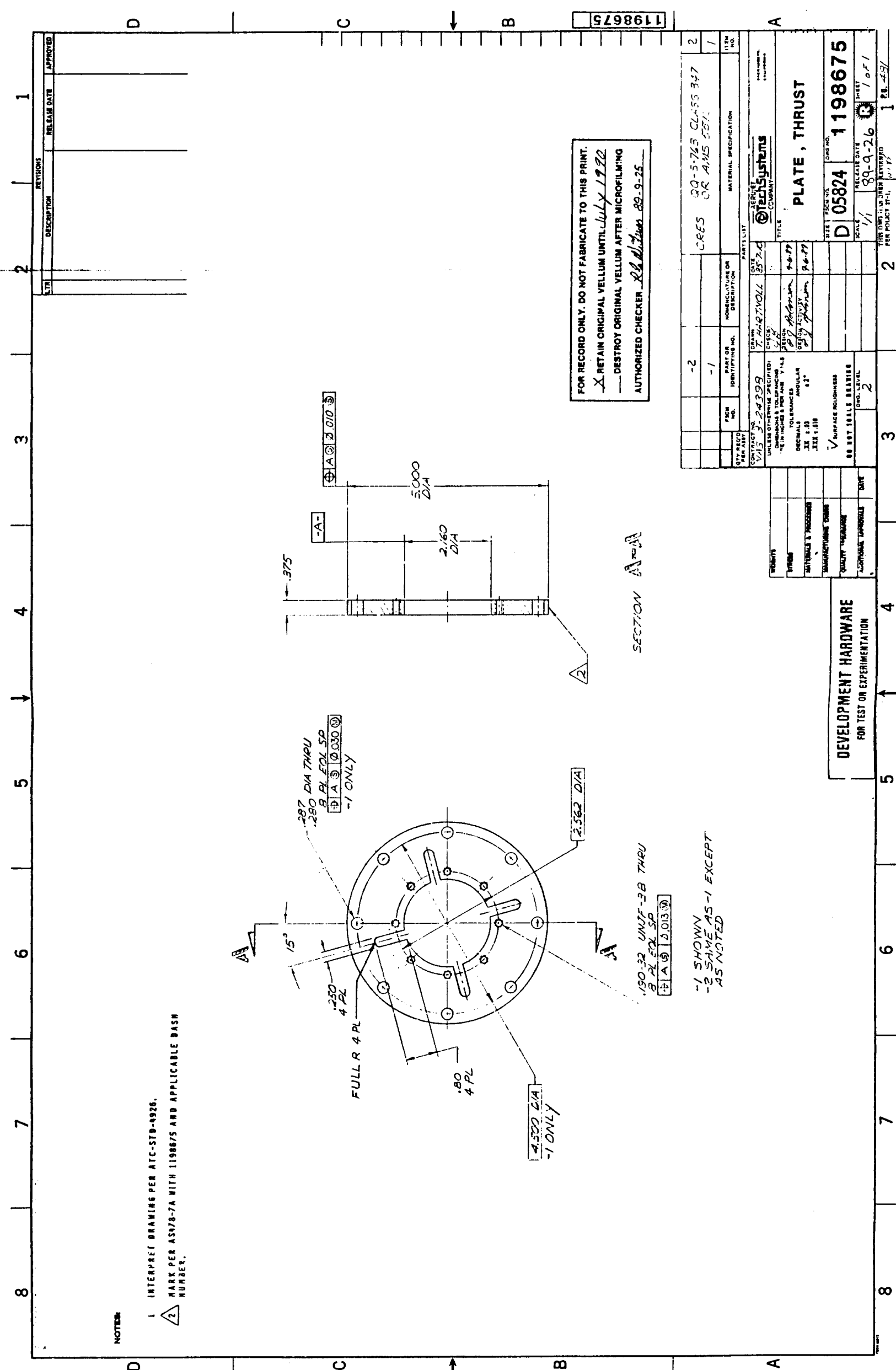
FOR RECORD ONLY. DO NOT FABRICATE TO THIS PRINT.
 RETAIN ORIGINAL VELLUM UNTIL July 1990
 DESTROY ORIGINAL VELLUM AFTER MICROFILMING
 AUTHORIZED CHECKER *R.L. Wilkes* 88-5-25

1198674

QTY REQD PER ASSY	FSCM NO	PART OR IDENTIFYING NO.	NOMENCLATURE OR DESCRIPTION	MATERIAL SPECIFICATION	ITEM NO
		-1		CRCS	
CONTRACT NO 153-2439B		DATE 85-7-1	PARTS LIST		
UNLESS OTHERWISE SPECIFIED: DIMENSIONS & TOLERANCING ARE IN INCHES & PER ANSI Y 14.5		DRAWN T. HARTMOLL	AEROJET @TechSystems COMPANY		
TOLERANCES		CHECKED D. J. [Signature]	TITLE FITTING		
DECIMALS .XX ± .03		DESIGN P. J. [Signature]	SIZE FSCM NO C 05824		
ANGULAR ± 2°		DESIGN ACTIVITY P. J. [Signature]	DWG NO 1198674		
XXX ± .010			SCALE 2/1		
√ SURFACE ROUGHNESS			RELEASE DATE 89-9-26		
DO NOT SCALE DRAWING			SHEET 1 OF 1		
DWG. LEVEL 2			P.C. 431		

DEVELOPMENT HARDWARE
FOR TEST OR EXPERIMENTATION

2 THIS DWG HAS BEEN REVIEWED PER POLICY 27-1, 1/1/85



NOTES:

- 1 INTERPRET DRAWING PER ATC-STD-492B.
- 2 MARK PER AS178-7A WITH 1198675 AND APPLICABLE DASH NUMBER.

FOR RECORD ONLY. DO NOT FABRICATE TO THIS PRINT.
 X-RETAIN ORIGINAL VELLUM UNTIL JULY 1992
 — DESTROY ORIGINAL VELLUM AFTER MICROFILMING
 AUTHORIZED CHECKER: *R. Williams 89-9-25*

REV. NO.	REV. DATE	DESCRIPTION	APPROVED
1			
2			

QTY. REQ'D	QTY. SUPPL'D	DATE

DESIGN NO.	REV.	DATE
1198675		

DESIGNER	CHECKED	DATE

DATE	SCALE	SHEET NO.	TOTAL SHEETS
89-9-26	1/1	1 of 1	1

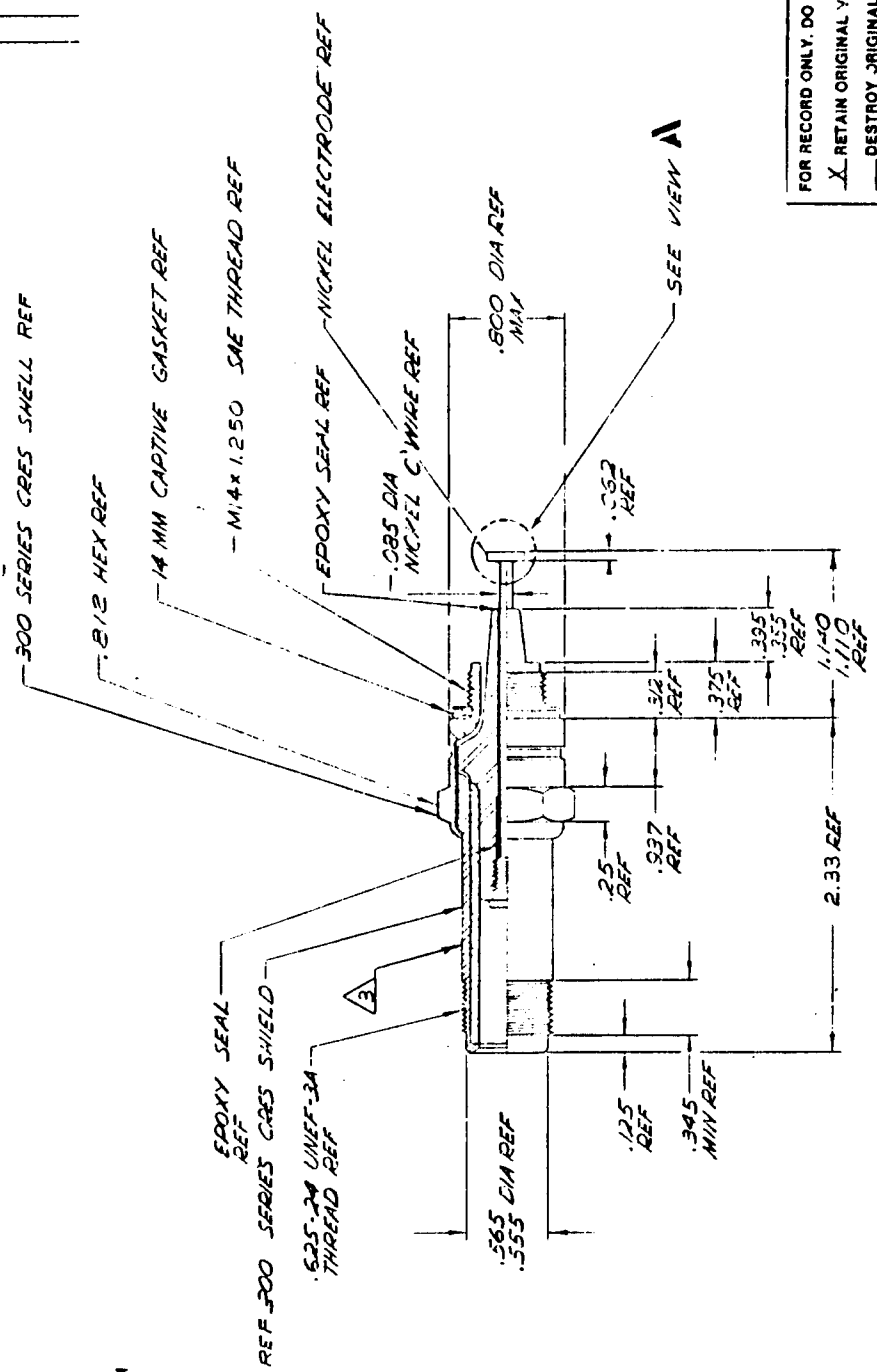
FILE NO.	PROJECT NO.	WORK CENTER

DATE	SCALE	SHEET NO.	TOTAL SHEETS
89-9-26	1/1	1 of 1	1

8 7 6 5 4 3 2 1

NOTES:

- 1 INTERPRET DRAWING PER ATC-STD-4926.
- 2 CENTER DRILL PERMISSIBLE, MAXIMUM SIZE PER COGNIZANT ENGINEER.
- 3 MARK PER AS478-7A WITH 1198692 AND APPLICABLE DASH NUMBER. OBLITERATE ORIGINAL IDENTIFICATION NO. WITHOUT DAMAGE TO THE PART.
- 4 S6L AUBURN SPARK PLUG CO., 89 YORK STREET, AUBURN, NEW YORK.
- 5 ALTER AS SHOWN.



FOR RECORD ONLY. DO NOT FABRICATE TO THIS PRINT.
 X RETAIN ORIGINAL YELLOW UNTIL NOV 19 1980
 — DESTROY ORIGINAL YELLOW AFTER MICROFILMING
 AUTHORIZED CHECKER R. J. Wilson 28.0.25

ALTERED ITEM DRAWING

REV. NO.	1	DATE	8-25-77	BY	7/10/T/M/OLL	DATE	8-25-77	BY	7/10/T/M/OLL
REV. NO.	2	DATE	9-4-77	BY	R. J. Wilson	DATE	9-4-77	BY	R. J. Wilson
REV. NO.	3	DATE	9-4-77	BY	R. J. Wilson	DATE	9-4-77	BY	R. J. Wilson
REV. NO.	4	DATE		BY		DATE		BY	
REV. NO.	5	DATE		BY		DATE		BY	
REV. NO.	6	DATE		BY		DATE		BY	
REV. NO.	7	DATE		BY		DATE		BY	
REV. NO.	8	DATE		BY		DATE		BY	
REV. NO.	9	DATE		BY		DATE		BY	
REV. NO.	10	DATE		BY		DATE		BY	
REV. NO.	11	DATE		BY		DATE		BY	
REV. NO.	12	DATE		BY		DATE		BY	
REV. NO.	13	DATE		BY		DATE		BY	
REV. NO.	14	DATE		BY		DATE		BY	
REV. NO.	15	DATE		BY		DATE		BY	
REV. NO.	16	DATE		BY		DATE		BY	
REV. NO.	17	DATE		BY		DATE		BY	
REV. NO.	18	DATE		BY		DATE		BY	
REV. NO.	19	DATE		BY		DATE		BY	
REV. NO.	20	DATE		BY		DATE		BY	
REV. NO.	21	DATE		BY		DATE		BY	
REV. NO.	22	DATE		BY		DATE		BY	
REV. NO.	23	DATE		BY		DATE		BY	
REV. NO.	24	DATE		BY		DATE		BY	
REV. NO.	25	DATE		BY		DATE		BY	
REV. NO.	26	DATE		BY		DATE		BY	
REV. NO.	27	DATE		BY		DATE		BY	
REV. NO.	28	DATE		BY		DATE		BY	
REV. NO.	29	DATE		BY		DATE		BY	
REV. NO.	30	DATE		BY		DATE		BY	
REV. NO.	31	DATE		BY		DATE		BY	
REV. NO.	32	DATE		BY		DATE		BY	
REV. NO.	33	DATE		BY		DATE		BY	
REV. NO.	34	DATE		BY		DATE		BY	
REV. NO.	35	DATE		BY		DATE		BY	
REV. NO.	36	DATE		BY		DATE		BY	
REV. NO.	37	DATE		BY		DATE		BY	
REV. NO.	38	DATE		BY		DATE		BY	
REV. NO.	39	DATE		BY		DATE		BY	
REV. NO.	40	DATE		BY		DATE		BY	
REV. NO.	41	DATE		BY		DATE		BY	
REV. NO.	42	DATE		BY		DATE		BY	
REV. NO.	43	DATE		BY		DATE		BY	
REV. NO.	44	DATE		BY		DATE		BY	
REV. NO.	45	DATE		BY		DATE		BY	
REV. NO.	46	DATE		BY		DATE		BY	
REV. NO.	47	DATE		BY		DATE		BY	
REV. NO.	48	DATE		BY		DATE		BY	
REV. NO.	49	DATE		BY		DATE		BY	
REV. NO.	50	DATE		BY		DATE		BY	
REV. NO.	51	DATE		BY		DATE		BY	
REV. NO.	52	DATE		BY		DATE		BY	
REV. NO.	53	DATE		BY		DATE		BY	
REV. NO.	54	DATE		BY		DATE		BY	
REV. NO.	55	DATE		BY		DATE		BY	
REV. NO.	56	DATE		BY		DATE		BY	
REV. NO.	57	DATE		BY		DATE		BY	
REV. NO.	58	DATE		BY		DATE		BY	
REV. NO.	59	DATE		BY		DATE		BY	
REV. NO.	60	DATE		BY		DATE		BY	
REV. NO.	61	DATE		BY		DATE		BY	
REV. NO.	62	DATE		BY		DATE		BY	
REV. NO.	63	DATE		BY		DATE		BY	
REV. NO.	64	DATE		BY		DATE		BY	
REV. NO.	65	DATE		BY		DATE		BY	
REV. NO.	66	DATE		BY		DATE		BY	
REV. NO.	67	DATE		BY		DATE		BY	
REV. NO.	68	DATE		BY		DATE		BY	
REV. NO.	69	DATE		BY		DATE		BY	
REV. NO.	70	DATE		BY		DATE		BY	
REV. NO.	71	DATE		BY		DATE		BY	
REV. NO.	72	DATE		BY		DATE		BY	
REV. NO.	73	DATE		BY		DATE		BY	
REV. NO.	74	DATE		BY		DATE		BY	
REV. NO.	75	DATE		BY		DATE		BY	
REV. NO.	76	DATE		BY		DATE		BY	
REV. NO.	77	DATE		BY		DATE		BY	
REV. NO.	78	DATE		BY		DATE		BY	
REV. NO.	79	DATE		BY		DATE		BY	
REV. NO.	80	DATE		BY		DATE		BY	
REV. NO.	81	DATE		BY		DATE		BY	
REV. NO.	82	DATE		BY		DATE		BY	
REV. NO.	83	DATE		BY		DATE		BY	
REV. NO.	84	DATE		BY		DATE		BY	
REV. NO.	85	DATE		BY		DATE		BY	
REV. NO.	86	DATE		BY		DATE		BY	
REV. NO.	87	DATE		BY		DATE		BY	
REV. NO.	88	DATE		BY		DATE		BY	
REV. NO.	89	DATE		BY		DATE		BY	
REV. NO.	90	DATE		BY		DATE		BY	
REV. NO.	91	DATE		BY		DATE		BY	
REV. NO.	92	DATE		BY		DATE		BY	
REV. NO.	93	DATE		BY		DATE		BY	
REV. NO.	94	DATE		BY		DATE		BY	
REV. NO.	95	DATE		BY		DATE		BY	
REV. NO.	96	DATE		BY		DATE		BY	
REV. NO.	97	DATE		BY		DATE		BY	
REV. NO.	98	DATE		BY		DATE		BY	
REV. NO.	99	DATE		BY		DATE		BY	
REV. NO.	100	DATE		BY		DATE		BY	
REV. NO.	101	DATE		BY		DATE		BY	
REV. NO.	102	DATE		BY		DATE		BY	
REV. NO.	103	DATE		BY		DATE		BY	
REV. NO.	104	DATE		BY		DATE		BY	
REV. NO.	105	DATE		BY		DATE		BY	
REV. NO.	106	DATE		BY		DATE		BY	
REV. NO.	107	DATE		BY		DATE		BY	
REV. NO.	108	DATE		BY		DATE		BY	
REV. NO.	109	DATE		BY		DATE		BY	
REV. NO.	110	DATE		BY		DATE		BY	
REV. NO.	111	DATE		BY		DATE		BY	
REV. NO.	112	DATE		BY		DATE		BY	
REV. NO.	113	DATE		BY		DATE		BY	
REV. NO.	114	DATE		BY		DATE		BY	
REV. NO.	115	DATE		BY		DATE		BY	
REV. NO.	116	DATE		BY		DATE		BY	
REV. NO.	117	DATE		BY		DATE		BY	
REV. NO.	118	DATE		BY		DATE		BY	
REV. NO.	119	DATE		BY		DATE		BY	
REV. NO.	120	DATE		BY		DATE		BY	
REV. NO.	121	DATE		BY		DATE		BY	
REV. NO.	122	DATE		BY		DATE		BY	
REV. NO.	123	DATE		BY		DATE		BY	
REV. NO.	124	DATE		BY		DATE		BY	
REV. NO.	125	DATE		BY		DATE		BY	
REV. NO.	126	DATE		BY		DATE		BY	
REV. NO.	127	DATE		BY		DATE		BY	
REV. NO.	128	DATE		BY		DATE		BY	
REV. NO.	129	DATE		BY		DATE		BY	
REV. NO.	130	DATE		BY		DATE		BY	
REV. NO.	131	DATE		BY		DATE		BY	
REV. NO.	132	DATE		BY		DATE		BY	
REV. NO.	133	DATE		BY		DATE		BY	
REV. NO.	134	DATE		BY		DATE		BY	
REV. NO.	135	DATE		BY		DATE		BY	
REV. NO.	136	DATE		BY		DATE		BY	
REV. NO.	137	DATE		BY		DATE		BY	
REV. NO.	138	DATE		BY		DATE		BY	
REV. NO.	139	DATE		BY		DATE		BY	
REV. NO.	140	DATE		BY		DATE		BY	
REV. NO.	141	DATE		BY		DATE		BY	
REV. NO.	142	DATE		BY		DATE		BY	
REV. NO.	143	DATE		BY		DATE		BY	
REV. NO.	144	DATE		BY		DATE		BY	
REV. NO.	145	DATE		BY		DATE		BY	
REV. NO.	146	DATE		BY		DATE		BY	
REV. NO.	147	DATE		BY		DATE		BY	
REV. NO.	148	DATE		BY		DATE		BY	
REV. NO.	149	DATE		BY		DATE		BY	
REV. NO.	150	DATE		BY		DATE		BY	
REV. NO.	151	DATE		BY		DATE		BY	
REV. NO.	152	DATE		BY		DATE		BY	
REV. NO.	153	DATE		BY		DATE		BY	
REV. NO.	154	DATE		BY		DATE		BY	
REV. NO.	155	DATE		BY		DATE		BY	
REV. NO.	156	DATE		BY		DATE		BY	
REV. NO.	157	DATE		BY		DATE		BY	
REV. NO.	158	DATE		BY		DATE		BY	
REV. NO.	159	DATE		BY		DATE		BY	

APPENDIX B
TEST DATA
FOR
THRUSTER NO. 1

SPACE STATION THRUSTER TEST SUMMARY

<u>Mixture Ratio</u> <u>O/F</u>	<u>Total Duration</u> <u>(sec)</u>	<u>Total Impulse</u> <u>(lbf-sec)</u>
2	60	1,302
3	240	5,107
4	3,735	89,526
5	224	5,576
6	221	4,728
7	17,563	428,997
8	<u>155</u>	<u>3,221</u>
Total:	22,198	538,457

SPACE STATION THRUSTER TEST SUMMARY

<u>Fuel Film Cooling (%)</u>	<u>Mixture Ratio O/F</u>	<u>Total Duration (sec)</u>	<u>Total Impulse (lbf-sec)</u>
59	3	60	1,662
	4	980	26,221
	5	55	1,386
	6	19	456
64	3	60	1,602
	4	687	16,458
	5	72	1,749
74	4	1,547	35,949
	5	97	2,441
85	4	271	6,314
	7	17,219	420,063
	8	51	1,056
87	2	60	1,302
	4	120	2,184
	6	120	2,376
	8	66	1,332
88	6	60	1,314
	8	38	833
92	3	120	1,843
	4	130	2,400
	6	22	582
95	7	344	8,934
		<u>22,198</u>	<u>538,457</u>
	Total:		



SPACE STATION AUXILIARY THRUST CHAMBER TECHNOLOGY

CONTRACT NAS 3-24398

TEST DATA SUMMARY FOR THRUSTER S/N 001

TEST CONFIGURATION CONSISTS OF INJECTOR S/N 002, ORIGINAL SLEEVE DESIGN, 87% FFC AND AMBIENT GH2 INLET TEMPERATURE

Test No.	O/F	F (lbf)	Pc (Psia)	ISP _v /ISP _n (lbf-sec/lbm)	T _{bulk} (°F)	T _{bs,max} (°F)	QF/CP	Duration (sec)	Comments
1	4.0								Fuel valve cold flow Test No. 1
2	4.0								Oxidizer valve cold flow Test No. 1
3	4.0								Oxidizer valve cold flow Test No. 2
4	4.0								Fuel valve cold flow Test No. 2
5	4.0								Simultaneous Fuel & Oxidizer valve cold flow
101	4.0								Simultaneous Fuel & Oxidizer valve cold flow
104	4.0							5	Ignition checkout
105	3.77							5	Ignition checkout
106								20	Ignition checkout
107								60	No data recorded during test
108	4.09	18.6	52.8	333	328	395	3.28	60	Data recorded, same conditions as No. 107
112	5.97	20.1	54.2	307	85	563	4.34	60	Ignition

TEST CONFIGURATION CONSISTS OF INJECTOR S/N 002, ORIGINAL SLEEVE DESIGN, 87% FFC AND AMBIENT GH2 INLET TEMPERATURE

Test No.	O/F	F (lbf)	Pc (Psia)	ISP _v /ISP _n (lbf-sec/lbm)	T bulk (°F)	T _{bs,max} (°F)	QF/CP	Duration (sec)	Comments
113	7.71	20.6	55.6	302	502	801	3.72	20	
GH2 Inlet Temp. Change from Ambient to Sub-Cooled (-80° F)									
114	4.18	17.8	50.9	329	212	283	3.26	60	
115	6.03	19.5	52.7	302	334	406	4.03	60	
116	7.76	20.0	52.4	306	546	812	4.93	46	TFJ kill @ 5500F
119	2.18	21.7	59.9	373	87.1	124	2.87	60	
Injector S/N Change from 002 to 001									
GH2 Inlet Temp. Change from Sub-Cooled to Ambient; % FFC Change from 87% to 92%									
123	4.04	17.4	47.8	326	212		1.80	10	Good test
124	3.96	25.8	69.6	340	346	376	4.51	60	517 OX; 303 Fuel Good test
125	4.17	11.3	32.9	341	388	464	2.25	60	237 OX; 303 Fuel Low Pc @ 33 Psia

TEST CONFIGURATION CONSISTS OF INJECTOR S/N 001, ORIGINAL SLEEVE DESIGN, 92% FFC AND AMBIENT GH2 INLET TEMPERATURE

Test No.	O/F	F (1bf)	Pc (Psia)	ISP _v /ISP _n (1bf-sec/lbm)	T bulk (OF)	Tbs,max (OF)	QF/CP	Duration (Sec)	Comments
126	3.43	6.21	18.5	371	328	396	1.15	60	Low Pc @ 18.5
128	6.19	26.2	70.9	345	543	783	5.24	22.2	Temp. kill @ 550OF
129	3.21	24.5	66.1	350	292	347	3.95	60	OK
%FFC Change from 92% to 63.9%									
134	4.14	32.4	85.2	404	498	549	7.13	60	High Pc, High F
140	3.96	25.9	68.5	410/410	504	561	6.07	60	
142	2.95	26.7	70.7	430/430	366	415	5.20	60	
146	4.69	24.1	63.6	393	545	609	5.62	25.6	TFJ kill @ 550OF Kill should have been 600° for this test
147	4.74	24.4	64.3	392	596	659	6.22	46.4	TFJ kill @ 600OF
% FFC Change from 63.9% to 59.2%									
153	3.93	26.6	69.8	421/421	504	607	6.10	60	Good test
154	3.03	27.7	73.1	438/439	388	470	5.57	60	Good test

66

TEST CONFIGURATION CONSISTS OF INJECTOR S/N 001, ORIGINAL SLEEVE DESIGN, 59.2% FFC AND AMBIENT GH2 INLET TEMPERATURE

Test No.	O/F	F (lbF)	Pc (Psia)	ISP _v /ISP _n (lbF-sec/lbm)	T bulk (OF)	T _{bs,max} (OF)	QF/CP	Duration (sec)	Comments
156	5.67	23.6	62.0	387	591	752	5.24	19.315	TFJ kill @ 600°F
164	5.03	25.2	65.8	399	596	771	6.07	55	TFJ kill @ 600°F
166	4.12	26.6	70.4	413	495	640	5.96	120	Good test
167	4.14	27.1	70.7	418/418	498	637	5.99	300	Good test - steady state (i.e. thermal equilibrium)
171	4.03	26.6	68.6	423/423	507	644	5.84	500.115	Manual kill to check facility temp.
172	4.13	21.6	57.8	381/380	485	559	4.67	60	Low F (21.6) and PC Hot test full duration
173	3.98	26.1	69.6	384/384	451	518	5.29	60	Good test
174	4.95	25.0	66.2	364/363	546	614	5.66	36.9	TFJ kill @ 550°F
175	4.99	25.3	66.6	365/365	590	663	6.19	60	Good test; full duration

% FFC change from 59.2% to 74%.
GH2 Inlet Temp. change from Ambient to -80°F.

TEST CONFIGURATION CONSISTS OF INJECTOR S/N 001, ORIGINAL SLEEVE DESIGN, 74% FFC AND AMBIENT GH2 INLET TEMPERATURE

Test No.	O/F	F (lbf)	Pc (Psia)	ISP _v /ISP _n (lbf-sec/lbm)	T bulk (°F)	T _{bs,max} (°F)	QF/CP	Duration (sec)	Comments
176	4.05	26.4	70.8	385/385	464	528		328	Facility kill @ 328 sec; One booster pump blower shut down
182	4.11	27.0	71.2	386/386	479	532	5.58	437	Facility kill @ 437 sec due to high cell pressure
183	4.01	21.9	58.9	385/385	507	562	5.00	217	21.9 lbf test - facility kill @ 217 sec due to high cell pressure
184	4.03	17.7	47.6	392/392	544	610	4.48	445	Facility kill due to high cell pressure

☐ Sleeve changed from original design to modified design. % FFC changed from 74% to 88%.

186	6.00	21.9	60.1	332/332	579	749	5.18	60	
187	7.63	22.0	60.2	341/341	583	949	4.31	20	

GH2 Inlet Temp. change from Ambient to -100°F

189	8.12	21.8	60.0	309/312	490	862	4.56	18	TC3 kill due to high temp
-----	------	------	------	---------	-----	-----	------	----	---------------------------

% FFC change from 88% to 85%.

191	8.09	20.7	54.3	291/295	575	780	5.33	51	TC3 kill @ 900°F
-----	------	------	------	---------	-----	-----	------	----	------------------

TEST CONFIGURATION CONSISTS OF INJECTOR S/N 001, MODIFIED SLEEVE DESIGN, 85% FFC AND 100°F GH2 INLET TEMPERATURE

Test No.	O/F	F (lbf)	Pc (Psia)	ISP/ISP _n (lbf-sec/lbm)	T _{bulk} (°F)	T _{DS,max} (°F)	QF/CP	Duration (sec)	Comments
192	7.08	20.8	54.4	302/306	561	656		60	Good run
193	7.17	21.4	54.4	307/310	556	628		600	Good run - TFJ=550°F TC4=750°F - Pduct=.32 ps
199	7.34	25.7	65.5	308/311	550	643		600	Good run - TFJ=540°F TC4=750°F - Pduct=.36 ps
GH2 Inlet Temp. change from -100°F to -90°F									
202	3.71	23.3	62.7	335/338	146	195	3.53	271	Kill due to high Pduct @ 0.66 psia
% FFC Change from 85% to 95% and GH2 Inlet Temp. change from -90°F to -100°F									
208	7.11	27.5	74.0	326/329	574	950	7.06	275	TC4 Temp kill @ 900°F
209	6.85	18.9	50.5	316/319	508	888		30	TC3A Temp kill @ 900°F
GH2 Inlet Temp. change from -100°F to -85°F									
214	6.99	20.6	55.8	312/315	479	824		39	TC3A Temp kill @ 900°F

TEST CONFIGURATION CONSISTS OF INJECTOR S/N 001, ORIGINAL SLEEVE DESIGN, 85% FFC and -90° F GH2 INLET TEMPERATURE

Test No.	O/F	F (lbf)	Pc (Psia)	ISP _v /ISP (lbf-sec/lbm)	T bulk (°F)	T _{bs,max} (°F)	QF/CP	Duration (sec)	Comments
215	6.78	21.1	55.5	294/297	454	843	5.19	16.8	TC3A kill @ >900° F
216	6.61	21.4	55.9	294/297	473	840	5.66	14.7	TC3A kill @ >900° F
Sleeve design change from Original to Modified. GH2 Inlet Temp. change from -90° F to -80° F									
219	7.27	21.3	56.5	311/314	523	723	5.38	60	Good test
222	7.26	22.9	58.8	322/326	560	669	5.87	600	Good test
224	7.29	24.4	61.9	327/331	563	707	6.20	900	Good test; Inspected sleeve & polished I.O.
231	7.38	24.3	61.6	327/330	552	701	6.03	900	Good test
232	7.48	23.6	62.0	318/321	597	810	6.33	54	TFJ @ 600° F
235	7.36	24.1	61.4	325/328	556	720	6.04	900	Good test; removed sleeve. Slight discoloration inside. Cleaned & reinstalled.
236	7.26	24.7	61.6	329/332	550	649	6.13	1200	Good test; Sleeve slightly rough at previous discoloration. Polished, cleaned & reinstalled.

TEST CONFIGURATION CONSISTS OF INJECTOR S/N 001, MODIFIED SLEEVE DESIGN, 85% FFC AND -80° F GH2 INLET TEMPERATURE

Test No.	O/F	F (lbF)	Pc (Psia)	ISP _v /ISP _n (lbF-sec/lbm)	T _{bulk} (°F)	T _{bs,max} (°F)	QF/CP	Duration (sec)	Comments
239	7.36	24.8	61.9	331/335	535	690	5.93	1200	Good test; sleeve appears smooth. Polished, cleaned & reinstalled
240	7.25	22.9	60.8	322/325	491	601	5.61	250	Manual kill due to rising P-cell = .14
244	7.42	23.9	59.9	332	509	612	5.74	572	Manual kill due to rising P-cell
245	7.24	24.4	60.5	315/318	516	614	5.71	1624	Kill due to high cell pressure
251	7.20	23.3	62.1	309/312	510	606	5.81	415	Kill due to high cell pressure
GH2 Inlet Temperature change from -80° F to -100° F									
260	7.14	23.2	62.4	310/313	510	603	5.84	364	Good test; Pduct = 0.5
269	7.15	20.4	52.4	315/318	576	688	5.31	664	Good test. Kill due to high cell pressure. Pduct=0.5
Sleeve design change from Modified to Original. % FFC change from 85% to 64%									
273	4.09	23.4	66.0	388/391	365	438	5.60	183	Good run; kill due to high cell pressure. Pduct=0.5

TEST CONFIGURATION CONSISTS OF INJECTOR S/N 001, ORIGINAL SLEEVE DESIGN, 64% FFC and -100° F GH2 INLET TEMPERATURE

<u>Test No.</u>	<u>O/F</u>	<u>F (1bF)</u>	<u>Pc (Psia)</u>	<u>ISP_v/ISP_n (1bF-sec/lbm)</u>	<u>T bulk (°F)</u>	<u>T_{bs,max} (°F)</u>	<u>QF/CP</u>	<u>Duration (sec)</u>	<u>Comments</u>
274	4.04	8.16	27.7	132/135	61.9	31.0	1.21	19	
277	4.09	23.4	65.9	388/391	360	429	5.57	182	Good run; Pduct = 0.5
279	4.14	23.3	65.8	386/389	364	430	5.61	183	Good run; Pduct = 0.5
Sleeve design change from Original to Modified. % FFC change from 64% to 85%, from -100° F to -85° F GH2 Inlet Temperature change									
285	7.32	25.5	66.5	331/335	565	627	6.35	1206	Good test
GH2 Inlet Temperature change from -85° F to -80° F									
304	7.31	25.4	66.1	330/333	566	632	6.40	1501	Good test
307	7.18	24.9	65.4	328/332	556	618	6.31	1317	Good test
311	7.47	25.6	66.3	327/331	568	637	6.39	2200	Good test

SPACE STATION AUXILIARY THRUST CHAMBER TECHNOLOGY

CONTRACT NAS 3-24398

SUMMARY OF TEST CONDITIONS FOR THRUSTER S/N 001

Sleeve Design	FFC	GH2 Inlet Temp.	F/Pc (1bF/psia)	O/F	Isp (lbF-sec / lbm)	T _{bulk} (°F)	T _{B.S.} (°F)	Comments
Original	87%	Ambient	20/54	4,6,8	302-333	328-502	395-801	3 Tests, 60 sec. each
Original	87%	Sub-Cooled	18-22/51-60	2,4,6,8	302-373	87-546	124-812	4 Tests, 60 sec. each
Original	92%	Ambient	6-26/18-71	3,4,6	340-371	292-543	347-783	5 Tests, 60 sec. each
Original	64%	Ambient	24-32/64-85	3,4,5	392-430	366-596	415-659	5 Tests, 60 sec. each
Original	59%	Ambient	24-28/62-73	3,4,5,6	387-438	388-596	470-771	7 Tests, 20 sec. to 500 sec.
Original	74%	Ambient	18-27/48-71	4,5	364-392	451-590	518-663	8 Tests, 40 sec. to 445 sec.
Modified	88%	Ambient	22/60	6,8	332-341	579-583	749-949	2 Tests, 60 sec. and 20 sec.
Modified	88%	Sub-Cooled	22/60	8	309	490	862	1 Test, 18 sec.
* Modified	85%	Sub-Cooled	21-26/54-66	4,7,8	291-335	146-575	195-780	5 Tests, 60 sec., 270 sec. and 600 sec.
*† Modified	95%	Sub-Cooled	19-28/50-74	7	312-326	479-574	824-950	3 Tests, 30 sec. to 275 sec.
Original	85%	Sub-Cooled	21/55	7	292-299	458-478	848	2 Tests, 15 sec. each

<u>Sleeve Design</u>	<u>FFC</u>	<u>GH2 Inlet Temp.</u>	<u>F/Pc (1bf/psia)</u>	<u>O/F</u>	<u>Isp (1bf-sec / 1bm)</u>	<u>T_{bulk} (°F)</u>	<u>T_{B.S.} (°F)</u>	<u>Comments</u>
Modified	85	Sub-Cooled	22-25/58-63	7	320-337	500-550	650-720	14 Tests, 9700 sec.
Original	64%	Sub-Cooled	23-24/66-67	4	380-397	360-364	437	4 Tests, 182 sec. each
Modified	85%	Sub-Cooled	25-26/65-67	7	329-340	552-573	~675	4 Tests, 1206 sec., 1500 sec., 1317 sec. and 2200 sec. Total: 6223 sec.

* Cell pressure instrumentation was reading incorrectly, i.e. bad calibration; therefore, Isp values can be as much as 20 1bf-sec/lbm higher than shown. Exact correction is being determined.

† Entries below the indicated run are based on "quick-look" data during testing; post test data reduction is still in progress.

APPENDIX C
OUTLINE OF PERFORMANCE PREDICTION
METHODOLOGIES

Simplified Procedure

$$I_{SP_{\text{Delivered}}} = I_{SP_{\text{ODE}}} \times \eta_{\text{KIN}} \eta_{\text{DIV}} \times \eta_{\text{ERE}} - \frac{\Delta FBL}{\dot{M}}$$

$\eta_{\text{KINETIC}} = I_{SP_{\text{ODK}}} / I_{SP_{\text{ODE}}}$
 $\eta_{\text{DIV}} = I_{SP_{\text{TDE}}} / I_{SP_{\text{ODE}}}$
 $\eta_{\text{ERE}} = \text{Vaporization/Mixing Analysis; Test Data.}$
 $\Delta FBL = \text{Turbulent Boundary Layer Code}$

Rigorous Procedure

$$I_{SP_{\text{Delivered}}} = \frac{1}{\dot{M}_T} \sum_{i=1}^N \dot{M}_i I_{SP_{\text{TDK}}} - \frac{FBL}{\dot{M}}$$

$\dot{M} = \text{Mass in Each Stream Tube From SDER/CICM}$
 $I_{SP_{\text{TDK}}} = \text{Two Dimension Kinetic ISP in Each Stream Tube}$
 $\Delta FBL = \text{Thrust Decrements in Boundary Layer From Blimp Code (or BLM Option of TDK)}$

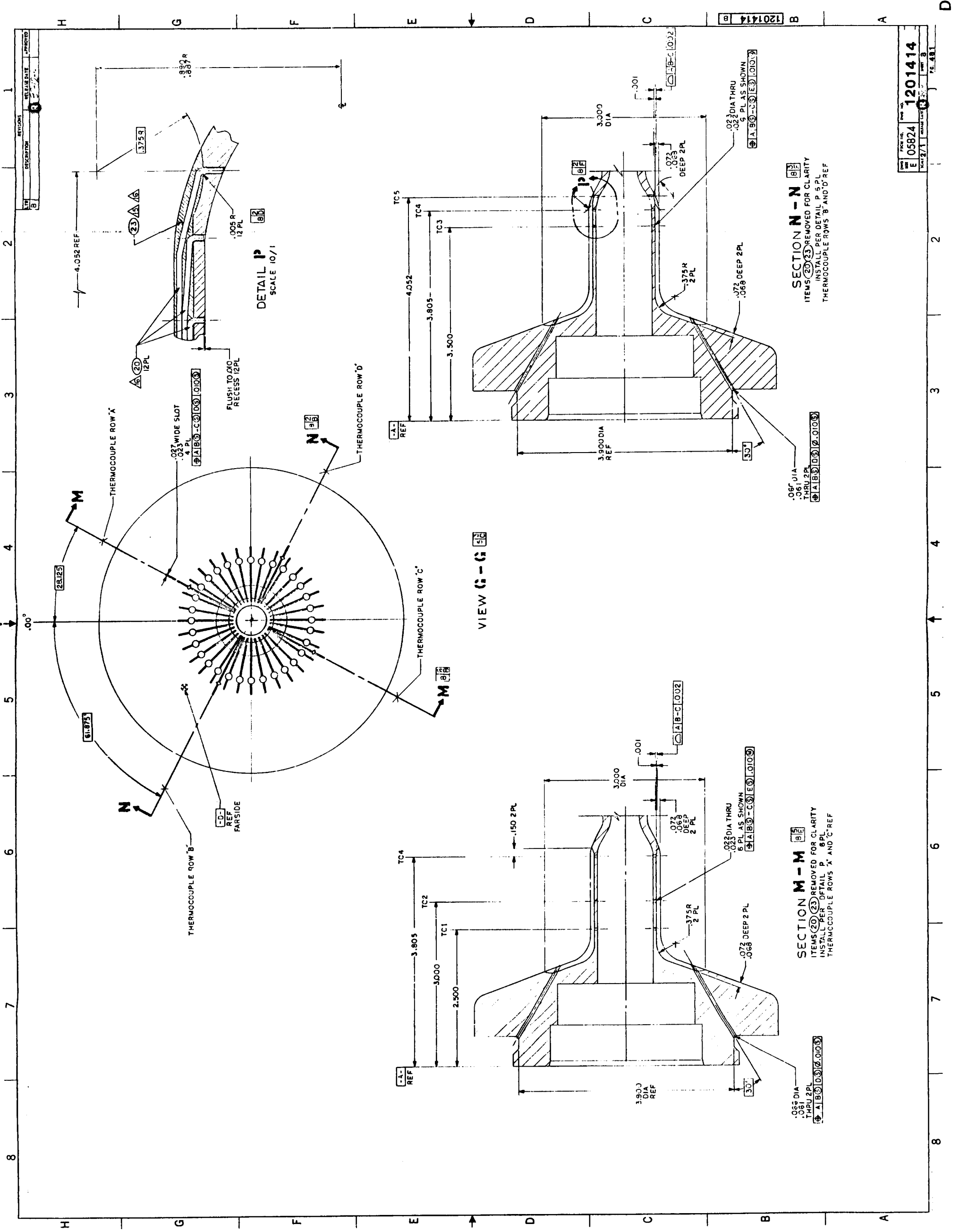
Figure C-1. Aerojet Has Used Both Simplified and Rigorous JANNAF Performance Procedure in Past to Predict Performance

- Define Engine Size and Operational Region Based on Requirements and Simplified Analysis
- Determine Chamber Length/Nozzle Size Which Best Meets Requirements
- Design Nozzle Contour Using RAO Design Code (Method of Characteristics)
- Run Two Dimensional Kinetics (TDK) Code With Boundary Layer Module (BLM) Option to Obtain
 - Kinetic Performance
 - Divergence Influence
 - Boundary Layer Loss
- Define Injector Energy Release Efficiency
 - Existing Hot Fire Test Data
 - Cold Flow Mixing Data
 - SDER/CICM Codes
 - Simplified Mixing and Vaporization Models

Figure C-2. The Standard Aerojet Prediction Procedure Follows the JANNAF Guidelines

APPENDIX D
DETAILED DRAWINGS
SPACE STATION THRUSTER NO. 2

<u>Drawing No.</u>	<u>Title</u>
1201414	Chamber Assembly
1201415	Thrust Chamber Assembly
1201417	Body Igniter
1201418	Integral Igniter Injector Assembly
1201419	Igniter Sleeve Assembly
1201420	Washer, Flow Balancing
1201422	Igniter, Spark
1201423	Valve, Propellant
1201424	Thrust Plate





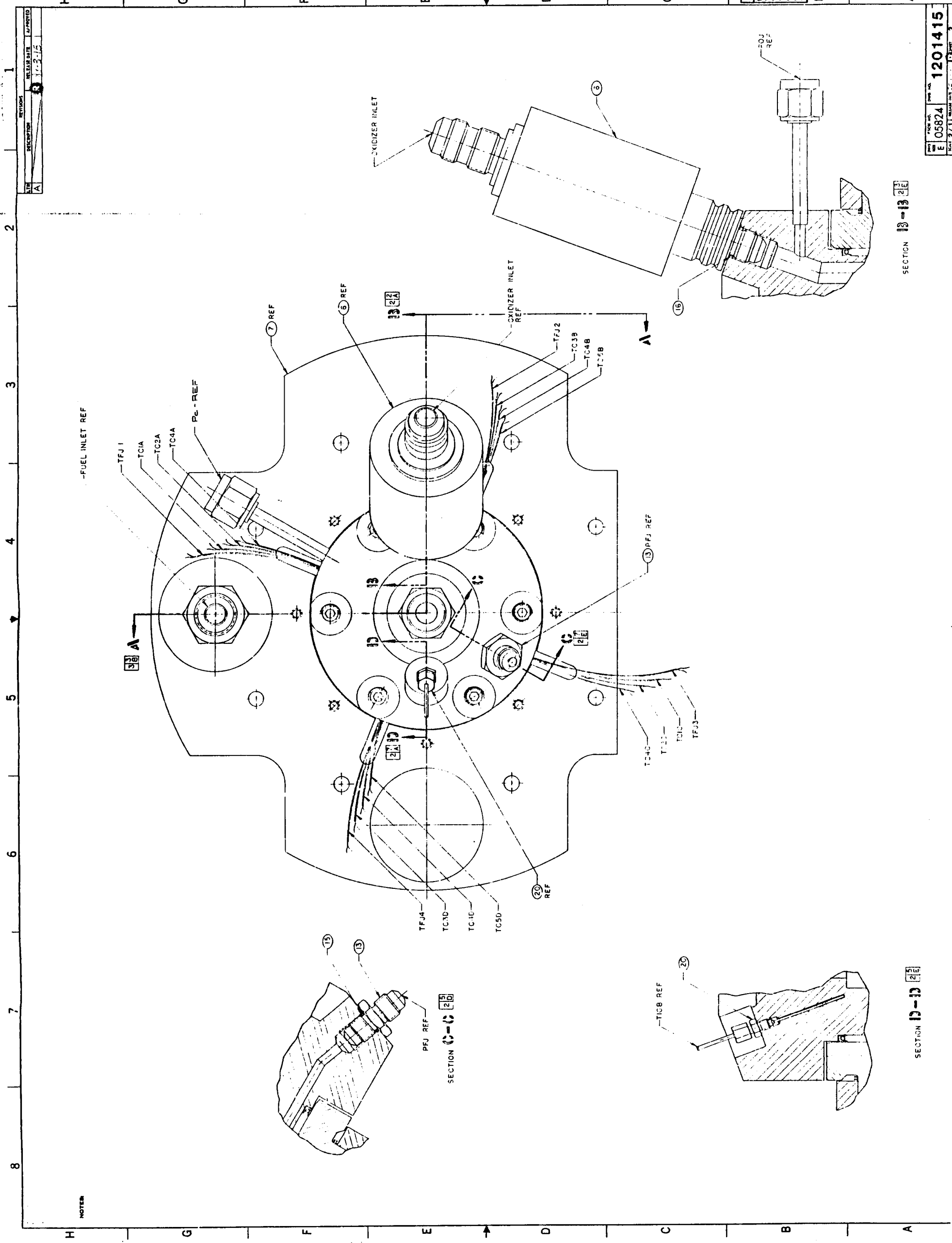
NOTES:

1. INTERPRET DRAINING PER ATC-STO-1926.
2. PROTECTIVE CLOSURES ARE REQUIRED ON ALL PROPELLANT INLETS, INSTRUMENTATION PORTS, AND NOZZLE EXIT DURING HANDLING, SHIPPING AND STORAGE. REMOVE DRY AS REQUIRED.
3. CONTAMINATION CRITICAL HARDWARE COMPONENT CLEANLINESS REQUIREMENTS SHALL BE MAINTAINED THROUGHOUT ASSEMBLY PROCEDURE.
4. MILLIPORE FILTERS (FSCM NO. 08071) RATED AT 200 MICRONS ABSOLUTE, OR LOWER, SHALL BE USED WHEN FLOWING ANY FLUIDS THROUGH THE HARDWARE.
5. APPLY A THIN FILM OF (3) LUBRICANT (MS-122) TO ALL SCREW THREADS PRIOR TO ASSEMBLY PER ATC-STO-1951.
6. TORQUE VALUES ARE TOTAL. TORQUE INFORMATION PER ATC-STO-1939.
7. TORQUE SEQUENCE FOR A GIVEN BOLT PATTERN SHALL BE PER ASD-3226.
8. REFERENCED INSTRUMENTATION TYPE AND LOCATION IS DEFINED ON DRAWINGS FOR (1) CHAMBER AND (2) INJECTOR. ADDITIONAL THERMOCOUPLE INSTRUMENTATION TO BE ADDED TO (3) PER COSHIZANT ENGINEER.
9. REQUIRED FLOW BALANCING WASHERS (DRAWING 1201420) SHALL BE SELECTED AND RECORDED BY THE QUALITY PART ENGINEER SUBSEQUENT TO COLD FLOW CALIBRATION TESTS PER DRAWING 1201418, NOTE 18.
10. PROOF AND LEAK TESTS: THE THRUST CHAMBER ASSEMBLY SHALL BE SUBJECTED TO PROOF AND LEAK TESTS AS FOLLOWS:
 - A. PROOF TEST - USING CLEAR DRY G₂, PRESSURIZE THE THRUST CHAMBER ASSEMBLY USING A SUITABLE BRONAT PLUG TO 225 ± 25 PSIG FOR 5 MINUTES MINIMUM.
 - B. LEAK TEST - USING CLEAR DRY G₂, PRESSURIZE THE THRUST CHAMBER ASSEMBLY TO 125 ± 10 PSIG FOR 5 MINUTES MINIMUM. THERE SHALL BE NO EVIDENCE OF LEAKAGE GREATER THAN 1.110⁻³ SCC ALLOWED.
11. MARK PER ASD78-35C WITH 1201415, APPLICABLE DASH NO. AND AEROJET TECHNOLOGIES COMPANY (ATC) ASSIGNED SERIAL NO.

QTY	PART NO.	DESCRIPTION	REV.
1	93768402-2103	LUBE	
1	05939480240890	THERMO-COUPLE	
1	AS33340E1-9102	SEAL ASSY	
1	AS30040E1-9102	O-RING	
1	AN924-85	O-RING	
1	AN815-45	NUT, BULKHEAD UNION	
14	NAS 620	WASHER, FLAT	
6	NAS 1351	SCREW, CAP	
8	NAS 1351	SCREW, CAP	
1	1201424-2	RING	
1	1201424-1	THRUST PLATE	
2	1201423-1	VALVE PROPELLANT INLET	
1	1201422-9	WASHER/BALANCE (1201420)	
1	1201419-1	SLIDES	
1	1201419-1	INJECTOR	
1	1201414-9	ASSEMBLY	

CONTRACT NO. **NAS 3-24308**
 DRAWING NO. **1201415**
 TITLE **THRUST CHAMBER ASSEMBLY**
 DATE **11-3-15**
 RELEASE DATE **11-3-15**
 APPROVED **[Signature]**
 CHECKED **[Signature]**
 DESIGNED **[Signature]**
 DRAWN **[Signature]**
 DATE **11-3-15**
 SHEET **1** OF **3**
 DEVELOPMENT HARDWARE FOR TEST ON EXPERIMENTATION

REVISION	DATE	BY	APPROVED
A	11-2-15		



NOTES

SECTION 13-13 21

SECTION D-D 21

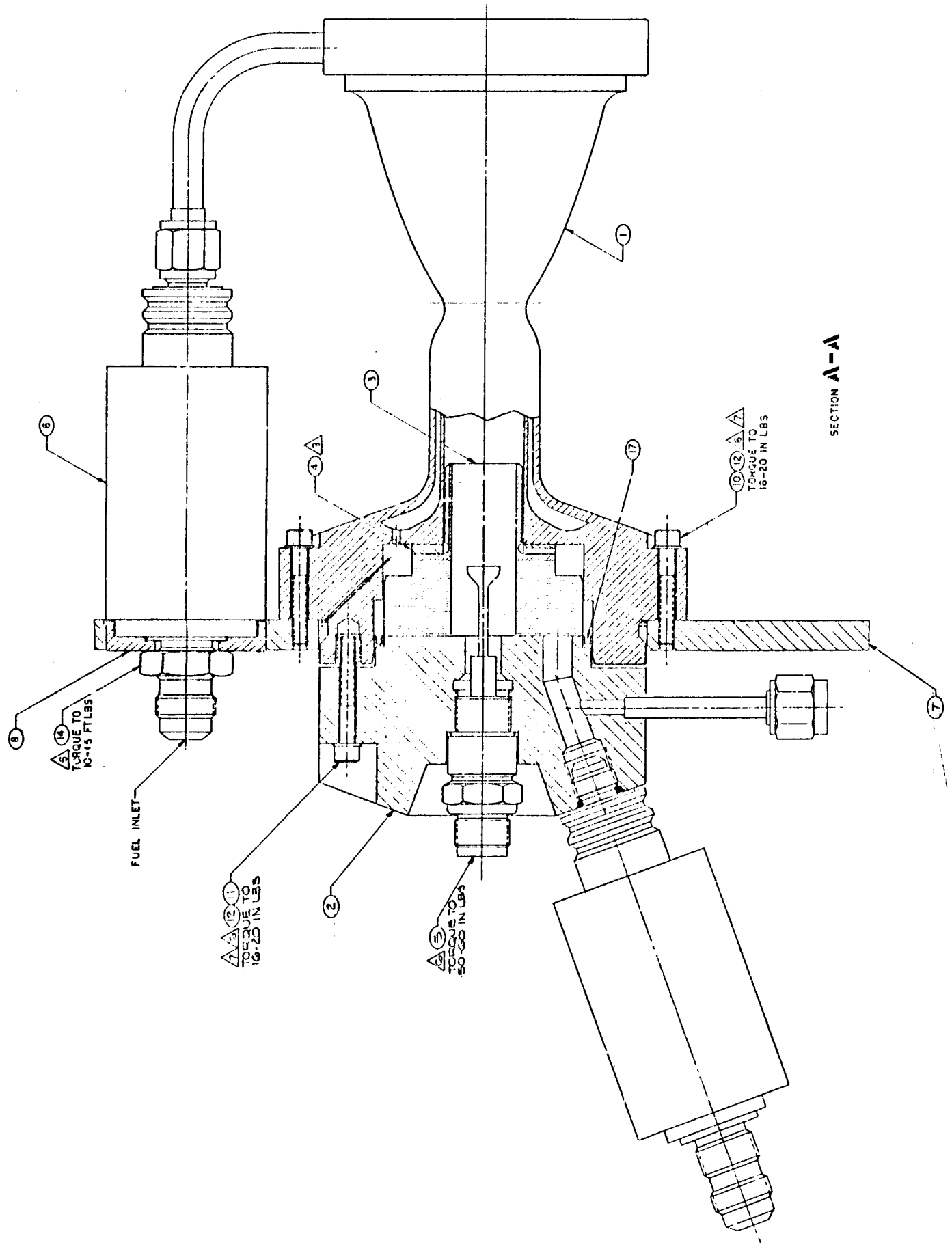
FIG. NO.	1201415
REV.	E
DATE	11-2-15
BY	
APPROVED	

H G F E D C B A

REV	DESCRIPTION	BY	DATE
1	APPROVED		
2			
3			

REV	DESCRIPTION	BY	DATE
1	APPROVED		
2			
3			

1 2 3 4 5 6 7 8



SECTION A-A

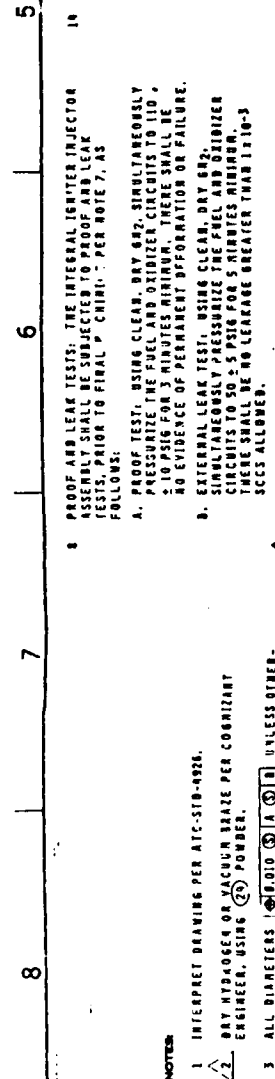
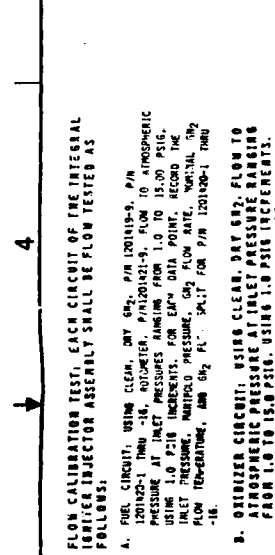
H G F E D C B A

1 2 3 4 5 6 7 8

NOTES

REV	DESCRIPTION	DATE	BY	CHKD
1	ASSEMBLY	12/12/68	R. NICKEL	

ITEM NO.	QTY	RECD
1	1	
2	1	
3	1	
4	1	
5	1	
6	1	
7	1	
8	1	
9	1	
10	1	
11	1	
12	1	
13	1	
14	1	
15	1	
16	1	
17	1	
18	1	



ITEM NO.	QTY	RECD
1	1	
2	1	
3	1	
4	1	
5	1	
6	1	
7	1	
8	1	
9	1	
10	1	
11	1	
12	1	
13	1	
14	1	
15	1	
16	1	
17	1	
18	1	

14 FLOW CALIBRATION TEST: EACH CIRCUIT OF THE INTEGRAL INJECTOR ASSEMBLY SHALL BE FLOW TESTED AS FOLLOWS:

A. FUEL CIRCUIT: USING CLEAN, DRY G₂, P/N 1201416-9, P/N 1201416-10, ROTOMETER, P/N 1201416-9, FLOW TO ATMOSPHERIC PRESSURE AT INLET PRESSURES RANGING FROM 1.0 TO 15.00 PSIG, RECORD THE FLOW IN INCREMENTS OF 0.50 PSIG. RECORD THE FLOW IN INCREMENTS OF 0.50 PSIG. RECORD THE FLOW IN INCREMENTS OF 0.50 PSIG. RECORD THE FLOW IN INCREMENTS OF 0.50 PSIG.

B. OXIDIZER CIRCUIT: USING CLEAN, DRY G₂, FLOW TO ATMOSPHERIC PRESSURE AT INLET PRESSURES RANGING FROM 1.0 TO 15.00 PSIG, RECORD THE FLOW IN INCREMENTS OF 0.50 PSIG. RECORD THE FLOW IN INCREMENTS OF 0.50 PSIG. RECORD THE FLOW IN INCREMENTS OF 0.50 PSIG.

15 MULLIPORE FILTERS RATED AT 400 MICRONS ABSOLUTE, OR LOWER, SHALL BE USED WHEN FLOWING ANY FLUID THROUGH THE INTEGRAL INJECTOR ASSEMBLY.

16 MARK PER AS929-7 WITH 1201416, APPLICABLE BASE NO. AND AEROMETRIC TECHNOLOGIES COMPANY (ATC) ASSIGNED SERIAL NO.

8 PROOF AND LEAK TESTS: THE INTEGRAL INJECTOR ASSEMBLY SHALL BE SUBJECTED TO PROOF AND LEAK TESTS, PRIOR TO FINAL CHECKOUT, PER NOTE 7, AS FOLLOWS:

A. PROOF TEST: USING CLEAN, DRY G₂, SIMULTANEOUSLY PRESSURIZE THE FUEL AND OXIDIZER CIRCUITS TO 1.0 TO 2.10 PSIG FOR 3 MINUTES MINIMUM. THERE SHALL BE NO EVIDENCE OF PERMANENT DEFORMATION OR FAILURE.

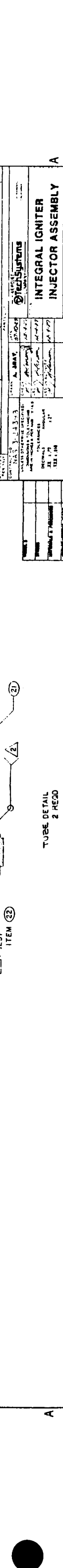
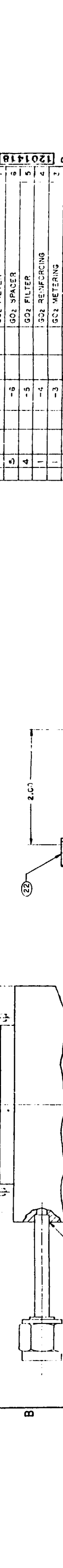
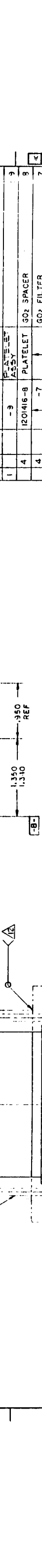
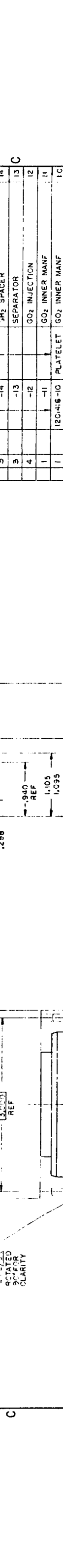
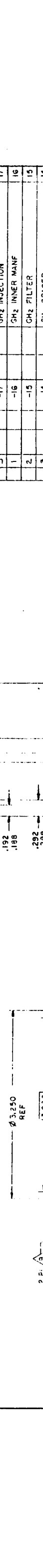
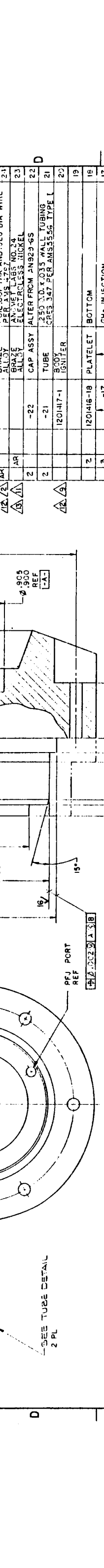
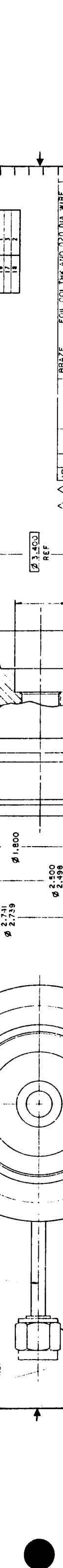
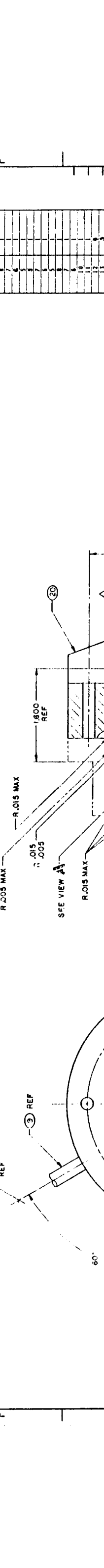
B. EXTERNAL LEAK TEST: USING CLEAN, DRY G₂, SIMULTANEOUSLY PRESSURIZE THE FUEL AND OXIDIZER CIRCUITS TO 2.5 PSIG FOR 5 MINUTES MINIMUM. THERE SHALL BE NO LEAKAGE GREATER THAN 1.0E-3 SCES ALLOWED.

C. CONTAMINATION CRITICAL HARDWARE: CLEARNESS PER ATC-STD-1028, LEVEL 6, EXCEPT PARTICLE SIZE AND VVA LIMITS PER ATC-STD-1028, LEVEL 1000 GENERAL, ALL LEVELS PER ATC-STD-1028, LEVEL 1000. NOTE: CONTAMINATION CRITICAL HARDWARE TO BE SUBMITTED TO FLOW CALIBRATION TESTS OF NOTE 14.

D. PROTECTIVE CLOSURES ARE REQUIRED TO PROTECT INTERNAL PASSAGES DURING HANDLING, SHIPPING AND STORAGE. REMOVE ONLY AS REQUIRED.

E. ALL DIMENSIONS APPLY AFTER BRAZING, UNLESS OTHERWISE INDICATED.

F. FINAL MACHINE AFTER PROOF AND LEAK TESTING PER NOTE 8.



ITEM NO.	QTY	RECD
1	1	
2	1	
3	1	
4	1	
5	1	
6	1	
7	1	
8	1	
9	1	
10	1	
11	1	
12	1	
13	1	
14	1	
15	1	
16	1	
17	1	
18	1	
19	1	
20	1	
21	1	
22	1	
23	1	

ITEM NO.	QTY	RECD
1	1	
2	1	
3	1	
4	1	
5	1	
6	1	
7	1	
8	1	
9	1	
10	1	
11	1	
12	1	
13	1	
14	1	
15	1	
16	1	
17	1	
18	1	
19	1	
20	1	
21	1	
22	1	
23	1	

ITEM NO.	QTY	RECD
1	1	
2	1	
3	1	
4	1	
5	1	
6	1	
7	1	
8	1	
9	1	
10	1	
11	1	
12	1	
13	1	
14	1	
15	1	
16	1	
17	1	
18	1	
19	1	
20	1	
21	1	
22	1	
23	1	

ITEM NO.	QTY	RECD
1	1	
2	1	
3	1	
4	1	
5	1	
6	1	
7	1	
8	1	
9	1	
10	1	
11	1	
12	1	
13	1	
14	1	
15	1	
16	1	
17	1	
18	1	
19	1	
20	1	
21	1	
22	1	
23	1	

ITEM NO.	QTY	RECD
1	1	
2	1	
3	1	
4	1	
5	1	
6	1	
7	1	
8	1	
9	1	
10	1	
11	1	
12	1	
13	1	
14	1	
15	1	
16	1	
17	1	
18	1	
19	1	
20	1	
21	1	
22	1	
23	1	

ITEM NO.	QTY	RECD
1	1	
2	1	
3	1	
4	1	
5	1	
6	1	
7	1	
8	1	
9	1	
10	1	
11	1	
12	1	
13	1	
14	1	
15	1	
16	1	
17	1	
18	1	
19	1	
20	1	
21	1	
22	1	
23	1	

ITEM NO.	QTY	RECD
1	1	
2	1	
3	1	
4	1	
5	1	
6	1	
7	1	
8	1	
9	1	
10	1	
11	1	
12	1	
13	1	
14	1	
15	1	
16	1	
17	1	
18	1	
19	1	
20	1	
21	1	
22	1	
23	1	

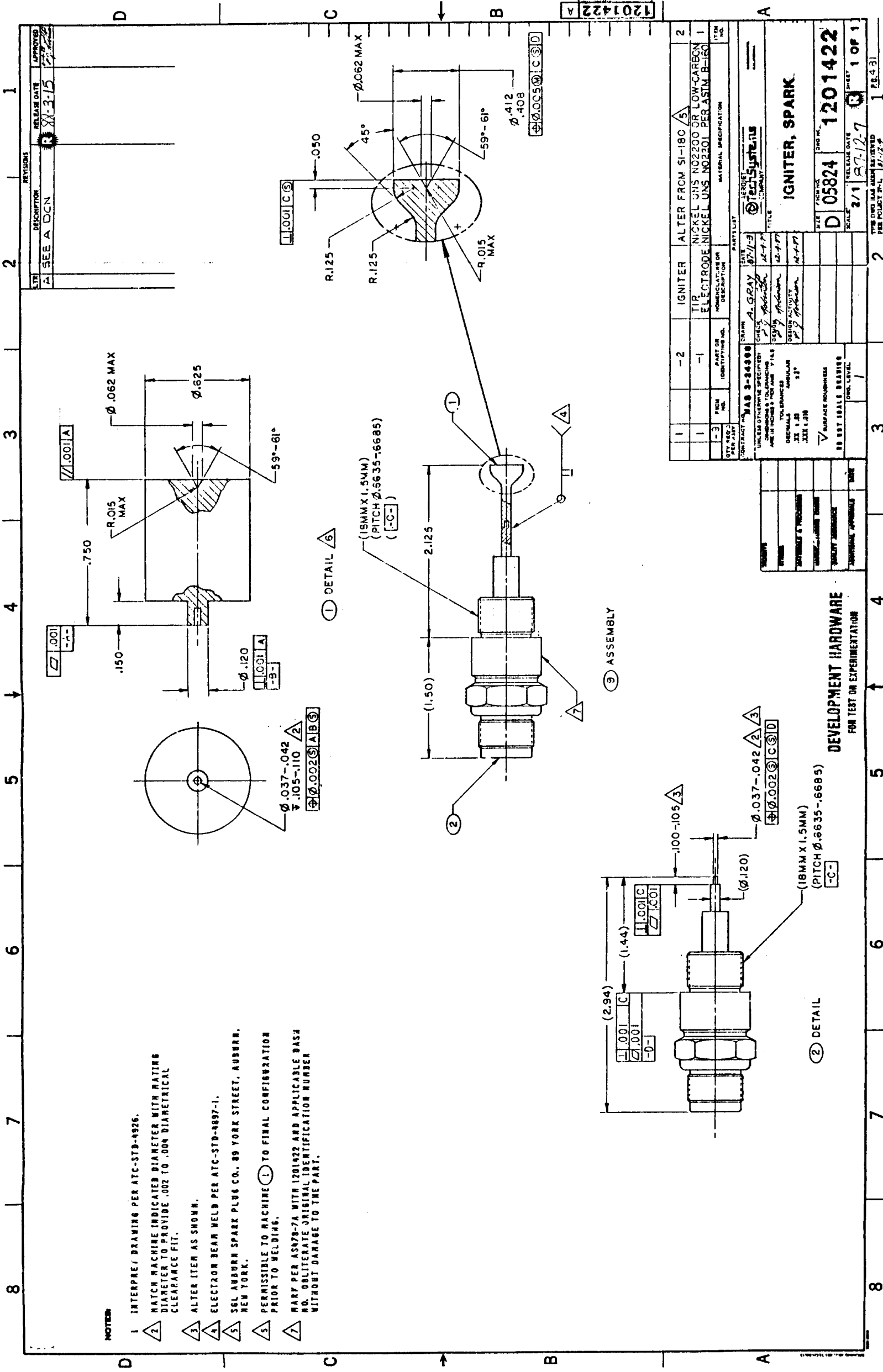
ITEM NO.	QTY	RECD
1	1	
2	1	
3	1	
4	1	
5	1	
6	1	
7	1	
8	1	
9	1	
10	1	
11	1	
12	1	
13	1	
14	1	
15	1	
16	1	
17	1	
18	1	
19	1	
20	1	
21	1	
22	1	
23	1	

INTEGRAL IGNITER INJECTOR ASSEMBLY

E 05824 1201418

2/1 2/12 1 OF 1

DEVELOPMENT HARDWARE FOR TEST OR EXPERIMENTATION



- NOTES:**
- 1 INTERPRET DRAWING PER ATC-STB-4926.
 - 2 MATCH MACHINE INDICATED DIAMETER WITH MATING DIAMETER TO PROVIDE .002 TO .004 DIAMETRICAL CLEARANCE FIT.
 - 3 ALTER ITEM AS SHOWN.
 - 4 ELECTRON BEAM WELD PER ATC-STB-4897-1.
 - 5 SGL ANADURN SPARK PLUG CO., 89 YORK STREET, AUBURN, NEW YORK.
 - 6 PERMISSIBLE TO MACHINE (1) TO FINAL CONFIGURATION PRIOR TO WELDING.
 - 7 MARY PER AS78-7A WITH 1201422 AND APPLICABLE BASH NO. OBLITERATE ORIGINAL IDENTIFICATION NUMBER WITHOUT DAMAGE TO THE PART.

REV	DESCRIPTION	RELEASE DATE	APPROVED
A	SEE A DCN	3-15	

REV	DESCRIPTION	RELEASE DATE	APPROVED
1	IGNITER ALTER FROM SI-18C		
2	TIP NICKEL UNS N02200 OR LOW-CARBON ELECTRODE NICKEL UNS N02201 PER ASTM B-160		

CONTRACT NO. 3-3498	DATE 12-7-7
UNLESS OTHERWISE SPECIFIED	ENGINEER A. GRAY
DIMENSIONS & TOLERANCES	DESIGNER
AS SHOWN ON THIS DRAWING	DATE 12-7-7
UNLESS OTHERWISE SPECIFIED	DESIGNER
XX 1.00	DATE 12-7-7
XX 1.20	DATE 12-7-7
XX 1.30	DATE 12-7-7
XX 1.40	DATE 12-7-7
XX 1.50	DATE 12-7-7
XX 1.60	DATE 12-7-7
XX 1.70	DATE 12-7-7
XX 1.80	DATE 12-7-7
XX 1.90	DATE 12-7-7
XX 2.00	DATE 12-7-7

ITEM NO.	1	2	3	4	5	6	7	8
DESCRIPTION	IGNITER	ALTER FROM SI-18C						
MATERIAL SPECIFICATION	NICKEL UNS N02200 OR LOW-CARBON ELECTRODE NICKEL UNS N02201 PER ASTM B-160							

ITEM NO.	1	2	3	4	5	6	7	8
DESCRIPTION	IGNITER	ALTER FROM SI-18C						
MATERIAL SPECIFICATION	NICKEL UNS N02200 OR LOW-CARBON ELECTRODE NICKEL UNS N02201 PER ASTM B-160							

ITEM NO.	1	2	3	4	5	6	7	8
DESCRIPTION	IGNITER	ALTER FROM SI-18C						
MATERIAL SPECIFICATION	NICKEL UNS N02200 OR LOW-CARBON ELECTRODE NICKEL UNS N02201 PER ASTM B-160							

ITEM NO.	1	2	3	4	5	6	7	8
DESCRIPTION	IGNITER	ALTER FROM SI-18C						
MATERIAL SPECIFICATION	NICKEL UNS N02200 OR LOW-CARBON ELECTRODE NICKEL UNS N02201 PER ASTM B-160							

ITEM NO.	1	2	3	4	5	6	7	8
DESCRIPTION	IGNITER	ALTER FROM SI-18C						
MATERIAL SPECIFICATION	NICKEL UNS N02200 OR LOW-CARBON ELECTRODE NICKEL UNS N02201 PER ASTM B-160							

ITEM NO.	1	2	3	4	5	6	7	8
DESCRIPTION	IGNITER	ALTER FROM SI-18C						
MATERIAL SPECIFICATION	NICKEL UNS N02200 OR LOW-CARBON ELECTRODE NICKEL UNS N02201 PER ASTM B-160							



REPORT DOCUMENTATION PAGE

1. Report No. NASA-CR-185296		2. Government Accession No.		3. Recipient's Catalog No.	
4. Title And Subtitle Space Station Auxiliary Thrust Chamber Technology			5. Report Date July 1990		
			6. Performing Organization Code		
7. Author(s) Philip J. Robinson			8. Performing Organization Report No.		
9. Performing Organization Name and Address GenCorp Aerojet Propulsion Division P.O. Box 13222 Sacramento, CA 95813-6000			10. Work Unit No. 506-42-31		
			11. Contract or Grant No. NAS 3-24398		
12. Sponsoring Agency Name and Address National Aeronautics and Space Administration Lewis Research Center Cleveland, Ohio 44135-3191			13. Type of Report and Period Covered Contractor Report Final		
			14. Sponsoring Agency Code		
15. Supplementary Notes Project Manager - Dr. Steven J. Schneider, Space Propulsion Technology Division NASA Lewis Research Center					
16. Abstract <p>The objective of the program documented herein was to establish a technical data base to support future development of GO₂/GH₂ flight thrusters for a Space Station Auxiliary Propulsion System. Specific issues of concern were thruster performance and cycle life. To address these issues, NASA funded Aerojet to design, fabricate and altitude test two 25-lbf GO₂/GH₂ thrusters. The first thruster was designed to operate at a nominal mixture ratio (O/F) of 4.0 and expansion area ratio (ϵ) of 100:1. It was tested over a range of O/F from 2.0 to 8.0, achieving a range of specific impulse (Isp) from 440 to 310 lbf-sec/lbm. The second thruster was optimized for a nominal O/F of 8.0 at a lower nozzle expansion area ratio ϵ of 30:1. This second thruster was tested over an O/F range of 3.0 to 9.5, achieving an Isp range of 416 to 3323 lbf-sec/lbm, respectively. At O/F = 8.0, the Isp was 360 lbf-sec/lbm, as predicted.</p>					
17. Key Words (Suggested by Author(s)) Rockets, Space Station, hydrogen/oxygen, regenerative, high-performance, long-life			18. Distribution Statement Unclassified Unlimited Subject Category 20		
19. Security Classif. (of this report) Unclassified		20. Security Classif. (of this page) Unclassified		21. No. of pages 172	22. Price A05